Analysis Report documenting the Assessment of the Solubility of Lead, EDTA and other Organic Ligands in non-Sulfide systems performed under TP 08-02 and under TP 20-01

Revision 0

Analysis Report for the Lead xperimental Data obtained under TP 08-02 Revision 0 and TP 20-01 Revision 0 per Analysis Plan AP-192 Revision 0

Jay Jang, Priya Hora, Leslie Kirkes Chammi Miller, and Luzheng Zhang

SNL WIPP Geochemistry (8882)

Sandia National Laboratories

Carlsbad, New Mexico, U.S.A.

Effective Date: November 23 2021
JJ 2/7/2 21

WIPP:4.4.2.2.1:TD:QA-L:RECERT:576380

Sandia National Laboratories is a multimission laboratory managed and operated by National Technology & Engineering Solutions of Sandia, LLC, a wholly owned subsidiary of Honeywell International Inc., for the U.S. Department of Energy's National Nuclear Security Administration under contract DE-NA0003525.

APPROVALS

	Print Name	Signature	Date
Authored by:	Jay Jang		11/18/2021
Authored by:	Priya Hora		11/18/2021
Authored by:	Leslie Kirkes		11/22/21
Authored by:	Chammi Miller		11/18/2021
Authored by:	Luzheng Zhang		11/18/2021
Reviewed by:	Carlos Jove-Colon Technical Reviewer	Signature on file	11/18/2021
Reviewed by:	Shelly R. Nielsen Quality Assurance Reviewer		11-19-2021
Approved by:	Paul Shoemaker Senior Manager		11/23/2021

I. INTRODUCTION

The objective of this report is to accept or reject the hypothesis that the experiments conducted under TP 08-02 Revision 0 (Ismail et al., 2008) were affected by CO_2(g) intrusion and sample contamination. The test of the hypothesis is accomplished by comparing the experimental data collected under the protocols of TP 08-02 Revision 0 and TP 20-01 Revision 0 (Kirkes and Zhang, 2020). The protocols of TP 20-01 Revision 0 minimize the possibilities of CO_2(g) intrusion and sample contamination. The experimental data sets obtained under both TPs will be assessed statistically to see if they are identical or not.

Under TP 08-02 Revision 0, lead solubility experiments were conducted under ambient atmosphere conditions where the partial pressure of CO_2(g) or $P_{CO_{2(g)}}$ is assumed to be $10^{-3.5}$ atm (Stumm and Morgan, 1996). On the other hand, experiments under TP 20-01 Revision 0 were conducted in minimum CO_2(g) gloveboxes. In this report we will discuss in detail the differences in experimental protocols under the two Test Plans (TP), and document and compare the results of solubility experiments performed under each TP.

I.1. Experiments conducted under TP 08-02 Revision 0

Under TP 08-02 Revision 0, the experiments were aged in sealed reactors, i.e., screw cap with a few rounds of paraffin film over the screw cap. The experiments were prepared in large volume reactors (typically larger than 50 mL) to allow for repeated sampling of supernatant over long aging times. The number of repeated sampling entries usually exceeded 5 times, and the aging time was typically on the order of multiple years. Thus, it is reasonable to hypothesize that the gas in the headspace of the reactors was replaced or mixed with the ambient atmosphere when the reactors were opened for repeated sampling over the duration of the experiments. Considering multiple years of aging time, possible diffusion of CO_2(g) through the container wall and cap, i.e., in or out depending on the partial pressure gradient, cannot be excluded. The solution chemistry inside the reactors may have been influenced by the gain or loss of CO_2(g). In addition, it is possible that contamination may have occurred in the samples, due to the repeated sample retrieval from the reactors.

To investigate the solubility of a lead sulfate mineral, $PbSO_4$(s) (anglesite), excess $PbSO_4$(s) was added to solutions of six incremental concentrations of sodium sulfate (Na_2SO_4) spiked with sodium chloride (NaCl) in duplicate (12 reactors in total). This set of experiments did not contain carbonate in the starting solution and solid; however, the experiments were prepared under ambient conditions open to the atmosphere, sealed, and aged under normal atmosphere where $P_{CO_{2(g)}} \approx 10^{-3.5}$ atm. Thus, the changes in the chemistry due to the $CO_2(g)$ intrusion would impact the measured concentrations of the reactive components, e.g., ΣPb.

To investigate the solubility of a lead carbonate mineral, $PbCO_3(s)$ (cerussite), excess $PbCO_3(s)$ was added in solutions of four incremental concentrations of sodium bicarbonate ($NaHCO_3$) spiked with sodium chloride (NaCl) at 0.15 m in duplicate (8 reactors). For the highest concentration of $NaHCO_3$, additional reactors spiked with 0.3 m NaCl were prepared in duplicates, thus, this set of experiments consisted of 10 reactors in total. The composition of background solutions indicates the partial pressure $CO_2(g)$ of this set of experiments ranges from $10^{-3.1}$ to $10^{-0.3}$ atm due to the $NaHCO_3$ loading. Considering the atmospheric partial pressure of $CO_2(g) \approx 10^{-3.5}$ atm (Stumm and Morgan, 1996), this set of reactors could have experienced loss of $CO_2(g)$. The reactors were aged under ambient atmosphere, and experienced repeated sampling events over long aging times. When the solids in the 10 reactors were analyzed with XRD at the termination of the experiments, a secondary mineral, abellaite ($NaPb_2(CO_3)_2(OH)(s)$), was identified from one of the duplicates representing one condition (Reactor ID: PbCO3 0.5/0.15-1; Kirkes and Xiong, 2019).

Formation of abellaite at the expense of cerussite can be expressed by the following reaction:

$$2PbCO_3(s)\ (\text{cerussite}) + Na^+ + OH^- = NaPb_2(CO_3)_2(OH)(s)\ (\text{abellaite}) \quad (1)$$

As shown in Reaction (1), the formation of abellaite at the expense of cerussite, $PbCO_3(s)$, requires excess Na^+ and/or OH^-. Discussion with DOE on the possible sources of the excess Na^+ and/or OH^- included the following: (i) sample contamination, and (ii) $CO_2(g)$ intrusion due to repeated entries for sampling over long aging time. However, $CO_2(g)$ intrusion cannot increase the OH^-.[1]

For the repeated sampling entries into the reactors, care has been exercised to not cross-contaminate the content of the reactors. It is part of general laboratory practice at SNL WIPP Geochemistry Program to (i) rinse the pH electrode with DI water prior to inserting the electrode into the reactors, and (ii) use new pipet tips, transfer pipets, syringes, filters, temporary containers, etc., in between the sampling of supernatants from individual reactors. However, the SNL WIPP Geochemistry Program did not exclude the possibility of inadvertent contamination due to the repeated entries.

[1] $CO_2(g)$ intrusion generates H^+ via the following reaction: $CO_2(g) + H_2O = H^+ + HCO_3^-$. $CO_2(g)$ intrusion cannot increase OH^-.

I.2. Verification experiments conducted under the protocols of TP 20-01

Three Experiments were selected through AP-192 Revision 0 (Jang et al., 2021) and prepared under the protocols described in TP 20-01 Revision 0 (Kirkes and Zhang, 2020). They resemble the experiments conducted under TP 08-02 Revision 0. The protocols of TP 20-01 Revision 0 were set up to exclude the uncertainties associated with the $CO_2(g)$ intrusion and sample contamination. At the same time, the protocols introduced new sources of uncertainty, such as different aging times and bottle materials. They are tabulated in Table 1 of AP-192 Revision 0 (Jang et al., 2021).

Under the protocols of TP 20-01 Revision 0, (1) the reactors were prepared and stored in minimal $CO_2(g)$ gloveboxes, and (2) instead of using large volume to allow repeated entries, replicates were prepared for each condition in smaller volume (20 mL) with the same solid:solution ratio as employed in TP 08-02 Revision 0 to allow for sacrificial sampling of the reactors. For time-dependent measurements of the components, two replicates representing a condition (i.e., composition of matrix solution) were used up to obtain filtered solution and solid after recording the pHr.[2] For filtration, 0.2 μm syringe filters were used.

Use of the gloveboxes would prevent the possible $CO_2(g)$ intrusion for non-carbonated experiment. For the carbonated experiment, the loss of $CO_2(g)$ could occur only once while taking the pHr from the selected replicates (usually less than 15 minutes without stirring). Remaining replicates would not be opened until the next sampling.

Experiments 1 and 2 below repeat two experiments conducted under TP 08-02 Revision 0. Experiment 3 was not conducted under TP 08-02 Revision 0. It was selected as a control experiment to explain the thermodynamics of the mineral paragenesis observed from the $PbCO_3(s)$ experiment (i.e., Experiment 2):

> Experiment 1. $PbSO_4(s)$ - Na_2SO_4 - NaCl - H_2O: The solid $PbSO_4(s)$, anglesite, was added in excess to the background solutions of incremental concentration of Na_2SO_4 (0.01, 0.10, 0.50, 1.00, 1.50, and 1.80 m) with NaCl concentration fixed at 0.15 m. This set is a repetition experiment for a direct comparison with data obtained from the same experiment performed under TP 08-02 Revision 0.

[2] pHr is the reading from the display of pH meters calibrated with commercial pH buffers of low ionic strength.

Experiment 2. $PbCO_3(s)$ - $NaHCO_3$ - $NaCl$ - H_2O: The solid $PbCO_3(s)$, cerussite, was added in excess to the background solutions of incremental concentration of $NaHCO_3$ (0.01, 0.05, 0.50, and 1.00 m) with NaCl concentration fixed at 0.15 m. Experiment of $NaHCO_3$ = 1.00 m solution is prepared with NaCl = 0.30 m in parallel. This set is a repetition experiment for direct comparison with data obtained from the same experiment performed under TP 08-02 Revision 0.

Experiment 3. $PbCO_3(s)$ - Na_2CO_3 - H_2O: The solid $PbCO_3(s)$, cerussite, will be added in excess to the solutions of incremental concentration of Na_2CO_3 (0, 0.01, 0.10, 0.50, 1.00, 1.50, 2.00, and 2.50 m). This experiment was not conducted under TP 08-02 Revision 0. This experiment requires measurement of ΣCO3 at concentrations lower than the detection limit of our current instrument (a Carbon Coulometer). This experiment was planned hoping for the timely procurement and operation of a new analytical instrument to measure total organic carbon (TOC analyzer). This instrument can also measure total inorganic carbon (TIC), with a lower detection limit. The TOC/TIC analyzer was installed and tested on 6/24/2021, and is in need of an approved activity specific procedure before data can be produced for project deliverables.[3]

II. EXPERIMENTS AND MEASUREMENTS

II.1. Experiment 1

Under TP 08-02 Revision 0, background solutions were prepared by mixing 1 kg of DI water with the prescribed mass of salts, Na_2SO_4 and NaCl (Table II.1-1). 100 mL of the prepared solution was mixed with 2.0 grams of $PbSO_4(s)$ (SN[4] WIPP-Solubility-3, pages 18, 20). Table II.1-1 summarizes the following: prescribed mass of salts, molality and Molarity of the salts in the prepared solutions, calculated and measured density of the prepared solutions, calculated pH[5] and Molarity-to-molality conversion factor (M:m, L/kg) (Jang, 2020). XRD scan of the purchased $PbSO_4(s)$ is presented in Figure II.1-1.

Table II.1-1. Recipe for the background solutions used for Experiment 1 under TP 08-02 Revision 0.

Recipe						molality (m, mol/kg)

[3] Technical Review of Activity Specific Procedure (SP) for the TOC under SNL WIPP QA program was completed on 11/4/2021.

[4] SN: Scientific Notebook, where laboratory activities are recorded.

[5] pH = - log $\{H^+\}$, i.e., pH is negative base 10 logarithm of H^+ activity.

Solution ID	Na_2SO_4, g	NaCl, g	H_2O, g			Na_2SO_4	NaCl	ΣNa	ΣSO4	ΣCl
0.01-Na2SO4+0.15-NaCl	1.4206	8.7663	1000			0.0100	0.150	0.171	0.0100	0.150
0.1-Na2SO4+0.15-NaCl	14.2027	8.7676	1000			0.100	0.150	0.351	0.100	0.150
0.5-Na2SO4+0.15-NaCl	71.0101	8.7669	1000			0.502	0.150	1.154	0.502	0.150
1.0-Na2SO4+0.15-NaCl	142.0393	8.7692	1000			1.00	0.151	2.16	1.00	0.151
1.5-Na2SO4+0.15-NaCl	213.05	8.7697	1000			1.50	0.151	3.16	1.50	0.151
1.8-Na2SO4+0.15-NaCl	255.66	8.7787	1000			1.81	0.151	3.76	1.81	0.151
Properties	Density, g/mL					Molarity (M, mol/L)				
Solution ID	Calculated	Measured#	%Deviation###	M:m, L/kg	pH##	Na_2SO_4	NaCl	ΣNa	ΣSO4	ΣCl
0.01-Na2SO4+0.15-NaCl	1.0075	1.0097	0.2%	1.0027	7.03	0.0100	0.150	0.170	0.0100	0.150
0.1-Na2SO4+0.15-NaCl	1.0156	1.0186	0.3%	1.0073	7.18	0.100	0.149	0.349	0.100	0.149
0.5-Na2SO4+0.15-NaCl	1.0508	1.0678	1.6%	1.0278	7.29	0.488	0.146	1.12	0.488	0.146
1.0-Na2SO4+0.15-NaCl	1.0929	1.1213	2.6%	1.0535	7.32	0.952	0.143	2.05	0.952	0.143
1.5-Na2SO4+0.15-NaCl	1.1329	1.1719	3.4%	1.0791	7.33	1.39	0.139	2.93	1.39	0.139
1.8-Na2SO4+0.15-NaCl	1.1561	1.1523	-0.3%	1.0945	7.34	1.65	0.138	3.44	1.65	0.138

WIPP-Solubility-21, p.89 per Jang (2021a).

Modeled pH using EQ3/6, Version 8.0a (Wolery and Jarek, 2003).[6] The pH is negative base 10 logarithm of H^+ activity, i.e., pH = - log $\{H^+\}$, of background solution calculated using PACE[7] and selected PIPs[8] in the approved data0.fm1, not taking into consideration the dissolution of anglesite. EQ3/6, Version 8.0a is not included in the Software List of AP-192 Revision 0 (Jang et al., 2021), thus, the calculation of pH in this report is considered a deviation from the AP per NP 9-1 Revision 11 Section 2.1.2. (Nielsen, 2020).

%Deviation of density = (Measured - Calculated)/Calculated × 100%.

Figure II.1-1. XRD scan for the initial $PbSO_4$(s) (Acros Organics LOT AO235161, WIPP-Solubility-3, page 20) used in Experiment 1 conducted under TP 08-02 Revision 0.

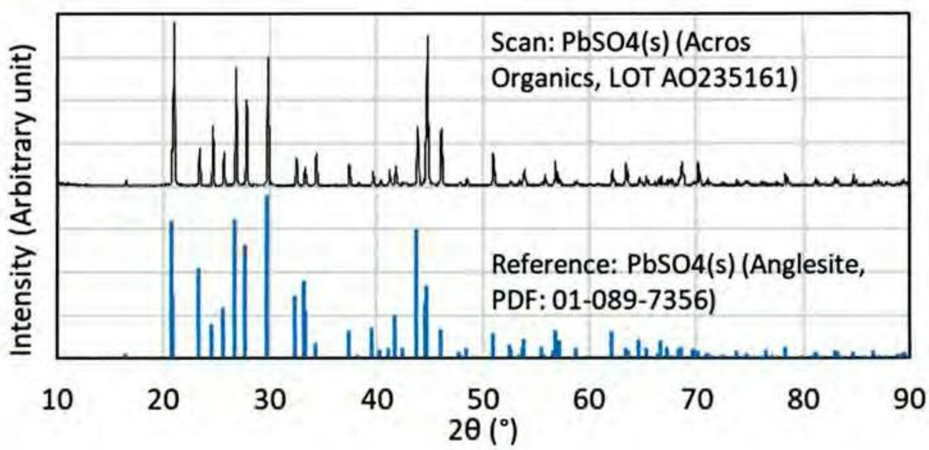

Under the protocols of TP 20-01 Revision 0, background solutions were prepared by mixing 500 g of de-gassed DI water with the prescribed masses of Na_2SO_4 and NaCl. 20 mL of the prepared solution was mixed with 0.4 g of $PbSO_4$(s) (SN WIPP-Pb-3, pages 5-8). Table II.1-2 summarizes the following: prescribed mass of salts, molality and Molarity of the salts in the prepared solutions,

[6] This reference is the users' manual for Version 8.0, and is applicable to Version 8.0a.
[7] PACE: Pitzer Activity Coefficient Equation
[8] PIPs: Pitzer Interaction Parameters

calculated density of the prepared solutions, calculated pH and Molarity-to-molality conversion factor (M:m, L/kg; Jang, 2020). For the fifth solution in Table II.1-2 (Solution ID: 1.5-Na2SO4+0.15-NaCl), slightly different concentrations of Na_2SO_4 and NaCl were applied due to addition of extra mass of DI water. XRD scan of the purchased $PbSO_4$(s) is presented in Figure II.1-2.

Table II.1-2. Recipe for the background solutions used for Experiment 1 under TP 20-01 Revision 0. For the fifth solution, slightly different concentrations of Na_2SO_4 and NaCl were applied, i.e., instead of 1.50 and 0.15 m, 1.47 m Na_2SO_4 and 0.147 m NaCl were applied.

Recipe						molality (m, mol/kg)				
Solution ID	Na_2SO_4, g	NaCl, g	H_2O, kg			Na_2SO_4	NaCl	ΣNa	ΣSO4	ΣCl
0.01-Na2SO4+0.15-NaCl	0.7106	4.3833	500.05			0.0100	0.150	1.70E-01	1.00E-02	1.50E-01
0.1-Na2SO4+0.15-NaCl	7.1016	4.3833	500.02			0.100	0.150	3.50E-01	1.00E-01	1.50E-01
0.5-Na2SO4+0.15-NaCl	35.5054	4.3831	500.02			0.500	0.150	1.15E+00	5.00E-01	1.50E-01
1.0-Na2SO4+0.15-NaCl	71.0197	4.3837	500.03			1.00	0.150	2.15E+00	1.00E+00	1.50E-01
1.5-Na2SO4+0.15-NaCl	106.525	4.3838	509.45			1.47	0.147	3.09E+00	1.47E+00	1.47E-01
1.8-Na2SO4+0.15-NaCl	127.8306	4.383	500.02			1.80	0.150	3.75E+00	1.80E+00	1.50E-01
Properties	Density, g/mL					Molarity (M, mol/L)				
Solution ID	Calculated	Measured	%Deviation###	M:m, L/kg	pH##	Na_2SO_4	NaCl	ΣNa	ΣSO4	ΣCl
0.01-Na2SO4+0.15-NaCl	1.0075	NA	NA	1.0027	7.03	0.0100	0.150	1.70E-01	9.98E-03	1.50E-01
0.1-Na2SO4+0.15-NaCl	1.0156	NA	NA	1.0073	7.18	0.0993	0.149	3.47E-01	9.93E-02	1.49E-01
0.5-Na2SO4+0.15-NaCl	1.0508	NA	NA	1.0278	7.29	0.486	0.146	1.12E+00	4.86E-01	1.46E-01
1.0-Na2SO4+0.15-NaCl	1.0929	NA	NA	1.0535	7.32	0.949	0.142	2.04E+00	9.49E-01	1.42E-01
1.5-Na2SO4+0.15-NaCl	1.1301	NA	NA	1.0772	7.33	1.37	0.137	2.87E+00	1.37E+00	1.37E-01
1.8-Na2SO4+0.15-NaCl	1.1561	NA	NA	1.0945	7.34	1.64	0.137	3.43E+00	1.64E+00	1.37E-01

Modeled pH using EQ3/6, Version 8.0a (Wolery and Jarek, 2003). The pH is negative base 10 logarithm of H^+ activity, i.e., pH = - log {H^+}, of background solution calculated using PACE and selected PIPs in the approved data0.fm1, not taking into consideration the dissolution of anglesite. EQ3/6, Version 8.0a is not included in the Software List of AP-192 Revision 0 (Jang et al., 2021), thus, the calculation of pH in this report is considered a deviation from the AP per NP 9-1 Revision 11 Section 2.1.2. (Nielsen, 2020).

%Deviation of density = (Measured - Calculated)/Calculated × 100%.

Figure II.1-2. XRD scan of the initial $PbSO_4$(s) used in Experiment 1 conducted under TP 20-01 Revision 0 (Acros Organics, LOT AO235161).

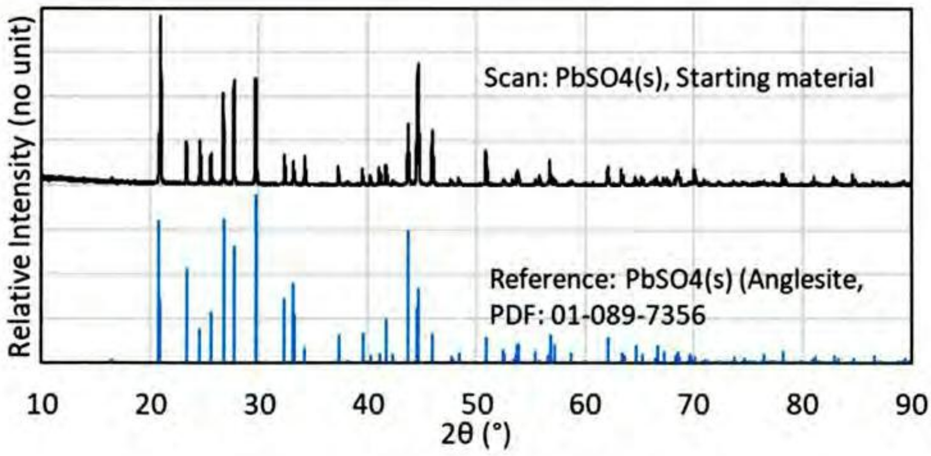

II.2. Experiment 2

Under TP 08-02 Revision 0, background solutions were prepared by mixing 1 L (i.e., 0.997 kg at 25 °C) of de-gassed DI water with the prescribed masses of $NaHCO_3$ and NaCl. 100 mL of the prepared solution was mixed with 2.0 g of $PbCO_3$(s) (SN WIPP-Solubility-3, pages 14, 15, 17). Table II.2-1 summarizes the prescribed mass of salts, molality and Molarity of the salts in the solutions, calculated and measured density of the solutions, calculated pH and Molarity-to-molality conversion factor (M:m, L/kg; Jang, 2020). Note that the actual molalities of $NaHCO_3$ are slightly different from the values used in the solution IDs. XRD of the purchased $PbCO_3$(s) is presented in Figure II.2-1.

Table II.2-1. Recipe for the background solutions used for Experiment 2 under TP 08-02 Revision 0.

Recipe						molality (m, mol/kg)				
Solution ID	$NaHCO_3$	NaCl	H_2O, kg			$NaHCO_3$	NaCl	ΣNa	ΣHCO3	ΣCl
0.01-NaHCO3+0.15-NaCl	0.7200	8.7664	0.997			8.60E-03	1.50E-01	1.59E-01	8.60E-03	1.50E-01
0.05-NaHCO3+0.15-NaCl	3.5998	8.7664	0.997			4.30E-02	1.50E-01	1.93E-01	4.30E-02	1.50E-01
0.5-NaHCO3+0.15-NaCl	35.9979	8.7664	0.997			4.30E-01	1.50E-01	5.80E-01	4.30E-01	1.50E-01
1.0-NaHCO3+0.15-NaCl	71.9959	8.7664	0.997			8.60E-01	1.50E-01	1.01E+00	8.60E-01	1.50E-01
1.0-NaHCO3+0.30-NaCl	71.9959	17.5328	0.997			8.60E-01	3.01E-01	1.16E+00	8.60E-01	3.01E-01
Properties	Density, g/mL					Molarity (M, mol/L)				
Solution ID	Calculated	Measured[#]	%Deviation[###]	M:m, L/kg	pH[##]	$NaHCO_3$	NaCl	ΣNa	ΣHCO3	ΣCl
0.01-NaHCO3+0.15-NaCl	1.0070	1.0073	0.0%	1.0025	8.64	8.58E-03	1.50E-01	1.59E-01	8.58E-03	1.50E-01
0.05-NaHCO3+0.15-NaCl	1.0088	1.0121	0.3%	1.0035	8.03	4.28E-02	1.50E-01	1.93E-01	4.28E-02	1.50E-01
0.5-NaHCO3+0.15-NaCl	1.0292	1.0327	0.3%	1.0151	7.89	4.23E-01	1.48E-01	5.72E-01	4.23E-01	1.48E-01
1.0-NaHCO3+0.15-NaCl	1.0512	1.0539	0.3%	1.0281	7.80	8.36E-01	1.46E-01	9.82E-01	8.36E-01	1.46E-01
1.0-NaHCO3+0.30-NaCl	1.0565	1.0602	0.4%	1.0313	7.76	8.34E-01	2.92E-01	1.13E+00	8.34E-01	2.92E-01

[#] WIPP-Solubility-21, p.91 per Jang (2021a).
[##] Modeled pH using EQ3/6, Version 8.0a (Wolery and Jarek, 2003). The pH is negative base 10 logarithm of H^+ activity, i.e., pH = - log $\{H^+\}$, of background solution calculated using PACE and selected PIPs in the approved data0.fm1, not taking into consideration the dissolution of cerussite. EQ3/6, Version 8.0a is not included in the Software List of AP-192 Revision 0 (Jang et al., 2021), thus, the calculation of pH in this report is considered a deviation from the AP per NP 9-1 Revision 11 Section 2.1.2. (Nielsen, 2020).
[###] %Deviation of density = (Measured - Calculated)/Calculated × 100%.

Figure II.2-1. XRD of initial solid used for Experiment 2 under TP 08-02 Revision 0: $PbCO_3(s)$ (Alfa Aesar, LOT F15S020; WIPP-Solubility-3, page 17).

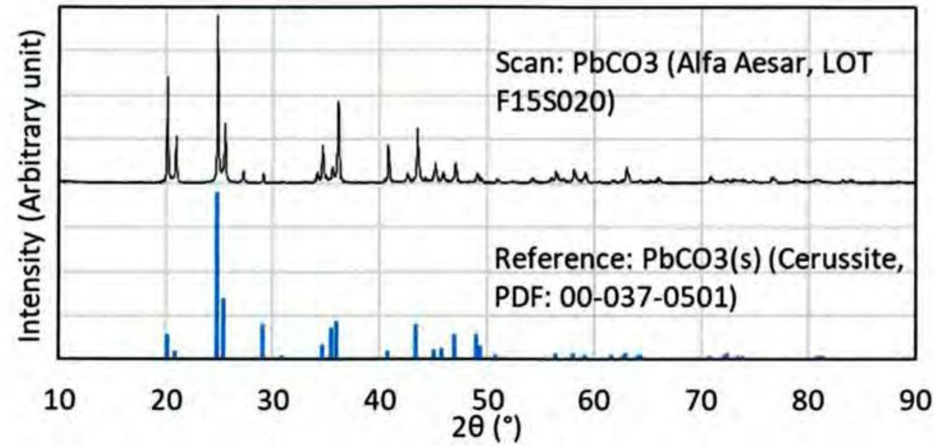

Under the protocols of TP 20-01 Revision 0, background solutions were prepared by mixing 500 g of de-gassed DI water with the prescribed masses of $NaHCO_3$ and NaCl salts. The prescribed mass of salts was mixed with de-gassed DI water inside a glove box. 20 mL of the prepared solution was mixed with 0.4 gram of $PbCO_3(s)$ (SN WIPP-Pb-3, pages 12-15). Table II.2-2 summarizes the following: prescribed mass of the salts, molality and Molarity of the salts in the solutions, calculated density of the solutions, calculated pH and Molarity-to-molality conversion factor (M:m, L/kg). Same $PbCO_3(s)$ as TP 08-02 was used as initial solid (Figure II.2-1).

Table II.2-2. Recipe for the background solutions used for Experiment 2 under TP 20-01 Revision 0.

Recipe						molality (m, mol/kg)				
Solution ID	$NaHCO_3$, g	NaCl, g	H_2O, g			$NaHCO_3$	NaCl	ΣNa	ΣCO3	ΣCl
0.01-NaHCO3+0.15-NaCl	0.4208	4.3830	500.00			0.0100	0.150	1.60E-01	1.00E-02	1.50E-01
0.05-NaHCO3+0.15-NaCl	2.1002	4.3828	500.00			0.0500	0.150	2.00E-01	5.00E-02	1.50E-01
0.5-NaHCO3+0.15-NaCl	21.0026	4.3829	500.07			0.500	0.150	6.50E-01	5.00E-01	1.50E-01
1.0-NaHCO3+0.15-NaCl	42.0056	4.3834	500.04			1.000	0.150	1.15E+00	1.00E+00	1.50E-01
1.0-NaHCO3+0.30-NaCl	42.0055	8.7664	500.80			0.998	0.300	1.30E+00	9.98E-01	3.00E-01
Properties	Density, g/mL					Molarity (M, mol/L)				
Solution ID	Calculated	Measured	%Deviation###	M:m, L/kg	pH##	$NaHCO_3$	NaCl	ΣNa	ΣCO3	ΣCl
0.01-NaHCO3+0.15-NaCl	1.0071	NA	NA	1.0025	8.05	0.0100	0.150	1.60E-01	9.99E-03	1.50E-01
0.05-NaHCO3+0.15-NaCl	1.0092	NA	NA	1.0037	8.03	0.0498	0.149	1.99E-01	4.98E-02	1.49E-01
0.5-NaHCO3+0.15-NaCl	1.0328	NA	NA	1.0173	7.88	0.491	0.147	6.39E-01	4.91E-01	1.47E-01
1.0-NaHCO3+0.15-NaCl	1.0583	NA	NA	1.0323	7.78	0.969	0.145	1.11E+00	9.69E-01	1.45E-01
1.0-NaHCO3+0.30-NaCl	1.0634	NA	NA	1.0354	7.75	0.964	0.289	1.25E+00	9.64E-01	2.89E-01

Modeled pH using EQ3/6, Version 8.0a (Wolery and Jarek, 2003). The pH is negative base 10 logarithm of H^+ activity, i.e., pH = - log $\{H^+\}$, of background solution calculated using PACE and selected PIPs in the approved data0.fm1, not taking into consideration the dissolution of cerussite. EQ3/6, Version 8.0a is not included in the Software List of AP-192 Revision 0 (Jang et al., 2021), thus, the calculation of pH in this report is considered a deviation from the AP per NP 9-1 Revision 11 Section 2.1.2. (Nielsen, 2020).

%Deviation of density = (Measured - Calculated)/Calculated × 100%.

Figure II.2-2. XRD starting $PbCO_3(s)$ for Experiment 2 under TP 20-01 Revision 0.

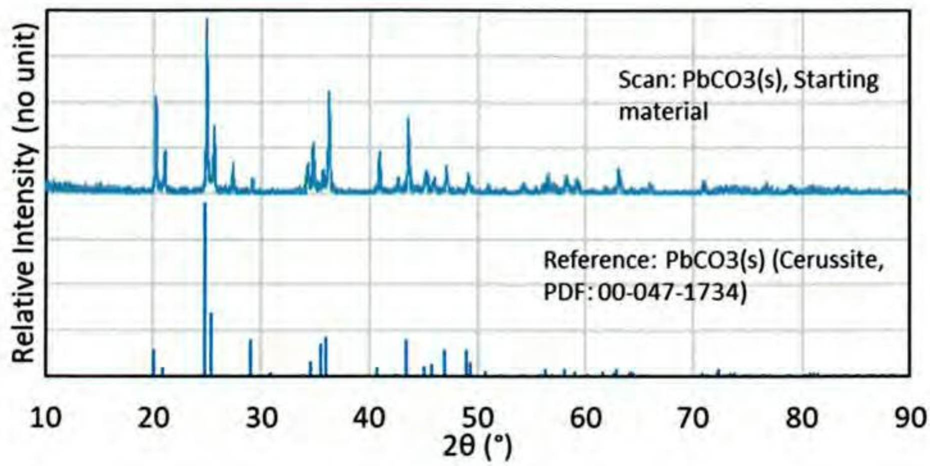

II.3. Sample Treatment and Measurements

Preparation of solution samples: Mass-to-volume dilutions were applied for filtered supernatants to prepare samples to measure the concentrations of components of interest under both TPs. When further dilutions were needed, volume-to-volume dilutions were applied. Some components in the background solutions used for Experiments 1 and 2 conducted under the protocols of TP 20-01 Revision 0 were measured from the prepared background solutions prior to adding $PbSO_4(s)$ or $PbCO_3(s)$ to confirm the preparation; samples injected to the instruments were diluted by volume-to-volume technique.

Preparation of solid samples: Under TP 08-02 Revision 0, solids were collected at the end of experiments. Under TP 20-01 Revision 0, solids were collected by filtering entire volume of replicates on the prescribed timed-investigation day.

Measurements: Concentrations of total dissolved cations, ΣPb and ΣNa, were measured using ICP-AES.[9] Concentrations of total dissolved anions, ΣSO4 and ΣCl, were measured using IC.[10] Concentration of total dissolved carbonate, ΣCO3, was measured by a Coulometer. Solids were characterized using XRD.[11] The pHr is recorded from the pH meter display after the pH reading stabilized when the pH electrode is in contact with the solution of interest. Most of solutions of

[9] Inductively Coupled Plasma - Atomic Emission Spectroscopy

[10] Ion Chromatography

[11] X-ray Diffraction

interest in this report have higher ionic strength, so the change of pHr reflects the change of pH, but pHr does not directly represent the pH.

III. RESULTS

The objective of this report is to directly compare data from Experiments 1 and 2 conducted under the experimental protocols of two test plans, TP 08-02 Revision 0 (Ismail et al., 2008) and TP 20-01 Revision 0 (Kirkes and Zhang, 2020). Even though experimental protocols are different, the recipes of Experiments 1 and 2 are nearly identical for data-to-data comparison (Table II.1-1 and Table II.1-2 for Experiment 1 under each TP; Table II.2-1 and Table II.2-2 for Experiment 2 under each TP). The measurement data are reported in units of Molarity (M, mol/L). The values for pHr[12] were compared without converting to pcH[13] and pmH.[14]

The measurement data obtained under TP 08-02 Revision 0 for Experiments 1 and 2 were imported from Kirkes et al. (2014). Exceptions are the measurement data of (i) pHr in Table III.1-1, Figure III.1-1, Table III.1-2, and Figure III.1-3A of Section III.1.1, and (ii) ΣPb in Table III.1-5, Figure III.1-4, Table III.1-6, and Figure III.1-6A of Section III.1.2. They were newly transcribed from the corresponding Scientific Notebooks (SNs).

Note that in Kirkes et al. (2014) the concentration values in the lead solubility sections are mistakenly reported in units of molality (m, mol/kg). The correct unit for the concentration values reported therein is Molarity (M, mol/L).

In Section III.1 below, results of Experiment 1 obtained under both TPs are compared in a component-by-component manner, including solid characterization results. The last Subsection III.1.7 provides a summary of the observation.

In Section III.2 below, results of Experiment 2 obtained under both TPs are compared in a component-by-component manner, including solid characterization results. The last Subsection III.2.7 provides a summary of the observation.

Black squares and red error bars in the time-dependent plots stand for the averages and twice the standard deviations (2SDs) of the time-dependent measurements. The time-dependent measurements

[12] pHr is the reading from the display of pH meters when the meter and pH electrode in use are calibrated with commercial pH buffers of low ionic strength.
[13] Negative base 10 logarithm of H^+ concentration in Molarity (M).
[14] Negative base 10 logarithm of H^+ concentration in molality (m).

are plotted individually to the right (blue dots and circles). For reactive/non-conservative components, the labels to the black squares list the following four statistics: average, 2SD,[15] %2SD,[16] and counts (i.e., number of measurements used to calculate the statistics) (Example: pHr in Figure III.1-1). For non-reactive/conservative components, the labels list the following five statistics: average, 2SD, %2SD, %Deviation, and the counts (i.e., number of measurements used to calculate the statistics) (Example: ΣNa in Figure III.1-10). %Deviation is calculated using the following equation:

$$\%Deviation = (Average - Loading)/Loading \times 100\% \quad (2)$$

Measurements contained in this report are traceable to the Scientific Notebooks through the associated Excel file, "VOL_CRC_GEOC-21-03_Mgmt.xlsx". The Excel file is archived at "/cvs/CVSLIB/WIPP_EXTERNAL/ap192".

III.1. Experiment 1: $PbSO_4(s) - Na_2SO_4 - NaCl - H_2O$

Recipes for this Experiment 1 under each TP are summarized in Table II.1-1 and Table II.1-2, respectively.

III.1.1. pHr

Table III.1-1 provides the pHr values recorded as a function of aging time from Experiment 1 conducted under TP 08-02 Revision 0. Plots of the pHr vs. aging time are in Figure III.1-1. The pHr values showed scatter. For PbSO4-0.01-(1,2), the scatter is confined around the averages within the maximum 2SD of 0.20 pH unit (%2SD = 7%), which means that the precision of the measurements was better than 7%. Statistically, the pHr for the first two loadings of Na_2SO_4 are experimentally resolved (i.e., statistically different average values), and the pHr values for the remainder are identical (Figure III.1-1, Table III.1-2, and Figure III.1-3A).

Listed in Table III.1-3 are the pHr values recorded as a function of aging time from Experiment 1 conducted under the protocols of TP 20-01 Revision 0. Plots of the pHr vs. aging time are displayed in Figure III.1-2. The pHr values showed scatter. The scatter is confined around the averages within the maximum 2SD of 0.14 pH unit (%2SD = 4%), which means that the precision of the measurements was better than 4%. Statistically, the pHr for the first two loadings of Na_2SO_4 are experimentally resolved (i.e., the average values are apart from each other with the difference exceeding the length of error bars), and the pHr values for the remainders are identical (Figure

[15] 2SD: Twice the Standard Deviation

[16] %2SD: Percentile Twice the Standard Deviation: 2SD/Average × 100 %

III.1-2, Table III.1-4, and Figure III.1-3B). The results of pHr measurements in Experiments 1 under both TPs are statistically identical (compare A and B of Figure III.1-3).

Table III.1-1. Time-dependent measurements of pHr in Experiment 1 under TP 08-02 Revision 0.

Aging time (Days)	PbSO4-0.01-1	PbSO4-0.01-2	PbSO4-0.1-1	PbSO4-0.1-2	PbSO4-0.5-1	PbSO4-0.5-2	PbSO4-1.0-1	PbSO4-1.0-2	PbSO4-1.5-1	PbSO4-1.5-2	PbSO4-1.8-1	PbSO4-1.8-2
360	2.78	2.82	3.11	3.12	3.37	3.36	3.49	3.47	3.57	3.55	3.52	3.53
743	2.45	2.54	3.09	3.19	3.52	3.51	3.49	3.40	3.36	3.35	3.49	3.31
1010	2.73	2.70	3.09	3.05	3.44	3.41	3.52	3.51	3.6	3.57	3.52	3.51
1059	2.75	2.75	3.12	3.05	3.41	3.42	3.53	3.51	3.58	3.63	3.58	3.55
1107	2.70	2.71	3.04	3.00	3.45	3.43	3.33	3.34	3.53	3.49	3.47	3.48
1158	2.75	2.82	3.28	3.14	3.42	3.41	3.56	3.45	3.62	3.62	3.68	3.55
1305	2.76	2.80	3.15	3.12	3.45	3.46	3.56	3.54	3.63	3.55	3.57	3.50
1368	2.75	2.77	3.14	3.09	3.44	3.43	3.55	3.53	3.61	3.58	3.59	3.60

Figure III.1-1. Plot of the time-dependent measurements of pHr from Experiment 1 under TP 08-02 Revision 0 in Table III.1-1. Black squares and red error bars located on 250 days are averages and twice the standard deviations of all the measurements displayed to the right at their aging time (blue dots and circles, which represent data from duplicate reactors).

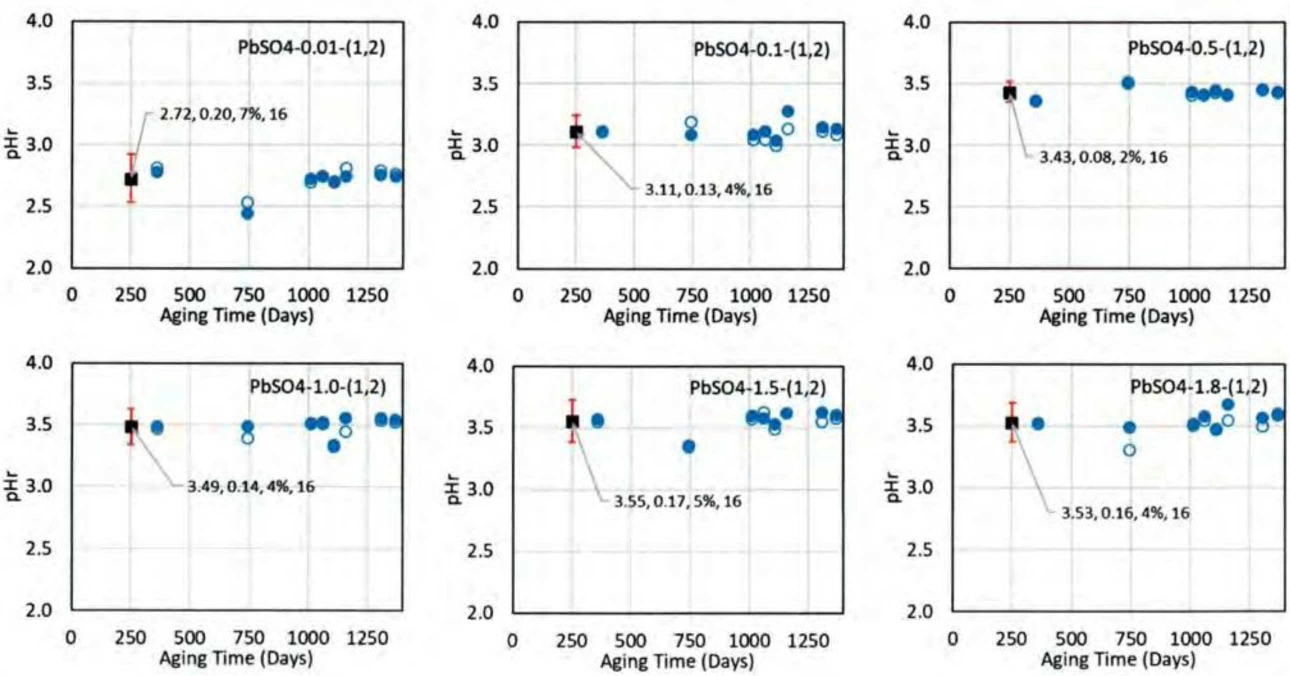

Table III.1-2. Statistics of measurements of pHr from Experiment 1 under TP 08-02 Revision 0 in Table III.1-1.

Reactor ID	Average	2SD	%2SD	Counts
PbSO4-0.01-(1,2)	2.72	0.20	7%	16
PbSO4-0.1-(1,2)	3.11	0.13	4%	16
PbSO4-0.5-(1,2)	3.43	0.08	2%	16
PbSO4-1.0-(1,2)	3.49	0.14	4%	16
PbSO4-1.5-(1,2)	3.55	0.17	5%	16
PbSO4-1.8-(1,2)	3.53	0.16	4%	16

Table III.1-3. Time-dependent measurements of pHr from Experiment 1 under TP 20-01 Revision 0.

Aging time (Days)	43	111
Reactor ID (n =)	1	2
PbSO4-0.01-SO4-1-n	2.91	2.92
PbSO4-0.01-SO4-2-n	2.88	2.97
PbSO4-0.1-SO4-1-n	3.27	3.27
PbSO4-0.1-SO4-2-n	3.19	3.27
PbSO4-0.5-SO4-1-n	3.55	3.62
PbSO4-0.5-SO4-2-n	3.57	3.63
PbSO4-1.0-SO4-1-n	3.62	*3.75*
PbSO4-1.0-SO4-2-n	3.66	3.73
PbSO4-1.5-SO4-1-n	3.68	3.69
PbSO4-1.5-SO4-2-n	3.70	3.74
PbSO4-1.8-SO4-1-n	3.73	3.82
PbSO4-1.8-SO4-2-n	3.69	3.83

Red italic: pH electrode broken while measurement. The value follows the trend but was not included in calculating the statistics. The value is displayed as the orange dot in Figure III.1-2.

Figure III.1-2. Plot of the time-dependent measurements of pHr from Experiment 1 under TP 20-01 Revision 0 in Table III.1-3. Black squares and red error bars are averages and twice the standard deviations of all the measurements displayed to the right at their aging time (blue dots and circles). Orange dot in the lower left panel is the value in red italic in Table III.1-3.

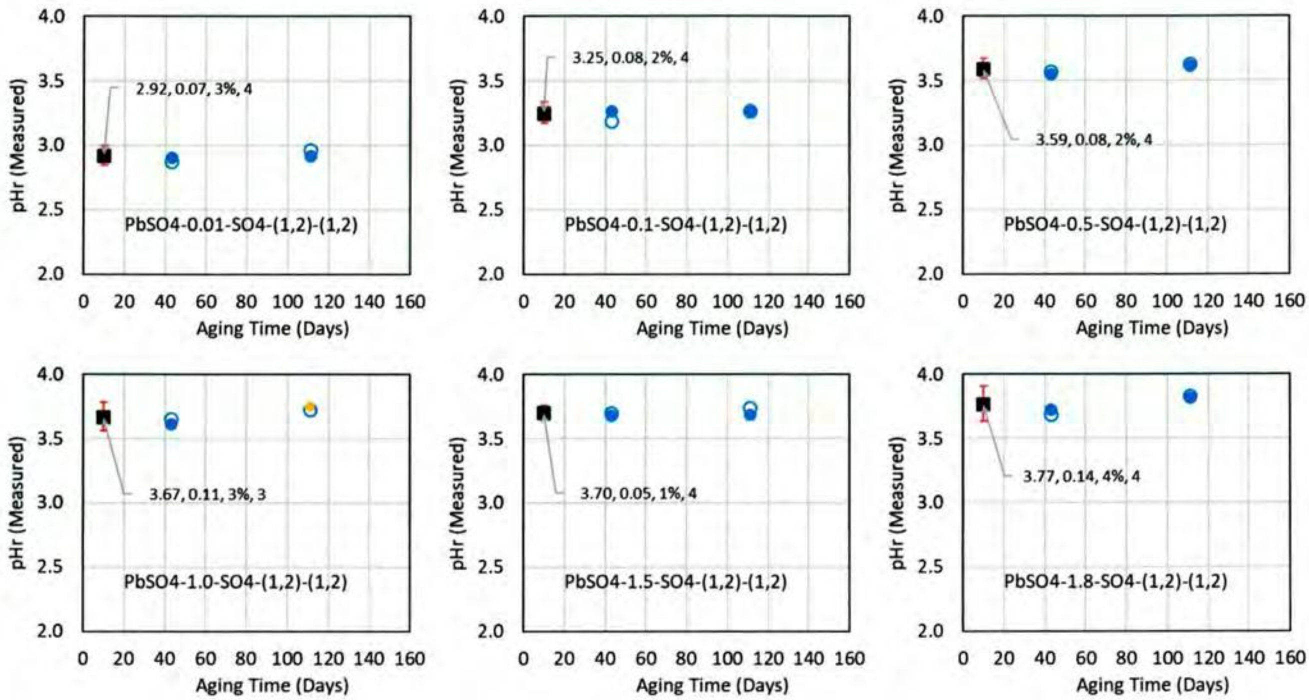

Table III.1-4. Statistics of measurements of pHr under TP 20-01 Revision 0 in Table III.1-3.

Reactor ID	Average	2SD	%2SD	Counts
PbSO4-0.01-SO4-(1,2)	2.92	0.07	3%	4
PbSO4-0.1-SO4-(1,2)	3.25	0.08	2%	4
PbSO4-0.5-SO4-(1,2)	3.59	0.08	2%	4
PbSO4-1.0-SO4-(1,2)	3.67	0.11	3%	3
PbSO4-1.5-SO4-(1,2)	3.70	0.05	1%	4
PbSO4-1.8-SO4-(1,2)	3.77	0.14	4%	4

Figure III.1-3. Plot of the statistics of pHr in: A. Table III.1-2 (TP 08-02 Revision 0), and B. Table III.1-4 (TP 20-01 Revision 0).

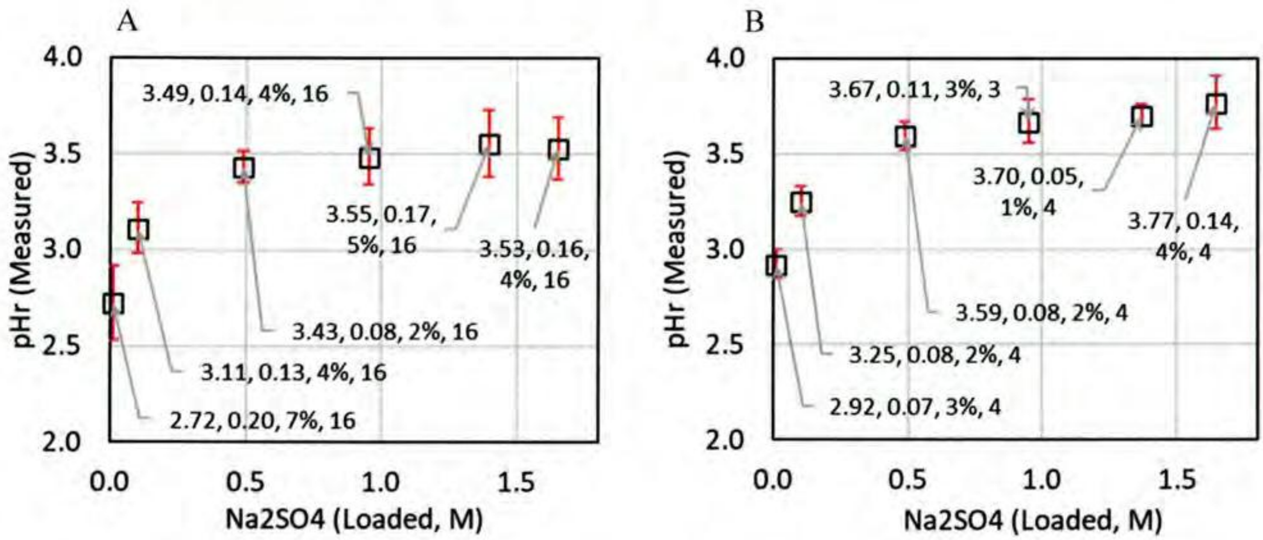

III.1.2. ΣPb

Listed in Table III.1-5 are the measured ΣPb values as a function of aging time from Experiment 1 conducted under TP 08-02 Revision 0. Plots of the measurements are in Figure III.1-4. Statistics are tabulated and displayed in Table III.1-6 and Figure III.1-6A.

From Experiment 1 conducted under TP 08-02 Revision 0, the ΣPb showed wider scatter at the beginning of the experiments and became stable at the later stage of the experiment. The scatter happened for the first measurements, including re-runs, made on the filtrates sampled on 360 days of aging (Figure III.1-4) indicating potential reproducibility issues initially with the method.

Open squares and dashed red error bars in Figure III.1-4 stand for the averages and 2SDs calculated for all valid measurements in Table III.1-5 using the normal distribution, including the data in red italics. The statistics of the open squares and dashed red error bars are listed in the upper half of Table III.1-6. Data points in green ovals are outliers because they are outside the range defined by average±2SD as shown in Figure III.1-4. From the statistical points (represented by the open squares and dashed red error bars), those data points are outside the 95% confidence intervals. The outliers were excluded from the overall dataset and averages and standard deviations were re-calculated (solid squares and solid red error bars in Figure III.1-4; new statistics are listed in the lower half of Table III.1-6). The new statistics are illustrated in Figure III.1-6A.[17]

Summarized in Table III.1-7 are the measured ΣPb values as a function of aging time from Experiment 1 conducted under the protocols of TP 20-01 Revision 0. Plots of the measurements are presented in Figure III.1-5. The ΣPb values are stable. Precision of the measurements was better than 9%. Statistics are summarized and presented in Table III.1-8 and Figure III.1-6B.

Figure III.1-6 indicates that the ΣPb measurements were not fully resolved (i.e., showed no statistical difference) as a function of the experimental conditions, i.e., loading of Na_2SO_4, under TP 08-02 Revision 0, and they are resolved under TP 20-01 Revision 0.[18] While the data points generated under TP 08-02 overlap within the error, they display a trend similar to the one observed for the data generated under TP 20-01.

The results of ΣPb measurements in Experiments 1 under both TPs are statistically identical (compare A and B of Figure III.1-6).

Table III.1-5. Time-dependent measurements of ΣPb (M, mol/L) from Experiment 1 under TP 08-02 Revision 0.

Aging time (Days)	PbSO4-0.01-1	PbSO4-0.01-2	Aging time (Days)	PbSO4-0.1-1	PbSO4-0.1-2	Aging time (Days)	PbSO4-0.5-1	PbSO4-0.5-2
360	*4.99E-05*	8.19E-05	360	*7.00E-05*	4.60E-05	360	*1.11E-05*	2.34E-05
360	6.33E-05	8.19E-05	360	*6.87E-05*	4.43E-05	360	*8.64E-06*	*1.12E-05*
743	6.08E-05	6.15E-05	743	2.21E-05	2.27E-05	360	2.85E-05	4.63E-05
743	6.28E-05[#]	6.31E-05[#]	743	2.46E-05[#]	2.46E-05[#]	743	3.30E-05	3.04E-05
1010	6.61E-05	6.41E-05	1010	2.27E-05	2.35E-05	743	3.36E-05[#]	3.45E-05[#]
1059	7.14E-05	7.24E-05	1059	2.67E-05	2.03E-05	1010	3.30E-05	3.30E-05
1107	6.36E-05	6.95E-05	1107	2.55E-05	2.55E-05	1059	3.23E-05	4.03E-05
1158	6.73E-05	6.75E-05	1158	3.23E-05	3.09E-05	1107	3.45E-05	3.16E-05
1305	6.85E-05	7.24E-05	1158	2.42E-05	2.46E-05	1158	3.70E-05	3.88E-05
1368	7.70E-05	7.11E-05	1305	2.95E-05	2.76E-05	1158	3.53E-05	3.50E-05
			1368	2.27E-05	2.48E-05	1305	3.28E-05	3.35E-05
						1368	3.17E-05	3.35E-05
Aging time (Days)	PbSO4-1.0-1	PbSO4-1.0-2	Aging time (Days)	PbSO4-1.5-1	PbSO4-1.5-2	Aging time (Days)	PbSO4-1.8-1	PbSO4-1.8-2
360	4.43E-05	2.07E-05	360	2.97E-05	3.02E-05	360	*1.49E-05*	*1.55E-05*
360	1.83E-05	*1.11E-05*	360	*1.47E-05*	*1.68E-05*	360	6.65E-05	6.65E-05
360	*8.12E-05*	5.12E-05	360	6.68E-05	6.71E-05	743	8.89E-05	7.45E-05
743	4.62E-05	4.79E-05	743	6.73E-05	6.92E-05	743	6.94E-05	NA
743	4.42E-05	4.47E-05	743	6.15E-05	6.24E-05	743	7.86E-05[#]	8.15E-05[#]

[17] This process is called statistical data reduction in this report. This process can be repeated until all data are encompassed within the 2SD but practiced once in this report.

[18] Goal of performing screening experiment at reduced scale is achieved.

743	5.30E-05[#]	5.29E-05[#]	743	7.21E-05[#]	7.13E-05[#]	1010	6.67E-05	6.00E-05
1010	5.19E-05	5.26E-05	1010	7.06E-05	6.99E-05	1059	7.68E-05	7.66E-05
1059	5.73E-05	4.95E-05	1059	7.33E-05	7.40E-05	1059	7.51E-05[##]	7.88E-05[##]
1107	5.28E-05	5.18E-05	1107	6.83E-05	6.97E-05	1107	8.24E-05	8.43E-05
1158	5.84E-05	5.31E-05	1158	7.65E-05	7.28E-05	1158	7.94E-05	8.46E-05
1305	5.13E-05	5.47E-05	1305	6.48E-05	6.88E-05	1305	8.55E-05	8.53E-05
1368	5.08E-05	5.36E-05	1368	6.92E-05	6.72E-05	1368	7.86E-05	7.82E-05

Italicized values in red are considered outliers because they fall outside the error range. Although they were not flagged by the lab (i.e., valid under SNL WIPP QA Program), they were not included in the further data processing tabulated in the lower half of Table III.1-6. See argument in Figure III.1-4. They are marked with green ovals/circles therein.

[#] High blank data: had to be discarded because the lower detection limit has never been defined, so never knew if such shift is larger or smaller than the uncertainty associated with the general laboratory operation. They are consistent with other valid measurements within the statistics, so could be useful to strengthen the statistics.

[##] Flagged by lab: had to be discarded a priori only because the readings did not fall within the calibration range, so never knew if such deviation is larger or smaller than the uncertainty associated with the general laboratory operation. They are consistent with other valid measurements within the statistics.

Figure III.1-4. Plot of the time-dependent measurements of ΣPb (M, mol/L) from Experiment 1 under TP 08-02 Revision in Table III.1-5. Open squares and red dashed error bars stand for the average and 2SD of all data in Table III.1-5, except those with # and ## therein. Solid squares and red solid error bars stand for the average and 2SD of data, excluding those in green ovals or circles.

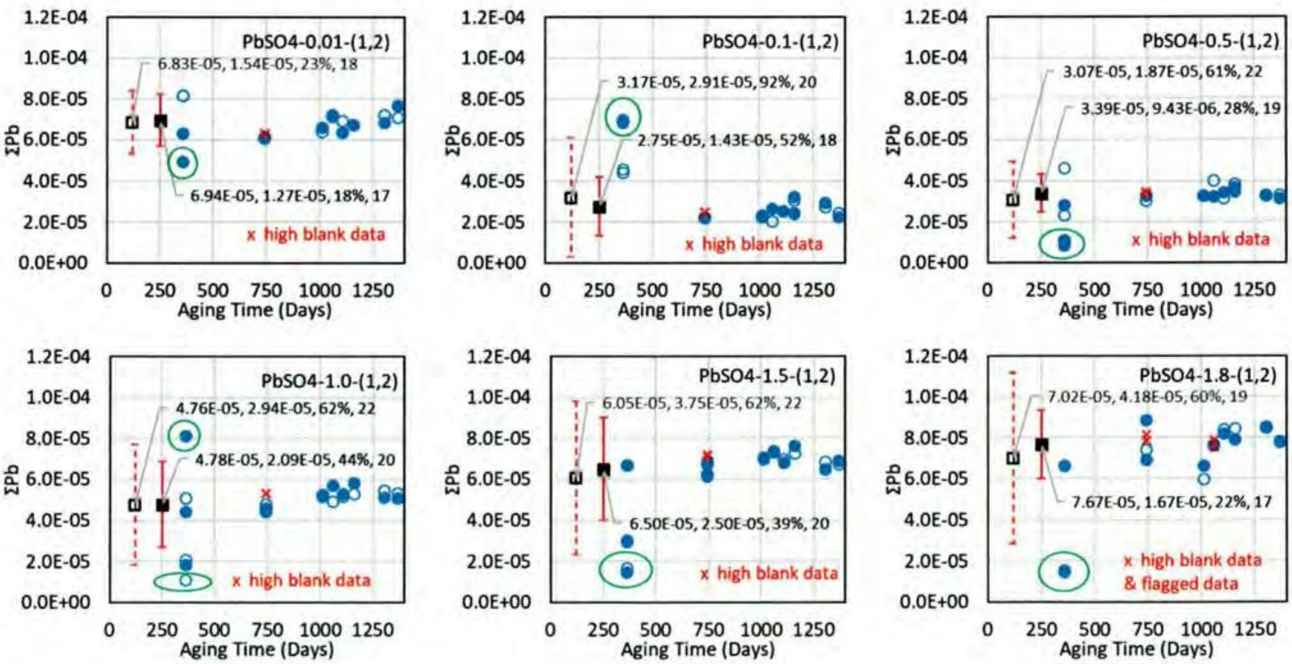

Table III.1-6. Statistics of measurements of ΣPb (M, mol/L) from Experiment 1 under TP 08-02 Revision 0 in Table III.1-5.

All Valid Data Statistics				
Reactor ID	Average	2SD	%2SD	Counts
PbSO4-0.01-(1,2)	6.83E-05	1.54E-05	23%	18
PbSO4-0.1-(1,2)	3.17E-05	2.91E-05	92%	20
PbSO4-0.5-(1,2)	3.07E-05	1.87E-05	61%	22

PbSO4-1.0-(1,2)	4.76E-05	2.94E-05	62%	22
PbSO4-1.5-(1,2)	6.05E-05	3.75E-05	62%	22
PbSO4-1.8-(1,2)	7.02E-05	4.18E-05	60%	19
Once-Reduced Data Statistics				
PbSO4-0.01-(1,2)	6.94E-05	1.27E-05	18%	17
PbSO4-0.1-(1,2)	2.75E-05	1.43E-05	52%	18
PbSO4-0.5-(1,2)	3.39E-05	9.43E-06	28%	19
PbSO4-1.0-(1,2)	4.78E-05	2.09E-05	44%	20
PbSO4-1.5-(1,2)	6.50E-05	2.50E-05	39%	20
PbSO4-1.8-(1,2)	7.67E-05	1.67E-05	22%	17

Table III.1-7. Time-dependent measurements of ΣPb (M, mol/L) from Experiment 1 under TP 20-01 Revision 0.

Aging time (Days)	43	111
Reactor ID (n =)	1	2
PbSO4-0.01-SO4-1-n	6.55E-05	7.07E-05
PbSO4-0.01-SO4-2-n	6.86E-05	7.05E-05
PbSO4-0.1-SO4-1-n	2.66E-05	2.45E-05
PbSO4-0.1-SO4-2-n	2.62E-05	2.43E-05
PbSO4-0.5-SO4-1-n	3.16E-05	3.18E-05
PbSO4-0.5-SO4-2-n	3.38E-05	3.39E-05
PbSO4-1.0-SO4-1-n	5.08E-05	5.45E-05
PbSO4-1.0-SO4-2-n	4.96E-05	5.21E-05
PbSO4-1.5-SO4-1-n	6.64E-05	6.83E-05
PbSO4-1.5-SO4-2-n	6.87E-05	6.82E-05
PbSO4-1.8-SO4-1-n	7.93E-05	7.83E-05
PbSO4-1.8-SO4-2-n	7.66E-05	8.03E-05

Figure III.1-5. Plot of the time-dependent measurements of ΣPb (M, mol/L) from Experiment 1 under TP 20-01 Revision in Table III.1-7. Black squares and red error bars located on 10 days are averages and twice the standard deviations of the measurements to the right (blue dots and circles).

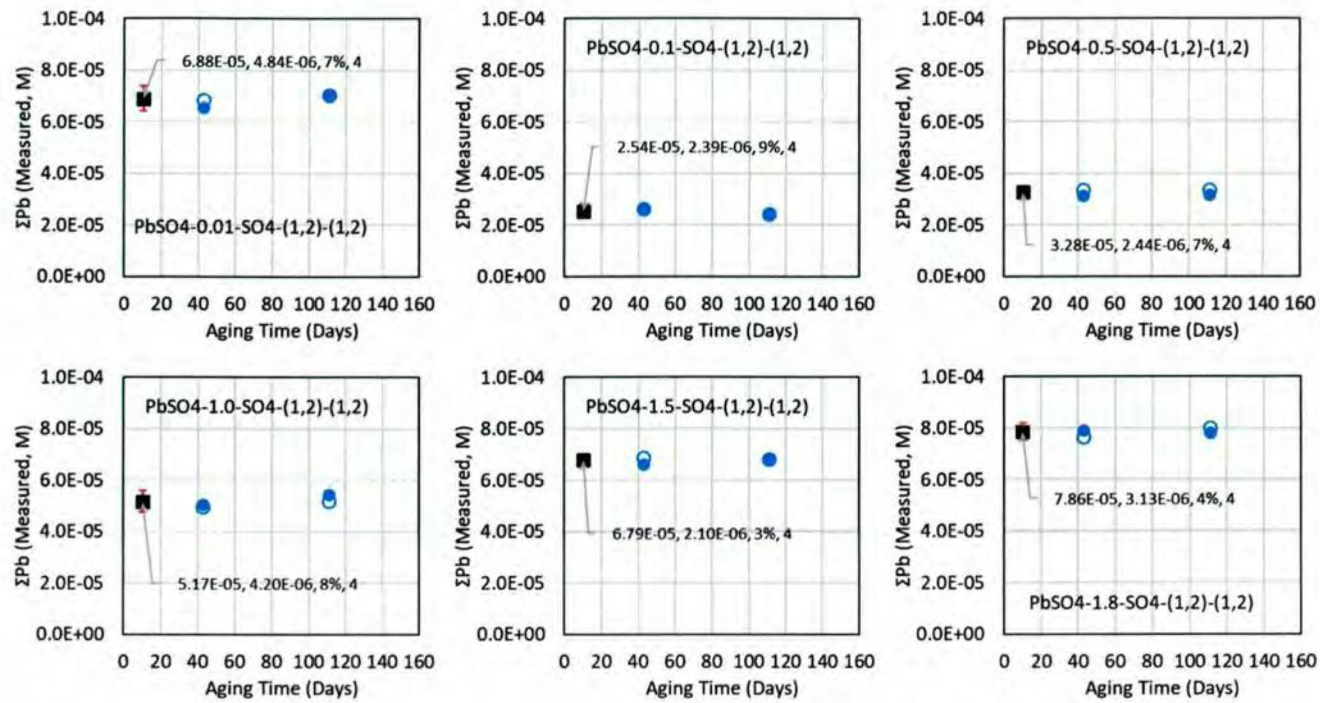

Table III.1-8. Statistics of measurements of ΣPb (M, mol/L) under TP 20-01 Revision 0 in Table III.1-7.

Reactor ID	Average	2SD	%2SD	Counts
PbSO4-0.01-SO4-(1,2)	6.88E-05	4.84E-06	7%	4
PbSO4-0.1-SO4-(1,2)	2.54E-05	2.39E-06	9%	4
PbSO4-0.5-SO4-(1,2)	3.28E-05	2.44E-06	7%	4
PbSO4-1.0-SO4-(1,2)	5.17E-05	4.20E-06	8%	4
PbSO4-1.5-SO4-(1,2)	6.79E-05	2.10E-06	3%	4
PbSO4-1.8-SO4-(1,2)	7.86E-05	3.13E-06	4%	4

Figure III.1-6. Plot of the statistics of ΣPb (M, mol/L) in Table III.1-6 (A) and Table III.1-8 (B).

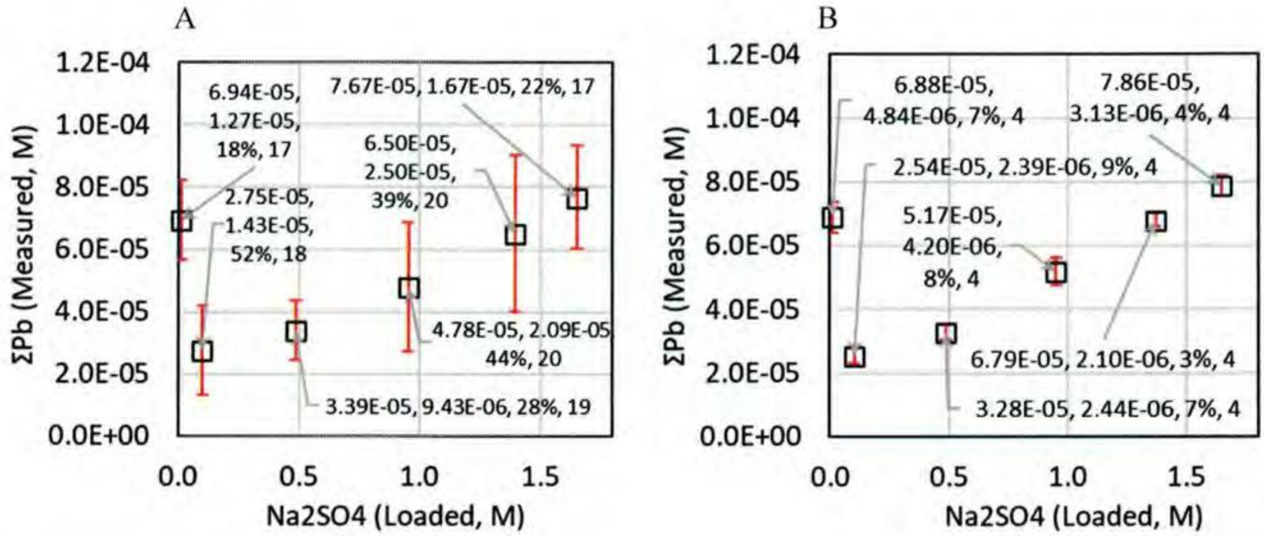

III.1.3. ΣSO4

In Experiment 1, known concentrations of sulfate were loaded by adding the salt, Na_2SO_4. Sulfate is a component of the solid $PbSO_4(s)$ (anglesite). Therefore, the dissolution of $PbSO_4(s)$ increases the ΣSO4 in addition to the sulfate loaded by Na_2SO_4.

$$\Sigma SO4 = [Na_2SO_4]_{Loaded} + [PbSO_4(s)]_{Dissolved}$$

$$= [Na_2SO_4]_{Loaded} + \Sigma Pb \quad (3)$$

where $[PbSO_4(s)]_{Dissolved} = \Sigma Pb$ by mass balance because $PbSO_4(s)$ is the sole source of dissolved lead. Sulfate is loaded by the salt, Na_2SO_4, and the lowest loading is 0.01 M (Table II.1-1). ΣPb is less than 10^{-4} M (Figure III.1-4 and Figure III.1-5). Thus, when assuming the measurements of ΣPb are accurate, the maximum %Deviation of the measured ΣSO4 from the loaded ΣSO4 that can be expected from the dissolution of $PbSO_4(s)$ is less than 1%. From Equation (3), $[Na_2SO_4]_{Loaded} >> [PbSO_4(s)]_{Dissolved} = \Sigma Pb$, thus, $\Sigma SO4 \equiv [Na_2SO_4]_{Loaded}$ within 1%. Therefore, although sulfate participates in the dissolution reaction, it can be considered a conservative component, and the dissolution does not affect the physical properties of the background solutions listed in Table II.1-1 and Table II.1-2.

Table III.1-9 provides the measured ΣSO4 values as a function of aging time from Experiment 1 conducted under TP 08-02 Revision 0. Plots of the time-dependent measurements are presented in Figure III.1-7. The ΣSO4 was stable through the aging time. Samples injected into the analytical instrument were prepared by mass-to-volume dilution techniques. Statistics are tabulated and displayed in Table III.1-10 and Figure III.1-9A.

Table III.1-11 lists the measured ΣSO4 as a function of aging time from Experiment 1 conducted under the protocols of TP 20-01 Revision 0. Plots of the time-dependent measurements are shown in Figure III.1-8. Only one timed measurement was available as of 6/22/2021. Statistics are tabulated and displayed in Table III.1-12 and Figure III.1-9B.

In performing Experiment 1 under the protocols of TP 20-01 Revision 0, ΣSO4 was measured from the background solutions prior to adding the solid $PbSO_4$(s). Additional measurements of ΣSO4 were conducted after commencing the dissolution. The samples injected to the instrument for the measurements of ΣSO4 in the background solution prior to the addition of $PbSO_4$(s) were prepared by volume-to-volume dilution. The samples for the measurements of ΣSO4 in the filtered supernatants sampled after commencing the dissolution were prepared by mass-to-volume dilution. All the measurements of ΣSO4 are summarized in Table III.1-11 and plotted in Figure III.1-8.

In theory, the volume-to-volume dilution could result in underestimation of analyte concentration. Volume-to-volume dilution means that a known volume of solution is mixed with diluent until the total volume reaches a known value. In our practice of the volume-to-volume dilution, the volume of a solution to be diluted is determined in the pipet tip by the vacuum held in the barrel of a fixed-volume pipet. The calibration check of the fixed-volume pipet is performed using DI water prior to use. When the calibration-checked pipet is used to transfer the same desired volume of a solution of higher density than DI water, the actual volume of the high-density solution in the pipet tip would be smaller than the desired volume because the vacuum held in the barrel of the fixed-volume pipet is calibrated to lift the mass of DI water occupying the desired volume. Same mass of solution of higher density occupies less volume than desired. In other words, the extent of the underestimation becomes larger with increasing solution density. However, from Figure III.1-8, noticeable underestimation of ΣSO4 by volume-to-volume dilution happened 2 out of 6 times (compare the orange $\times$ and two black circles on each vertical axis) without showing density-dependency of the underestimation (i.e., the measured concentration was lower than the loaded concentration irrespective of solution density). Meanwhile, underestimation by mass-to-volume dilution (blue circles and dots) happened 4 out of 6 times. When both techniques showed underestimation (third and sixth panels of Figure III.1-8), the extent of underestimation by volume-to-volume dilution is smaller or equal to the mass-to-volume dilution. Precision was higher for the data obtained by volume-to-volume dilution (compare the scatter of two black circles and blue dot/circles in Figure III.1-8). The extent of underestimation is comparable for the two dilution techniques at the highest loading of ΣNa (sixth panel in Figure III.1-8), where the most visual difference would have been observed if the two dilution techniques are distinct from each other under SNL WIPP Geochemistry Program's general laboratory practice. Two dilution technique are indistinguishable from each other under the overall laboratory operation at SNL WIPP Geochemistry Program.[19] Thus, statistics in Table III.1-12 were calculated using all measurements in Table III.1-11.

From the statistics illustrated in Figure III.1-9A, it can be stated with 95% confidence that the loaded ΣSO4 was reproduced except for the one at the lowest loading of ΣSO4 under TP 08-02 Revision 0. From the statistics presented in Figure III.1-9B, it can be stated with 95% confidence that the loaded ΣSO4 was reproduced except the one at the highest loading of ΣSO4 under TP 20-01 Revision 0.

The results of ΣSO4 measurements in Experiments 1 under both TPs are statistically identical (compare the black squares at a condition at a time in A and B of Figure III.1-9).

Table III.1-9. Time-dependent measurements of ΣSO4 (M, mol/L) under TP 08-02 Revision 0.

	Aging time (Days)							
Reactor ID	360	743	1010	1059	1107	1158	1305	1368
PbSO4-0.01-1	NA	1.18E-02	1.17E-02	1.11E-02	1.11E-02	1.11E-02	1.15E-02	1.15E-02
PbSO4-0.01-2	NA	1.14E-02	1.21E-02	1.10E-02	1.12E-02	1.11E-02	1.15E-02	1.15E-02
PbSO4-0.1-1	NA	1.13E-01	1.13E-01	9.94E-02	9.96E-02	1.01E-01	1.04E-01	1.04E-01
PbSO4-0.1-2	NA	1.81E-01	1.10E-01	9.96E-02	1.02E-01	1.02E-01	1.05E-01	1.05E-01
PbSO4-0.5-1	5.18E-01	6.18E-01	5.60E-01	5.00E-01	5.07E-01	4.94E-01	5.05E-01	5.08E-01
PbSO4-0.5-2	5.27E-01	4.90E-01	5.38E-01	5.02E-01	4.87E-01	4.94E-01	5.01E-01	5.09E-01
PbSO4-1.0-1	1.01E+00	9.77E-01	1.01E+00	9.75E-01	9.62E-01	9.77E-01	1.01E+00	1.01E+00
PbSO4-1.0-2	1.04E+00	9.84E-01	1.03E+00	9.77E-01	9.88E-01	9.80E-01	9.89E-01	1.01E+00
PbSO4-1.5-1	1.46E+00	1.47E+00	1.48E+00	1.40E+00	1.44E+00	1.47E+00	1.32E+00	1.47E+00
PbSO4-1.5-2	1.39E+00	1.47E+00	1.55E+00	1.41E+00	1.44E+00	1.46E+00	1.31E+00	1.43E+00
PbSO4-1.8-1	1.36E+00	1.07E+00	1.48E+00	1.22E+00	1.38E+00	1.55E+00	1.31E+00	1.40E+00
PbSO4-1.8-2	1.40E+00	1.12E+00	1.31E+00	1.30E+00	1.39E+00	1.55E+00	1.33E+00	1.43E+00

Figure III.1-7. Plot of the time-dependent measurements of ΣSO4 (M, mol/L) under TP 08-02 Revision 0 in Table III.1-9 (M, mol/L). Orange ×s on the vertical axes are the loading of ΣSO4 by the recipe. Black squares and red error bars located on

[19] Mass-to-volume dilution is more labor-intensive, and subject to higher chance of introducing error when practiced inside gloveboxes due to limited dexterity, continuous vibration, and airflow over the balance.

250 days are averages and twice the standard deviations of all the measurements displayed to the right at their aging time (blue dots and circles, which represent data from duplicate reactors).

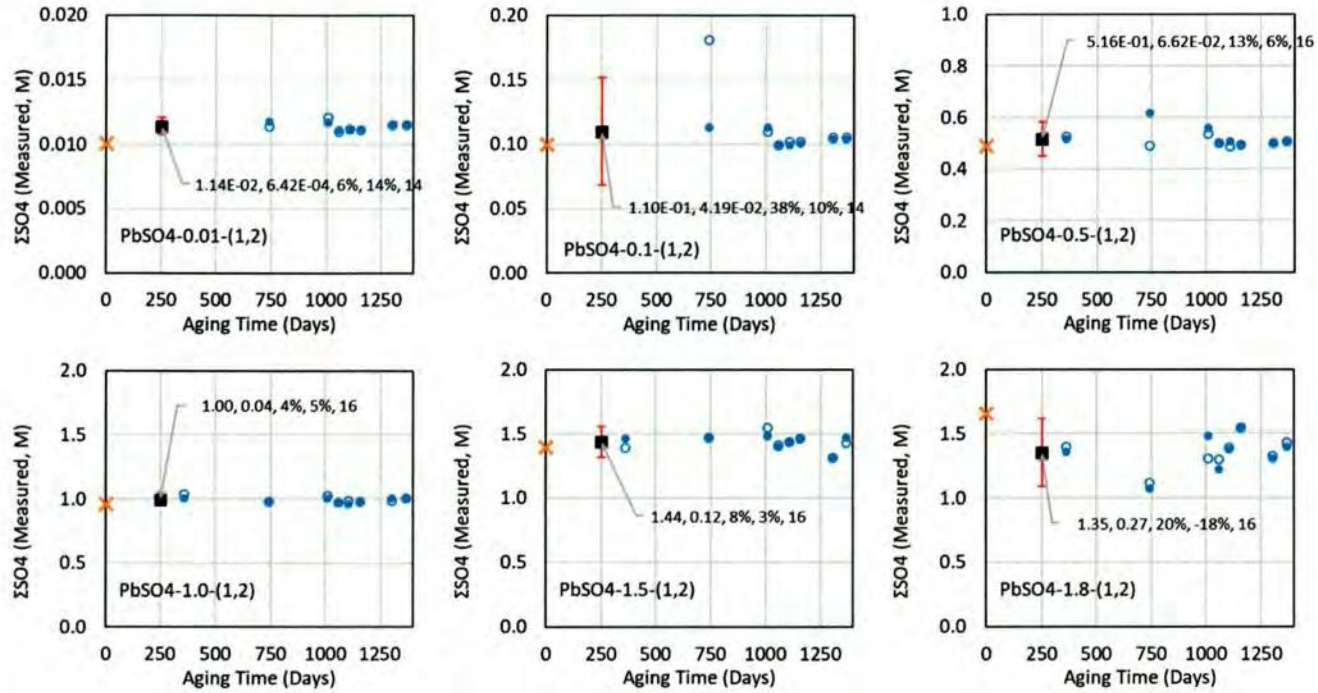

Table III.1-10. Statistics of measurements of ΣSO4 (M, mol/L) under TP 08-02 Revision 0 in Table III.1-9.

Reactor ID	Average	2SD	%2SD	%Deviation	Counts
PbSO4-0.01-(1,2)	1.14E-02	6.42E-04	6%	14%	14
PbSO4-0.1-(1,2)	1.10E-01	4.19E-02	38%	10%	14
PbSO4-0.5-(1,2)	5.16E-01	6.62E-02	13%	6%	16
PbSO4-1.0-(1,2)	9.96E-01	4.40E-02	4%	5%	16
PbSO4-1.5-(1,2)	1.44E+00	1.20E-01	8%	3%	16
PbSO4-1.8-(1,2)	1.35E+00	2.66E-01	20%	-18%	16

Table III.1-11. Time-dependent measurements of ΣSO4 (M, mol/L) under TP 20-01 Revision 0.

Aging time (Days)	0	43
Reactor ID (n =)	Before adding PbSO4(s)[#]	1
PbSO4-0.01-SO4-1-n	9.64E-03	2.07E-02
PbSO4-0.01-SO4-2-n	9.72E-03	1.91E-02
PbSO4-0.1-SO4-1-n	9.86E-02	7.86E-02
PbSO4-0.1-SO4-2-n	9.82E-02	8.08E-02
PbSO4-0.5-SO4-1-n	4.25E-01	3.71E-01
PbSO4-0.5-SO4-2-n	4.34E-01	3.78E-01

PbSO4-1.0-SO4-1-n	9.52E-01	8.07E-01
PbSO4-1.0-SO4-2-n	9.46E-01	7.51E-01
PbSO4-1.5-SO4-1-n	1.37E+00	1.17E+00
PbSO4-1.5-SO4-2-n	1.38E+00	1.16E+00
PbSO4-1.8-SO4-1-n	1.39E+00	1.39E+00
PbSO4-1.8-SO4-2-n	1.38E+00	1.35E+00

#Duplicate measurements of the six solutions described in Table II.1-2 prior to adding to the solid-containing vials. Samples injected to the instrument were prepared by volume-to-volume dilution.

Figure III.1-8. Plot of the time-dependent measurements of ΣSO4 under TP 20-01 Revision in Table III.1-11 (M, mol/L). Orange ×s on the vertical axes are the initial loadings. Black circles are the measurements of ΣSO4 from the background solutions prior to commencing the dissolution, where samples injected to the instrument (IC) were prepared by volume-to-volume dilution. Black squares and red error bars located on 20 days are averages and twice the standard deviations of all the measurements displayed (black circles, blue dots and circles. Blue dots and circles represent data from duplicate reactors).

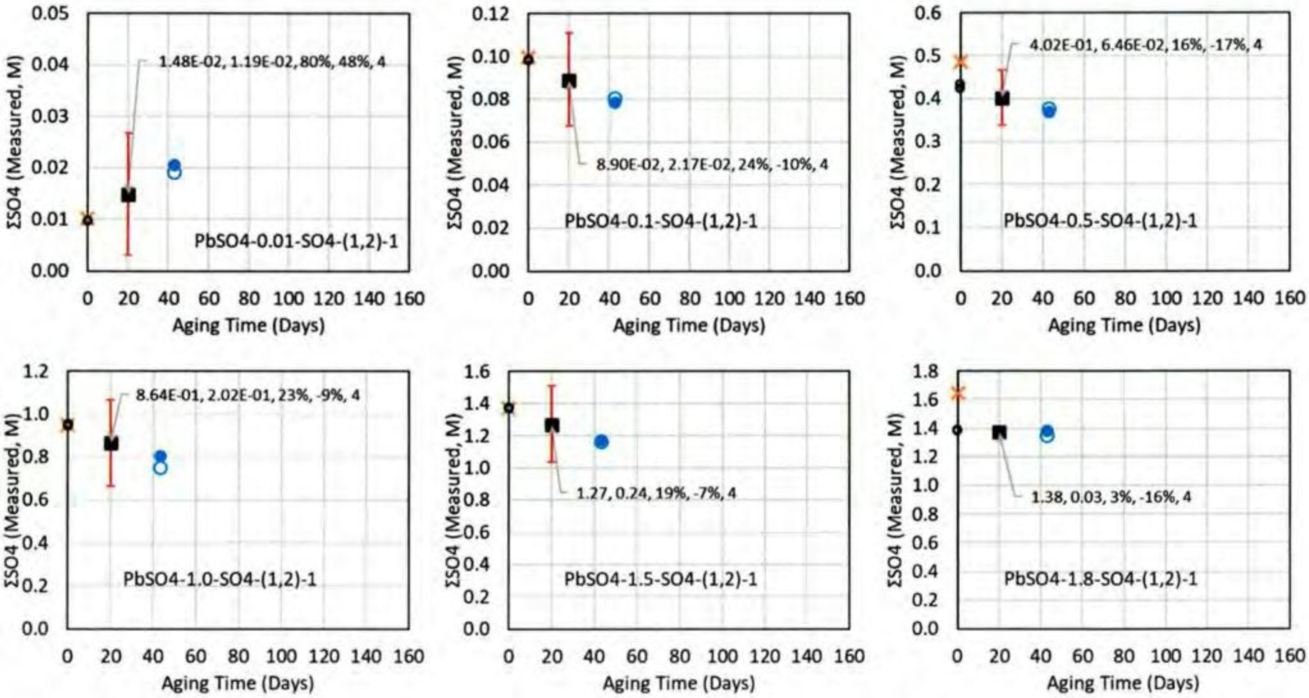

Table III.1-12. Statistics of measurements of ΣSO4 under TP 20-01 Revision 0 in Table III.1-11 (M, mol/L).

Reactor ID	Average	2SD	%2SD	%Deviation	Counts
PbSO4-0.01-SO4-(1,2)	1.48E-02	1.19E-02	80%	48%	4
PbSO4-0.1-SO4-(1,2)	8.90E-02	2.17E-02	24%	-10%	4
PbSO4-0.5-SO4-(1,2)	4.02E-01	6.46E-02	16%	-17%	4
PbSO4-1.0-SO4-(1,2)	8.64E-01	2.02E-01	23%	-9%	4

PbSO4-1.5-SO4-(1,2)	1.27	0.24	19%	-7%	4
PbSO4-1.8-SO4-(1,2)	1.38	0.03	3%	-16%	4

Figure III.1-9. Plot of the statistics of ΣSO4 in Table III.1-10 (A) and Table III.1-12 (B) (M, mol/L).

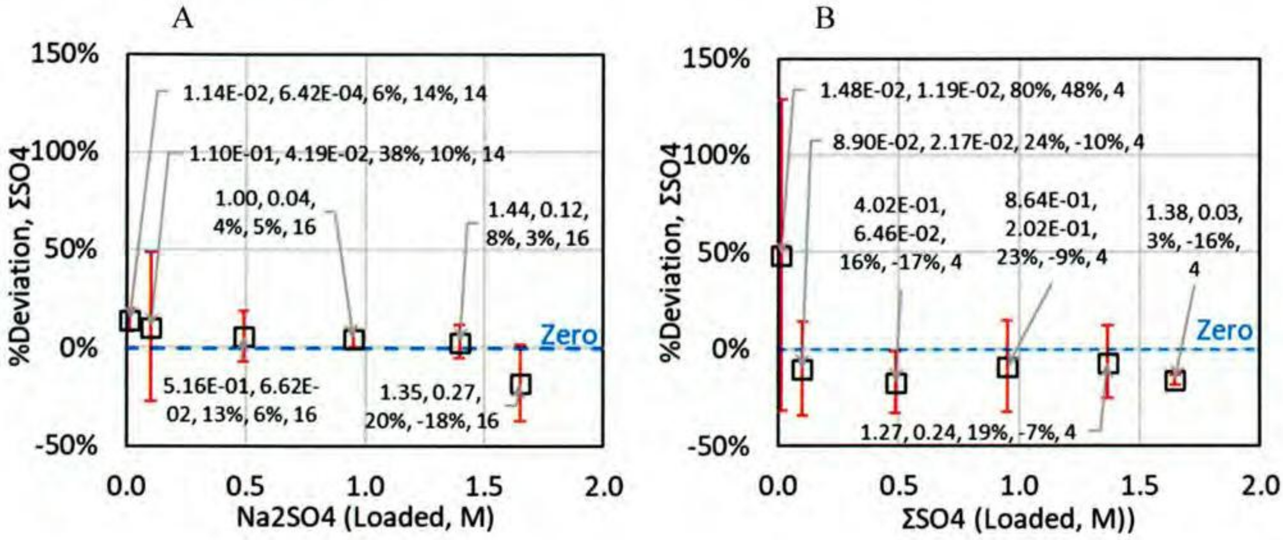

III.1.4. ΣNa

Sodium can be considered a non-reactive/conservative component, if there is no precipitation of solid(s) containing sodium. Total dissolved sodium concentration, ΣNa, can be defined as:

$$\Sigma Na = 2 \times [Na_2SO_4]_{Loaded} + [NaCl]_{Loaded} \quad (4)$$

Presented in Table III.1-13 are the ΣNa measured as a function of aging time from Experiment 1 conducted under TP 08-02 Revision 0. Plots of the time-dependent measurements are presented in Figure III.1-10. The ΣNa were stable through the aging time (1368 days). Statistics are tabulated and displayed in Table III.1-14 and Figure III.1-12A.

The measurements were accurate within -6 to 2% deviation from the loaded ΣNa, except at the highest loading of ΣNa, which showed the largest negative deviation from the loaded amount (Figure III.1-10, Table III.1-14, and Figure III.1-12A). Our precision indicates that, at 95% confidence, we reproduced the loaded ΣNa concentration (Figure III.1-12A).

In performing the Experiment 1 under the protocols of TP 20-01 Revision 0, ΣNa was measured from the background solutions prior to adding the solid, $PbSO_4(s)$. Additional measurements were conducted after commencing solid dissolution. The samples injected to the instrument for measurements of ΣNa in the background solution prior to the addition of $PbSO_4(s)$ were prepared by volume-to-volume dilution. The samples injected into the instrument for the measurements of ΣNa in the filtered supernatants sampled after commencing the dissolution were prepared by mass-to-volume dilution. All the measurements of ΣNa are summarized in Table III.1-15, and plotted in Figure III.1-11.

Similar to the measurements of ΣSO4 described in Section III.1.3, no trend of underestimation of ΣNa by volume-to-volume dilution was observed as a function of solution density. Black circles and orange ×'s on the vertical axes in Figure III.1-11 stand for the ΣNa measurements from the samples diluted by the volume-to-volume technique prior to commencing the dissolution and the loading of ΣNa, respectively. Blue circles and dots are ΣNa measured from samples diluted by mass-to-volume technique. No noticeable difference is observed between the two dilution techniques. Both dilution techniques underestimated the ΣNa at the highest loading of ΣNa, where the two techniques would have shown clearer difference. The extent of the underestimation of both techniques was comparable to each other, meaning that the both dilution techniques have little or any discernable impact from the solution density under the practice of SNL WIPP Geochemistry Program. Until SNL WIPP Geochemistry Program improves the accuracy and precision of the overall laboratory operation, volume-to-volume dilutions should suffice.[20]

Orange dots in Figure III.1-11 are the measurements flagged by the lab because the instrument readings were outside the range of calibration. They are not included in calculating the statistics. However, those values are consistent with other measurements valid under SNL WIPP QA, which could make analysts wonder about the need to discard them prior to statistical testing and comprehensive review of the data. Statistical determinations would be strengthened by increasing the number of observations. Knowledge of the interval for linear responses and low detection limit could prevent discarding potentially useful data *a priori*.[21]

---

[20] Inside gloveboxes, increased chance of introducing larger uncertainty exists, such as limited dexterity, continuous air flow, and vibration interfering with accurate determination of mass of filtered solution in tared volumetric flasks.

[21] SNL WIPP Geochemistry is considering to set low/high detection limits for analytical instruments, including mandating the use of a calibration standard of lowest concentration of analyte in the sample injection queue as a check standards.

The results of ΣNa measurements in Experiments 1 under both TPs are statistically identical (compare one black square in A and B of Figure III.1-12 at a condition at a time).

Table III.1-13. Time-dependent measurements of ΣNa under TP 08-02 Revision 0 (M, mol/L).

	Aging time (Days)							
Reactor ID	360	743	1010	1059	1107	1158	1305	1368
PbSO4-0.01-1	NA	1.66E-01	1.62E-01	1.68E-01	1.68E-01	1.70E-01	1.67E-01	1.66E-01
PbSO4-0.01-2	NA	1.73E-01	1.60E-01	1.64E-01	1.68E-01	1.70E-01	1.68E-01	1.68E-01
PbSO4-0.1-1	NA	3.34E-01	3.21E-01	3.38E-01	3.15E-01	3.35E-01	3.31E-01	3.42E-01
PbSO4-0.1-2	NA	3.30E-01	3.18E-01	3.50E-01	3.01E-01	3.13E-01	3.31E-01	3.35E-01
PbSO4-0.5-1	1.09E+00	1.09E+00	1.05E+00	1.06E+00	1.03E+00	1.10E+00	1.08E+00	1.08E+00
PbSO4-0.5-2	1.10E+00	1.09E+00	1.06E+00	1.04E+00	9.79E-01	1.08E+00	1.09E+00	1.11E+00
PbSO4-1.0-1	2.11E+00	2.14E+00	2.07E+00	2.06E+00	2.01E+00	2.20E+00	2.11E+00	2.11E+00
PbSO4-1.0-2	2.07E+00	2.15E+00	2.05E+00	2.00E+00	2.01E+00	2.05E+00	2.10E+00	2.08E+00
PbSO4-1.5-1	2.79E+00	2.98E+00	2.80E+00	3.05E+00	2.75E+00	3.11E+00	2.62E+00	2.92E+00
PbSO4-1.5-2	2.74E+00	3.06E+00	2.88E+00	3.09E+00	2.66E+00	3.08E+00	2.60E+00	2.86E+00
PbSO4-1.8-1	2.70E+00	2.28E+00	2.57E+00	2.83E+00	2.49E+00	3.27E+00	2.69E+00	2.90E+00
PbSO4-1.8-2	2.70E+00	2.23E+00	2.56E+00	2.80E+00	2.70E+00	3.27E+00	2.72E+00	2.96E+00

Figure III.1-10. Plot of the time-dependent measurements of ΣNa under TP 08-02 Revision in Table III.1-13 (M, mol/L). Orange ×s on the vertical axes are initial loading of ΣNa = 2×[Na_2SO_4] + [NaCl]. Black squares and red error bars located on 250 days are averages and twice the standard deviations of all the measurements displayed to the right at their aging time (blue dots and circles, which represent data from duplicate reactors).

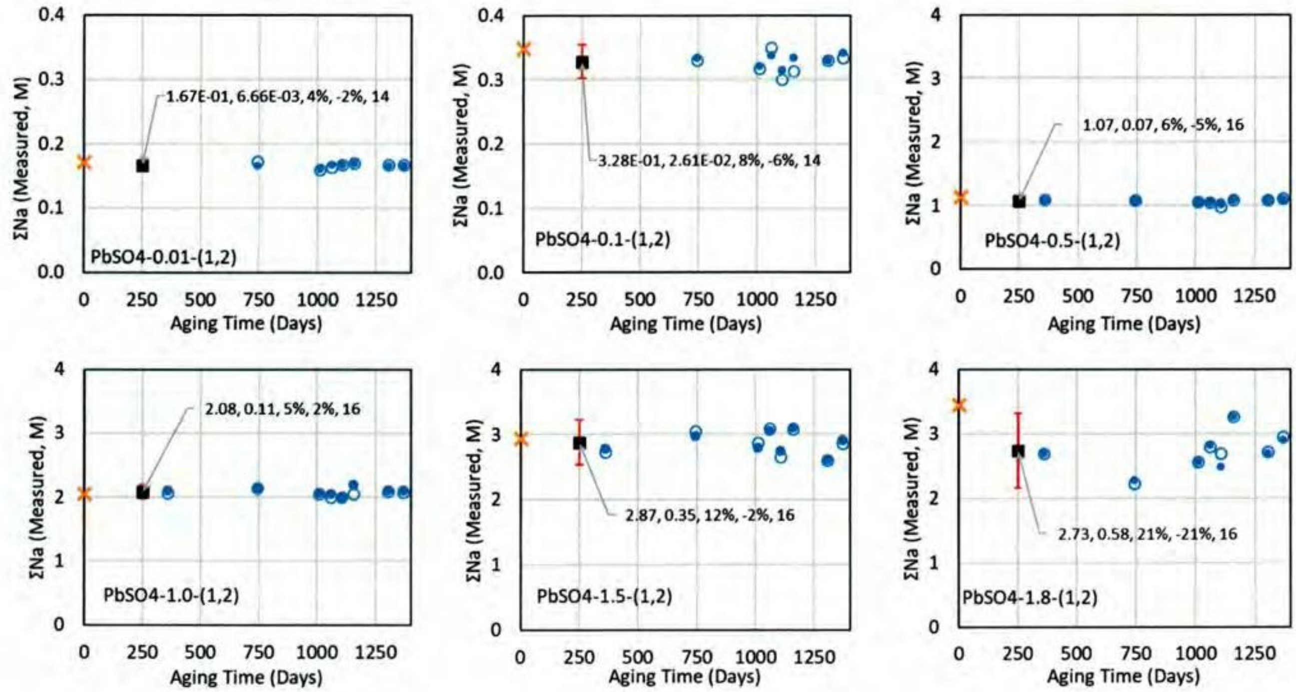

Table III.1-14. Statistics of measurements of ΣNa (M, mol/L) under TP 08-02 Revision 0 in Table III.1-13.

Reactor ID	Average	2SD	%2SD	%Deviation	Counts
PbSO4-0.01-(1,2)	1.67E-01	6.66E-03	4%	-2%	14
PbSO4-0.1-(1,2)	3.28E-01	2.61E-02	8%	-6%	14
PbSO4-0.5-(1,2)	1.07E+00	6.67E-02	6%	-5%	16
PbSO4-1.0-(1,2)	2.08E+00	1.09E-01	5%	2%	16
PbSO4-1.5-(1,2)	2.87E+00	3.48E-01	12%	-2%	16
PbSO4-1.8-(1,2)	2.73E+00	5.77E-01	21%	-21%	16

Table III.1-15. Time-dependent measurements of ΣNa under the protocols of TP 20-01 Revision 0 (M, mol/L).

Aging time (Days)	0	43	111
Reactor ID (n =)	Before adding PbSO4(s)[#]	1	2
PbSO4-0.01-SO4-1-n	1.57E-01	1.63E-01	1.51E-01
		1.75E-01	*1.55E-01*
PbSO4-0.01-SO4-2-n	1.57E-01	1.62E-01	1.47E-01
		1.75E-01	*1.54E-01*
PbSO4-0.1-SO4-1-n	3.78E-01	3.25E-01	3.21E-01
PbSO4-0.1-SO4-2-n	3.83E-01	3.26E-01	3.20E-01
PbSO4-0.5-SO4-1-n	1.01E+00	9.96E-01	9.91E-01

PbSO4-0.5-SO4-2-n	1.03E+00	1.02E+00	1.01E+00
PbSO4-1.0-SO4-1-n	1.96E+00	1.93E+00	1.94E+00
		2.09E+00	*1.96E+00*
PbSO4-1.0-SO4-2-n	1.96E+00	1.93E+00	1.90E+00
		2.10E+00	*1.97E+00*
PbSO4-1.5-SO4-1-n	2.83E+00	2.75E+00	2.39E+00
PbSO4-1.5-SO4-2-n	2.84E+00	2.72E+00	2.42E+00
PbSO4-1.8-SO4-1-n	2.99E+00	3.17E+00	2.73E+00
PbSO4-1.8-SO4-2-n	3.04E+00	3.15E+00	2.89E+00

Italics in red fonts: Flagged by lab. Not used in the statistics. Presented here and in Figure III.1-11 to address importance of establishing sensitivity and/or low detection limit of analytical instruments.
#Duplicate measurements of the six solutions described in Table II.1-2 prior to adding to the solid-containing vials. Samples injected to the instrument were prepared by volume-to-volume dilution.

Figure III.1-11. Plot of the time-dependent measurements of ΣNa from Experiment 1 under TP 20-01 Revision in Table III.1-15 (M, mol/L). Yellow dots were not included in calculating the statistics. See discussion in the text. Black squares and red error bars located on 20 days are averages and twice the standard deviations of all the measurements displayed to the right at their aging time (blue dots and circles, which represent data from duplicate reactors).

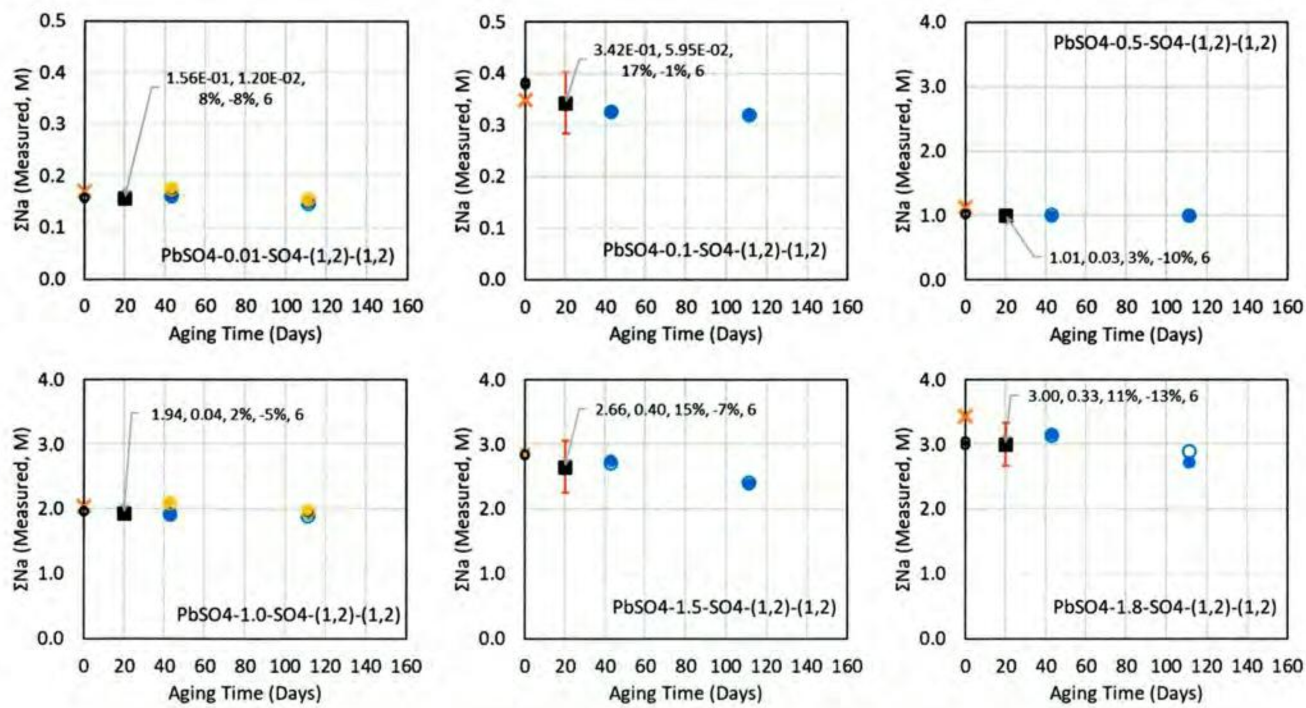

Table III.1-16. Statistics of measurements of ΣNa under TP 20-01 Revision 0 in Table III.1-15 (M, mol/L).

Reactor ID	Average	2SD	%2SD	%Deviation	Counts
PbSO4-0.01-(1,2)	1.56E-01	1.20E-02	8%	-8%	6

PbSO4-0.1-(1,2)	3.42E-01	5.95E-02	17%	-1%	6
PbSO4-0.5-(1,2)	1.01	0.03	3%	-10%	6
PbSO4-1.0-(1,2)	1.94	0.04	2%	-5%	6
PbSO4-1.5-(1,2)	2.66	0.40	15%	-7%	6
PbSO4-1.8-(1,2)	3.00	0.33	11%	-13%	6

Figure III.1-12. Plot of the statistics of ΣNa in A. Table III.1-14 (TP 08-02 Revision 0); B. Table III.1-16 (TP 20-01 Revision 0). $\Sigma Na_{Loaded} = [NaCl]_{Loaded} + 2\times[Na_2SO_4]_{Loaded}$.

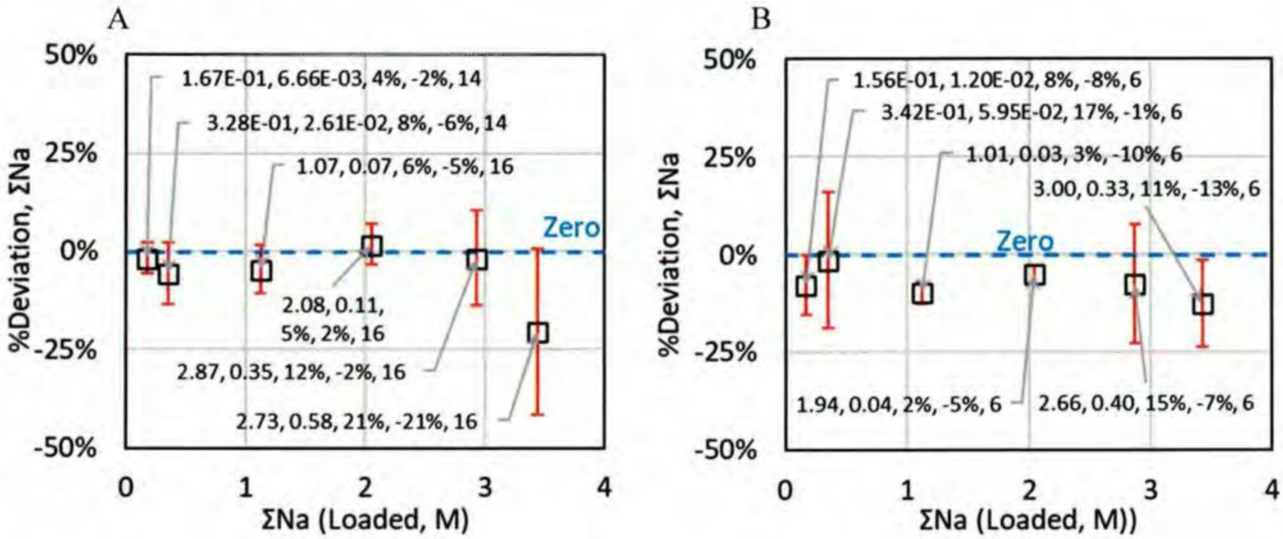

III.1.5. ΣCl

Chloride can be considered a conservative component. Total dissolved chloride concentration, ΣCl, should be close to the loaded NaCl concentration, if there is no precipitation of solid(s) containing chloride:

$$\Sigma Cl = [NaCl]_{Loaded} \quad (5)$$

Summarized in Table III.1-17 are the ΣCl measured as a function of aging time from Experiment 1 conducted under TP 08-02 Revision 0. Plots of the time-dependent measurements are presented in Figure III.1-13. The ΣCl were stable over the aging time. The observed scatters were confined within maximum %2SD of 24%. Statistics are tabulated and displayed in Table III.1-18 and Figure III.1-15A.

The measurements were accurate with the %Deviation ranging 0 to 18% from the loaded ΣCl (Figure III.1-13, Table III.1-18, and Figure III.1-15A). Our precision indicates that, with 95% confidence, we reproduced the loaded ΣCl concentration (Figure III.1-15A), with one exception at the highest loading of ΣCl.

In performing the Experiment 1 under the protocols of TP 20-01 Revision 0, ΣCl was measured only from the background solutions without $PbSO_4$(s). Additional measurements after commencing the dissolution are not available as of 6/22/2021 (Table III.1-19).[22] The samples injected on the instrument for measurements of ΣCl in the background solution prior to the addition of $PbSO_4$(s) were prepared by volume-to-volume dilution. Solid black squares in Figure III.1-14 are the averages of two measurements in Table III.1-19.

The results of ΣCl measurements in Experiments 1 under both TPs are statistically identical (compare one black square in A and B of Figure III.1-15 at a condition at a time), except two data points at the highest Cl loading. We have no explanation for the overestimations for the last 4 data points with high precision in Figure III.1-15B.

Table III.1-17. Time-dependent measurements of ΣCl under TP 08-02 Revision 0 (M, mol/L).

	Aging time (Days)							
Reactor ID	360	743	1010	1059	1107	1158	1305	1368
PbSO4-0.01-1	NA	1.63E-01	1.58E-01	1.55E-01	1.52E-01	1.55E-01	1.50E-01	1.47E-01
PbSO4-0.01-2	NA	1.58E-01	1.58E-01	1.51E-01	1.52E-01	1.53E-01	1.50E-01	1.49E-01
PbSO4-0.1-1	NA	1.51E-01	1.58E-01	1.32E-01	1.52E-01	1.51E-01	1.47E-01	1.47E-01
PbSO4-0.1-2	NA	1.44E-01	1.54E-01	1.57E-01	1.55E-01	1.44E-01	1.49E-01	1.48E-01
PbSO4-0.5-1	1.52E-01	1.90E-01	1.60E-01	2.18E-01	1.54E-01	1.50E-01	1.47E-01	1.46E-01
PbSO4-0.5-2	1.54E-01	1.61E-01	1.54E-01	1.54E-01	1.49E-01	1.52E-01	1.47E-01	1.47E-01
PbSO4-1.0-1	1.53E-01	1.88E-01	1.43E-01	1.48E-01	1.46E-01	1.48E-01	1.45E-01	1.45E-01
PbSO4-1.0-2	1.53E-01	1.44E-01	1.44E-01	1.51E-01	1.46E-01	1.47E-01	1.45E-01	1.45E-01
PbSO4-1.5-1	1.48E-01	1.43E-01	1.45E-01	1.47E-01	1.49E-01	1.47E-01	1.55E-01	1.43E-01
PbSO4-1.5-2	1.40E-01	1.43E-01	1.55E-01	1.43E-01	1.48E-01	1.47E-01	1.54E-01	1.46E-01
PbSO4-1.8-1	1.60E-01	1.76E-01	1.71E-01	1.61E-01	1.58E-01	1.48E-01	1.62E-01	1.57E-01
PbSO4-1.8-2	1.60E-01	1.76E-01	1.66E-01	1.63E-01	1.57E-01	1.49E-01	1.60E-01	1.56E-01

[22] The DIQ (Days In Queue) for the measurements of ΣCl for filtered supernatants sampled from -1 and -2 reactors of this Experiment 2 under the protocols of TP 20-01 Revision 0 appear to be quite long. The "-1" reactors were terminated on 2/25/2021, and "-2" on 5/4/2021. No measurements of ΣCl from them are completed, and they are not listed in Table III.1-19.

Figure III.1-13. Plot of the time-dependent measurements of ΣCl under TP 08-02 Revision in Table III.1-17 (M, mol/L).

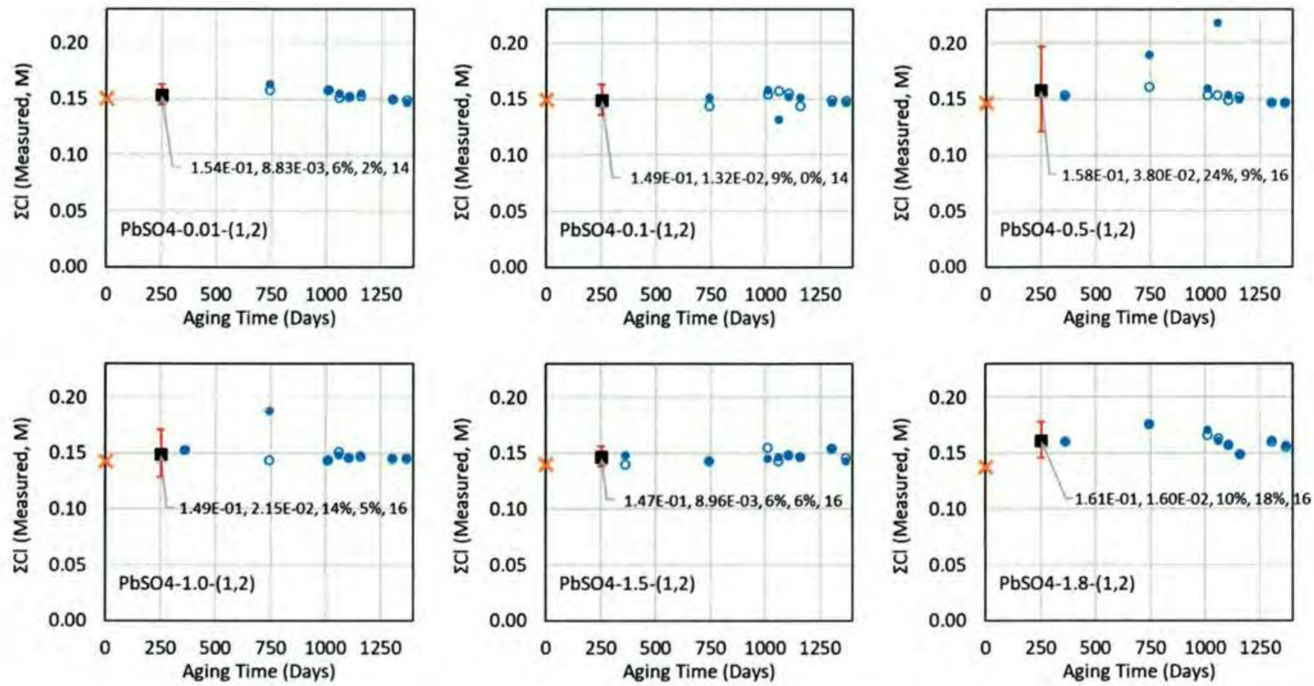

Table III.1-18. Statistics of measurements of ΣCl (M, mol/L) under TP 08-02 Revision 0 in Table III.1-17.

Reactor ID	Average	2SD	%2SD	%Deviation	Counts
PbSO4-0.01-(1,2)	1.54E-01	8.83E-03	6%	2%	14
PbSO4-0.1-(1,2)	1.49E-01	1.32E-02	9%	0%	14
PbSO4-0.5-(1,2)	1.58E-01	3.80E-02	24%	9%	16
PbSO4-1.0-(1,2)	1.49E-01	2.15E-02	14%	5%	16
PbSO4-1.5-(1,2)	1.47E-01	8.96E-03	6%	6%	16
PbSO4-1.8-(1,2)	1.61E-01	1.60E-02	10%	18%	16

Table III.1-19. Time-dependent measurements of ΣCl under the protocols of TP 20-01 Revision 0 (M, mol/L).

Aging time (Days)	0
Reactor ID (n =)	Before adding PbSO4(s)[#]
PbSO4-0.01-SO4-1-n	1.47E-01
PbSO4-0.01-SO4-2-n	1.48E-01
PbSO4-0.1-SO4-1-n	1.48E-01
PbSO4-0.1-SO4-2-n	1.48E-01
PbSO4-0.5-SO4-1-n	1.81E-01
PbSO4-0.5-SO4-2-n	1.74E-01
PbSO4-1.0-SO4-1-n	1.75E-01

PbSO4-1.0-SO4-2-n	1.77E-01
PbSO4-1.5-SO4-1-n	1.73E-01
PbSO4-1.5-SO4-2-n	1.76E-01
PbSO4-1.8-SO4-1-n	1.88E-01
PbSO4-1.8-SO4-2-n	1.87E-01

Duplicate measurements of the six solutions described in Table II.1-2 prior to adding to the solid-containing vials. v-v dilution.

Figure III.1-14. Plot of the time-dependent measurements of ΣCl under TP 20-01 Revision in Table III.1-19 (M, mol/L).

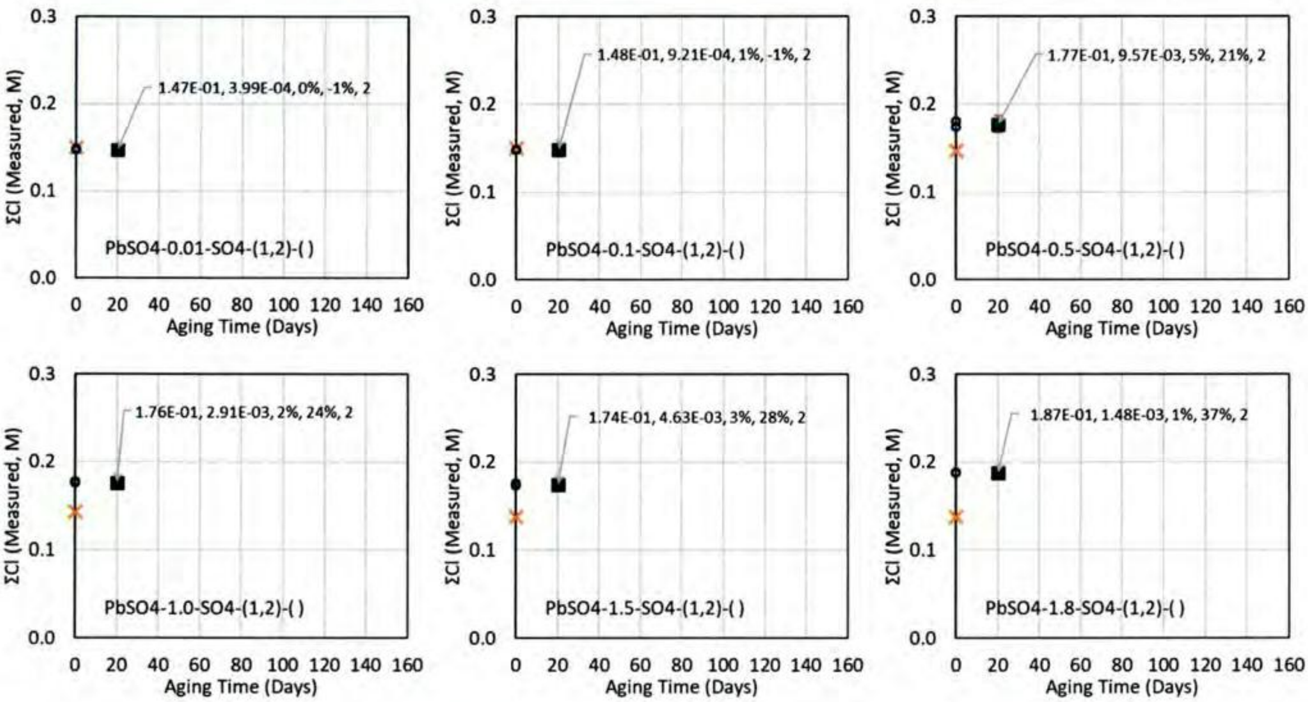

Table III.1-20. Statistics of measurements of ΣCl (M, mol/L) under TP 20-01 Revision 0 in Table III.1-19.

Reactor ID	Average	2SD	%2SD	%Deviation	Counts
PbSO4-0.01-(1,2)	1.47E-01	3.99E-04	0%	-1%	2
PbSO4-0.1-(1,2)	1.48E-01	9.21E-04	1%	-1%	2
PbSO4-0.5-(1,2)	1.77E-01	9.57E-03	5%	21%	2
PbSO4-1.0-(1,2)	1.76E-01	2.91E-03	2%	24%	2
PbSO4-1.5-(1,2)	1.74E-01	4.63E-03	3%	28%	2
PbSO4-1.8-(1,2)	1.87E-01	1.48E-03	1%	37%	2

Figure III.1-15. Plot of the statistics of ΣCl in: A. Table III.1-18 (TP 08-02 Revision 0), B. Table III.1-20 (TP 20-01 Revision 0). The horizontal axes are reversed to be consistent with the order of increase of the loading of ΣNa (See lower halves of

Table II.1-1 and Table II.1-2, i.e., Molarity of loaded ΣCl decreases as Molarity of loaded ΣNa increases).

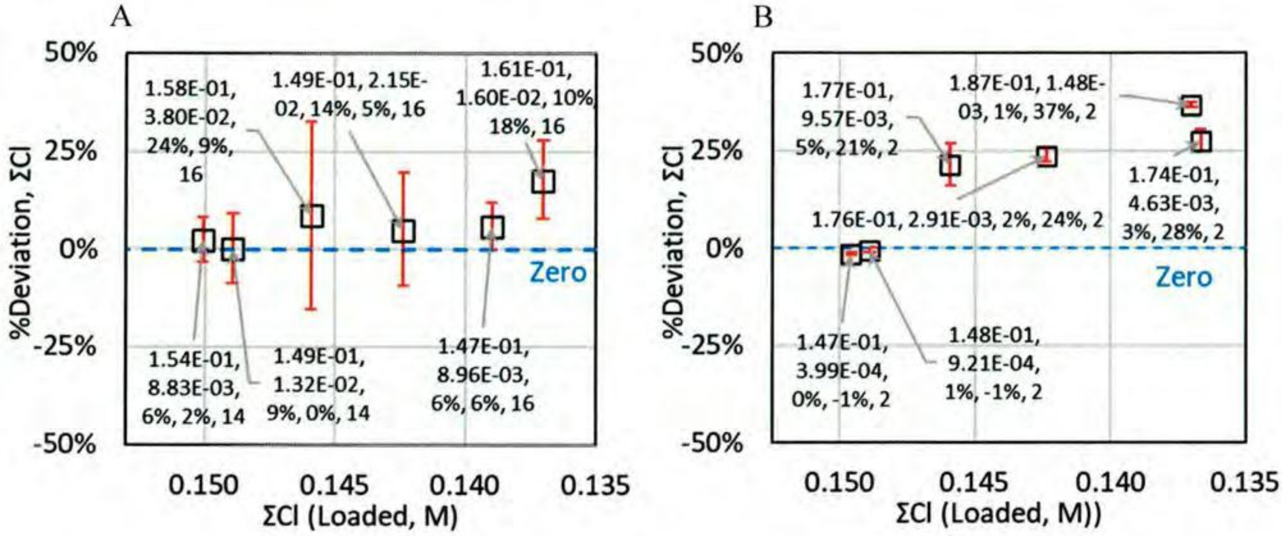

III.1.6. Solid Characterization

Under TP 08-02 Revision 0, a large volume of reactors was terminated to collect the solids after final sampling of the supernatants. One of the duplicate reactors for each condition (six conditions in total) was terminated. Six XRD scans are presented in Figure III.1-16.

Under TP 20-01 Revision 0, solids were collected at each sample date. As of 6/27/2021, XRD patterns for the first timed experiments, i.e., reactors with ID ending with "-1", are available and presented in Figure III.1-17.

Figure III.1-16. XRD scans of solids collected from Experiment 1 conducted under TP 08-02 Revision 0. Aging time exceeds 1300 days.

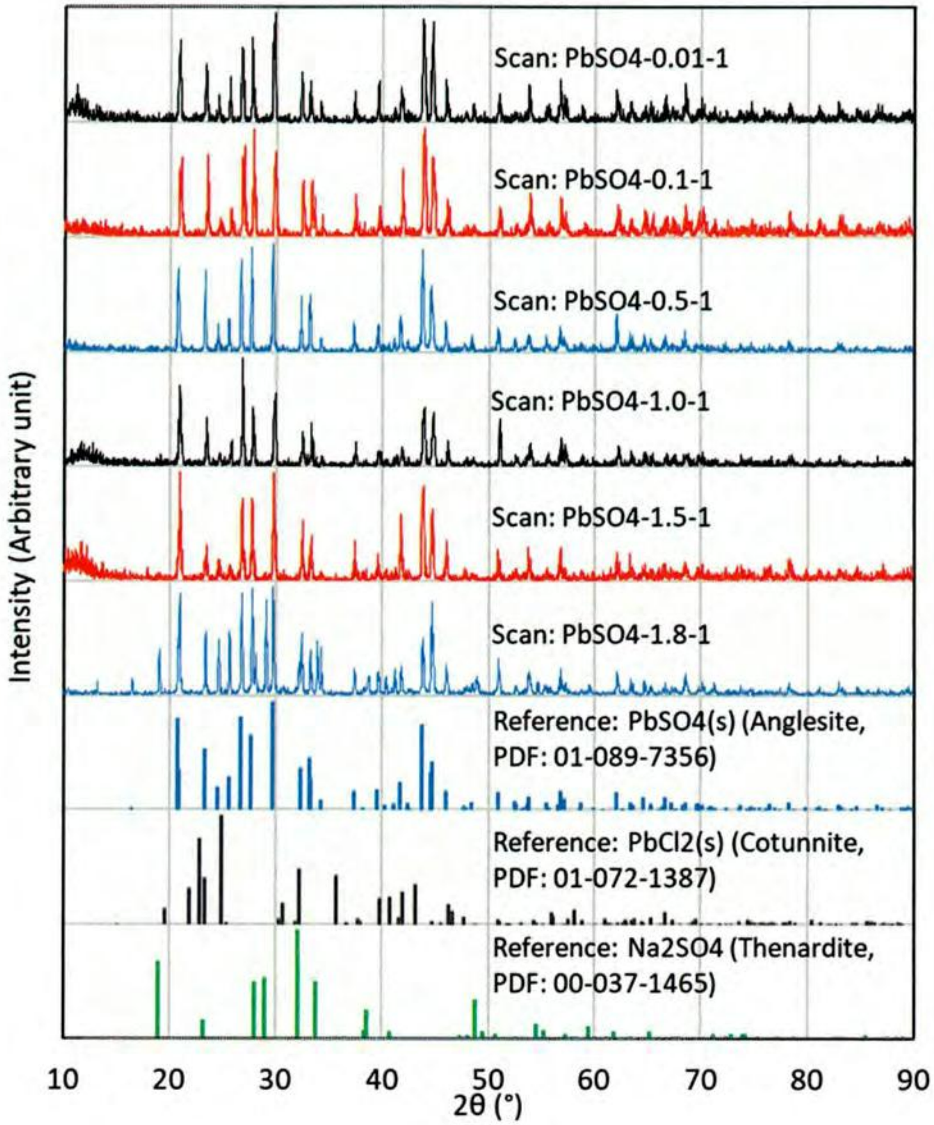

Figure III.1-17. XRD scans of solids collected from Experiment 1 conducted under TP 20-01 Revision 0 (The last digit of the scan ID, i.e., -1, means that the aging time = 43 days).

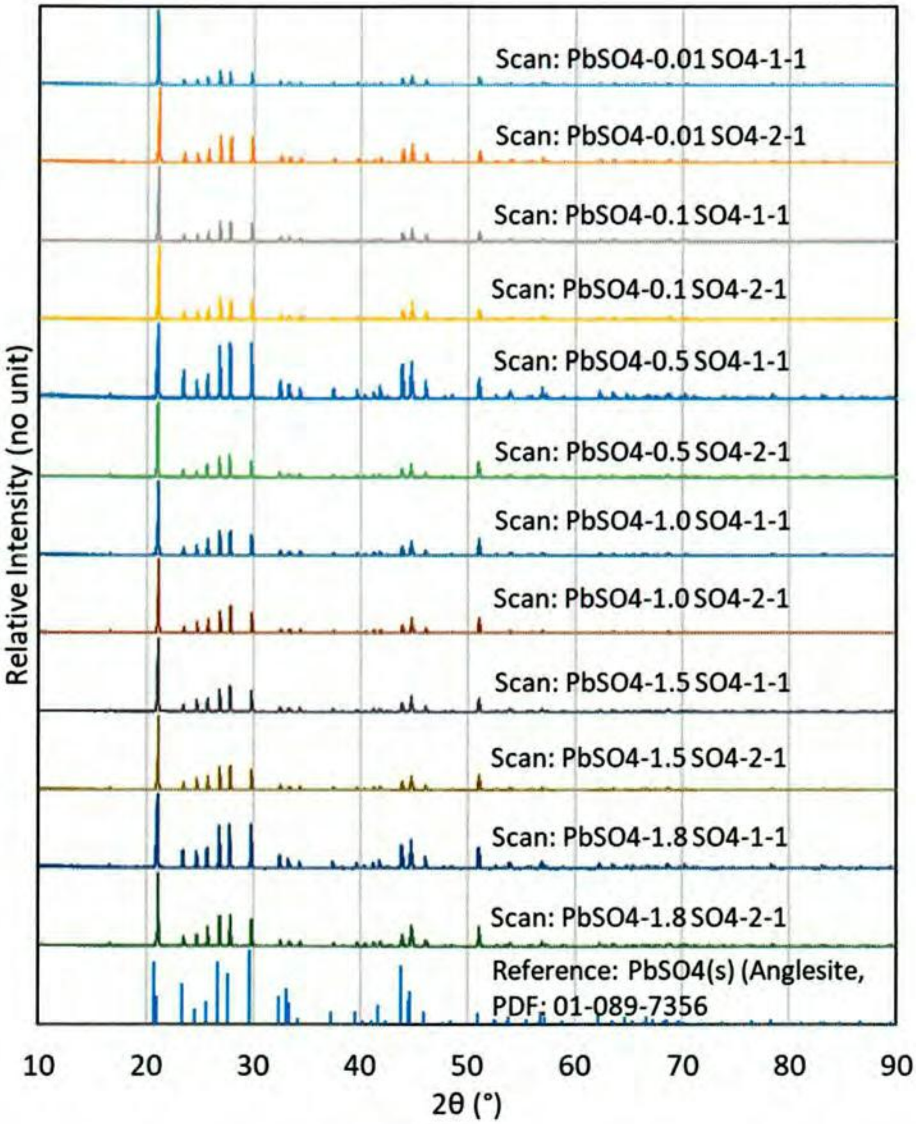

III.1.7. Summary

Experiment 1, where excess $PbSO_4$(s) (anglesite) was added to background solutions of incremental concentrations of Na_2SO_4 spiked with a constant NaCl concentration, was performed using protocols in TP 08-02 Revision 0 (assumed to be subject to CO_2(g) intrusion and inadvertent contamination of the reactors by unknown sources due to repeated entries for sampling and aging time extending multiple years). The same experiment was performed under the protocols of TP 20-01 Revision 0: use of minimal CO_2(g) gloveboxes and preparation of multiple replicates for termination at each timed investigation to exclude the possibilities of CO_2(g) intrusion and inadvertent contamination of the reactors. The last sampling under TP 20-01 Revision 0 was conducted on 111 days, which is much earlier than the first sampling under TP 08-02 Revision 0 (360 days).

The recorded pHr values are statistically identical (Figure III.1-3). The measured ΣPb are statistically identical (Figure III.1-6). The measured ΣSO4 are statistically identical (Figure III.1-9). The measured ΣNa are statistically identical (Figure III.1-12). Measured ΣCl cannot be compared due to the low accuracy observed in Figure III.1-15B. The accuracy demonstrated in the measurements of other conservative components, i.e., ΣSO4 and ΣNa (Figure III.1-9 and Figure III.1-12), shows that the inaccuracy of ΣCl measurements could be due to a sensitivity artifact of the ion chromatography column.

Mineralogical transformation of the initial $PbSO_4$(s) did not happen under the protocols of both TPs (Figure III.1-16 and Figure III.1-17). One possible explanation for the observation of thenardite (Na_2SO_4) in Figure III.1-16 (scan: PbSO4-1.8-1) is the precipitation of thenardite from the evaporation of background solutions captured in the pore space of collected solids. A second possible explanation could be precipitation of thenardite in the reactor due to its own supersaturation. The second explanation needs further investigation on what triggered thenardite supersaturation, and why Experiment 1 conducted under TP 20-01 did not show the same observation, i.e., thenardite was not observed in Figure III.1-17.

By repeating the Experiment 1 under the protocols of TP 20-01 Revision 0 where the two contamination possibilities are eliminated by the experimental protocols, we proved that the influence of CO_2(g) intrusion and contamination was not statistically observable, and the influence of such contamination on the thermodynamic interpretation of the measurements would fall within analytical and experimental uncertainties. Additionally, it was demonstrated that equilibrium was achieved within 111 days suggesting that experimental durations can be reduced while still achieving valid and representative results.

III.2. Experiment 2: $PbCO_3$(s) - $NaHCO_3$ - NaCl - H_2O

Recipes for this Experiment 2 under each TP are summarized in Table II.2-1 and Table II.2-2, respectively.

III.2.1. pHr

In Table III.2-1 the pHr values are recorded as a function of aging time from Experiment 2 conducted under TP 08-02 Revision 0. Plots of the measurements are displayed in Figure III.2-1. The observed scatters are confined around the averages within the maximum 2SD of 0.64 pH unit (7%), which means that the precision of the measurements was better than 7%. Statistically, they are identical at around 9 (Figure III.2-1, Table III.2-2, and Figure III.2-3A). Note that the last two background solutions have the same loading of $NaHCO_3$ (0.9 m) but different NaCl loadings (0.15 and 0.30 m) (Table II.2-1). $NaHCO_3$ buffers the pH, so the pHr should remain close to each other, and they are at 95% confidence (Table III.2-2; Figure III.2-3A).

Table III.2-3 presents the pHr values recorded as a function of aging time from Experiment 2 conducted under the protocols of TP 20-01 Revision 0. Plots of the measurements are presented in Figure III.2-2. The scatter in pHr values is confined around the averages within the maximum 2SD of 0.14 pH unit (2%), indicating that the precision of the measurements was better than 2%. Unlike the pHr obtained under TP 08-02 Revision 0, the measurements of pHr illustrated resolution for the loadings of $NaHCO_3$ with 95% confidence (Figure III.2-2, Table III.2-4, and Figure III.2-3B). In other words, the error bars = 2SD or %2SD and they are not overlapping with each other. Note that the last two background solutions have the same loading of $NaHCO_3$ (1.0 m), and different NaCl loadings (0.15 and 0.30 m) (Table II.2-2). $NaHCO_3$ buffers the pH, so the pHr should remain close to each other, and they are at 95% confidence (Table III.2-4; Figure III.2-3B).

Two groups are identified in Figure III.2-3. Green ovals indicate one group of reactors of statistically identical pHr values. Interpretation is minimal loss of $CO_2(g)$ due to lower partial pressure of $CO_2(g)$ (i.e., lower loading of $NaHCO_3$), so the minimal loss of $CO_2(g)$ did not show up in pHr regardless of the experimental protocols. Orange ovals indicate the other group of reactors of statistically different pHr values. The interpretation is that significant loss of $CO_2(g)$ due to higher partial pressure of $CO_2(g)$ (i.e., higher loading of $NaHCO_3$ in the recipe) over long aging times and repeated sampling entries under TP 08-02 Revision 0 (orange oval in Figure III.2-3A), relative to the same experiment conducted under the protocols of TP 20-01 Revision 0 (orange oval in Figure III.2-3B). Loss of $CO_2(g)$ drives the following reaction to the right by Le Chatelier's principle, producing OH^- (and increasing pH):

$$HCO_3^- \rightarrow OH^- + CO_2(g)\uparrow \quad (6)$$

Under the protocols of TP 20-01 Revision 0, multiples of identical reactors of one condition were prepared, and two of them for each condition were terminated at each timed investigation to capture the solution chemistry before Reaction (6) proceeds to the right.

Table III.2-1. Time-dependent measurements of pHr from Experiment 2 under TP 08-02 Revision 0.

pHr	Aging time (Days)							
Reactor ID	741	1020	1069	1118	1167	1293	1379	1461
PbCO3 0.01/0.15-1	9.18	8.79	8.76	8.65	8.68	8.60	8.58	8.60
PbCO3 0.01/0.15-2	9.45	9.25	9.23	9.32	9.22	9.30	9.24	9.23
PbCO3 0.05/0.15-1	9.11	9.01	9.05	9.16	9.08	9.14	9.12	9.11
PbCO3 0.05/0.15-2	9.10	9.16	9.17	9.26	9.18	9.24	9.21	9.19
PbCO3 0.5/0.15-1	8.82	9.68	9.55	9.59	9.49	9.54	9.50	9.14
PbCO3 0.5/0.15-2	8.92	9.08	9.09	9.16	9.09	9.17	9.10	9.12
PbCO3 1.0/0.15-1	8.70	8.89	8.89	8.97	8.90	8.99	8.92	8.94
PbCO3 1.0/0.15-2	8.63	8.80	8.82	8.91	8.85	8.94	8.89	8.91
PbCO3 1.0/0.3-1	8.62	8.96	8.97	9.05	8.98	9.06	8.99	9.01
PbCO3 1.0/0.3-2	8.60	8.80	8.80	8.89	8.83	8.93	8.87	8.88

Figure III.2-1. Plot of the time-dependent measurements of pHr under TP 08-02 Revision 0 in Table III.2-1. Solid and open symbols indicate duplicate reactors of each condition. Black squares and red error bars located on 550 days are averages and twice the standard deviations of all the measurements displayed to the right at their aging time (blue dots and circles, which represent data from duplicate reactors).

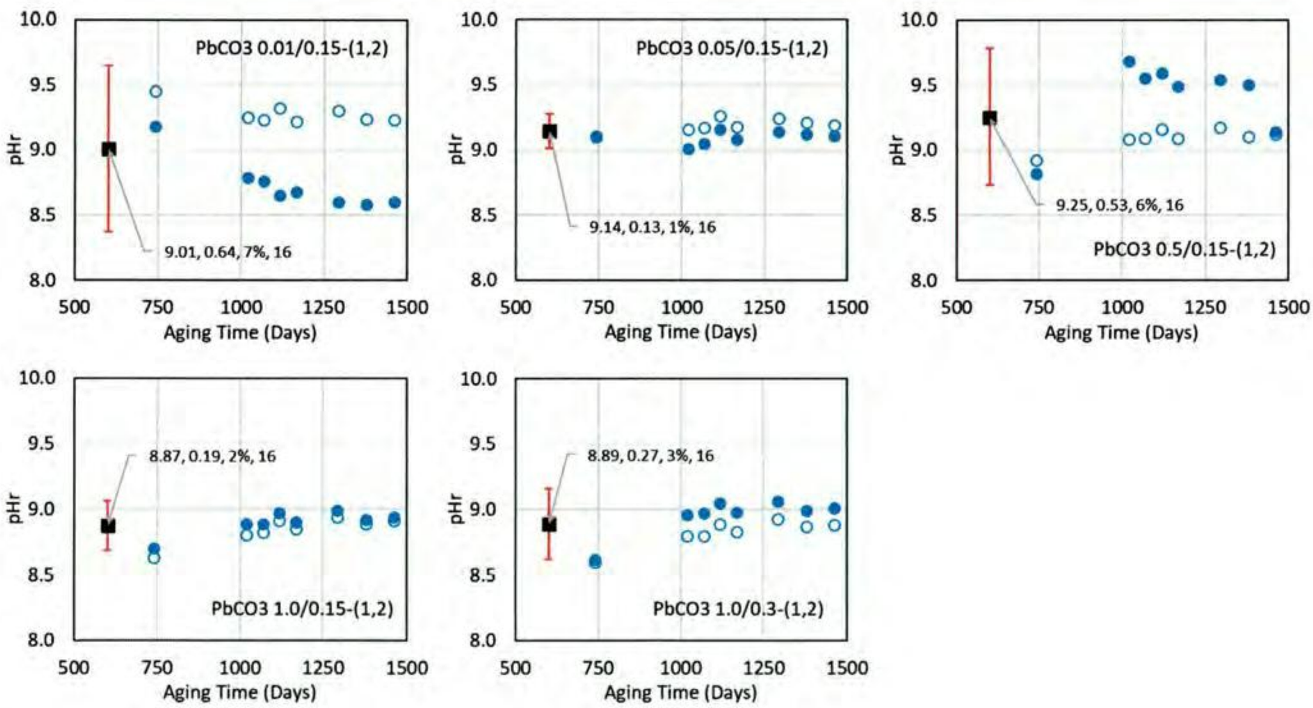

Table III.2-2. Statistics of measurements of pHr under TP 08-02 Revision 0 in Table III.2-1.

Reactor ID	Average	2SD	%2SD	Counts
PbCO3 0.01/0.15-1	9.01	0.64	7%	16
PbCO3 0.05/0.15-1	9.14	0.13	1%	16
PbCO3 0.5/0.15-1	9.25	0.53	6%	16
PbCO3 1.0/0.15-1	8.87	0.19	2%	16
PbCO3 1.0/0.3-1	8.89	0.27	3%	16

Table III.2-3. Time-dependent measurements of pHr under the protocols of TP 20-01 Revision 0. The n specifies the timed investigation.

Aging time (Days)	47	91
Reactor ID (n =)	1	2
PbCO3-0.01-NaHCO3-1-n	9.26	9.34
PbCO3-0.01-NaHCO3-2-n	9.26	9.35
PbCO3-0.05-NaHCO3-1-n	9.00	9.04
PbCO3-0.05-NaHCO3-2-n	8.89	9.04
PbCO3-0.5-NaHCO3-1-n	8.30	8.35
PbCO3-0.5-NaHCO3-2-n	8.32	8.35
PbCO3-1.0-NaHCO3-1-n	8.03	8.11
PbCO3-1.0-NaHCO3-2-n	8.12	8.13
PbCO3-1.0/0.3-NaHCO3-1-n	8.06	8.10
PbCO3-1.0/0.3-NaHCO3-2-n	8.11	8.14

Figure III.2-2. Plot of the time-dependent measurements of pHr under TP 20-01 Revision in Table III.2-3. Black squares and red error bars located on 10 days are averages and twice the standard deviations of all the measurements displayed to the right at their aging time (blue dots and circles, which represent data from duplicate reactors).

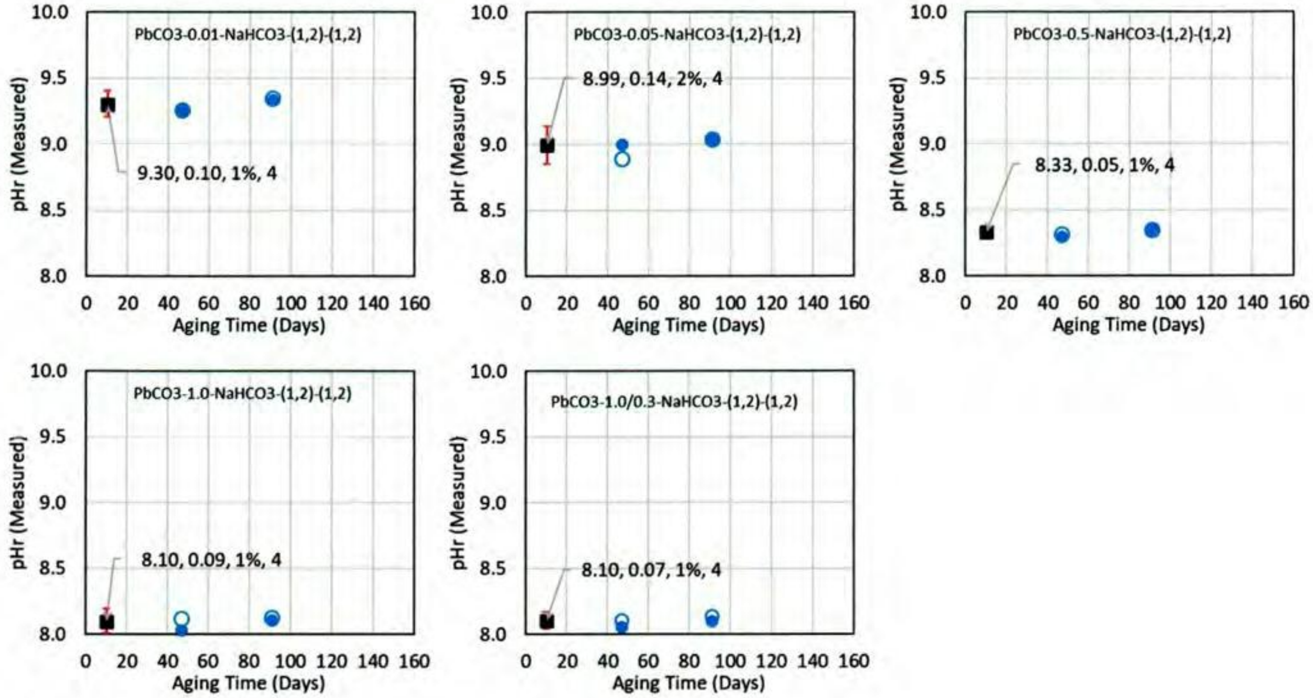

Table III.2-4. Statistics of measurements of pHr under TP 20-01 Revision 0 in Table III.2-3.

Reactor ID	Average	2SD	%2SD	Counts
PbCO3-0.01-NaHCO3-(1,2)-(1,2)	9.30	0.10	1%	4
PbCO3-0.05-NaHCO3-(1,2)-(1,2)	8.99	0.14	2%	4
PbCO3-0.5-NaHCO3-(1,2)-(1,2)	8.33	0.05	1%	4
PbCO3-1.0-NaHCO3-(1,2)-(1,2)	8.10	0.09	1%	4
PbCO3-1.0/0.3-NaHCO3-(1,2)-(1,2)	8.10	0.07	1%	4

Figure III.2-3. Plots of the statistics for pHr in Table III.2-2 and Table III.2-4. Green ovals indicate a group of reactors showing statistically similar pHr values between

A and B, and yellow ovals indicate another group of reactors showing different pHr values between A and B.

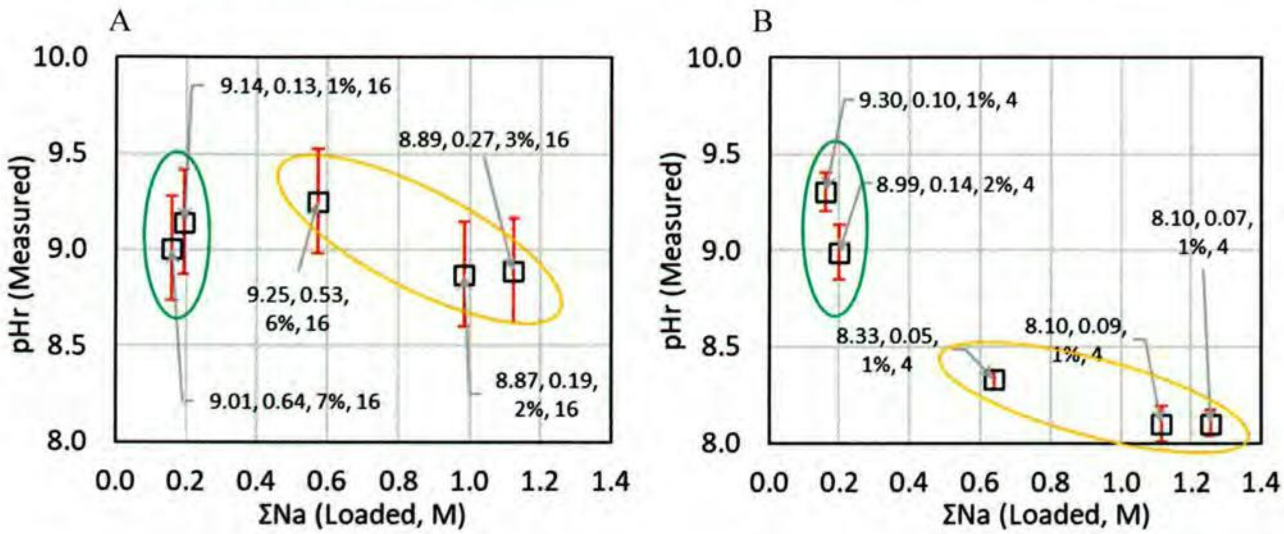

III.2.2. ΣPb

Table III.2-5 lists the ΣPb measured as a function of aging time from Experiment 2 conducted under TP 08-02 Revision 0. Plots of the measurements are presented in Figure III.2-4. The ΣPb values showed scatter.

Statistical data reduction as described in Section III.1.2 was performed on the ΣPb measurements due to the outliers shown in Figure III.2-4. The possible outliers are marked with green ovals (values in red italics in Table III.2-5). They are parts of valid measurements under SNL WIPP QA. Open squares and dashed red error bars in Figure III.2-4 stand for the averages and 2SDs calculated for all valid measurements, including those in the green ovals, in Table III.2-5 using the normal distribution. The statistics are listed in the upper half of Table III.2-6. Data points in green ovals were confirmed to be outliers based on the statistics represented by the open squares and dashed red error bars. They were excluded with 95% confidence (red dashed error bars) to calculate the new statistics (solid squares and solid red error bars in Figure III.2-4; the new statistics are listed in the lower half of Table III.2-6). At high loading of NaCl of 0.3 m, no outliers were noticed for the reactors PbCO3 1.0/0.3-(1,2) when all measurements were considered, and no reduction was performed for the reactors of higher loading of 0.3 m NaCl.

The recalculated 2SDs encompass the remaining data (Compare dashed and solid red error bars in Figure III.2-4). Those outliers are valid records under SNL WIPP QA Program.[23]

The error bars extending to negative concentrations even after the statistical data reduction for reactors $PbCO_3$ 0.01/0.15-(1,2) may indicate that the diluted samples injected on the ICP-AES for ΣPb measurements had ΣPb lower than the detection limit of ICP-AES.[24]

The last three panels in Figure III.2-4 showed a trend of ΣPb increasing over time. The last three panels in this figure describe the experiments of elevated pHr under TP 08-02 Revision 0, relative to those under TP 20-01 Revision 0 (Figure III.2-3; A and B, orange ovals), and the interpretation of the elevated pHr was the $CO_2(g)$ loss. Loss of $CO_2(g)$ can drive the following reaction to the right, resulting in increased dissolution of cerussite, i.e., higher ΣPb;

$$PbCO_3(s) + 2H^+ \rightarrow Pb^{+2} + H_2O + CO_2(g)\uparrow \quad (7)$$

Statistical analysis of the measurements in Figure III.2-4 are summarized in Table III.2-6 (lower half of the Table) and Figure III.2-6A.

Table III.2-7 shows the measured ΣPb values as a function of aging time from Experiment 2 conducted under the protocols of TP 20-01 Revision 0. Plots of the measurements as a function of time are displayed in Figure III.2-5. The ΣPb values are scattered. The observed scattering of the data is confined within the maximum %2SD of 48%. Table III.2-8 and Figure III.2-6B show the summary of statistical analysis.

Suppression of ΣPb was observed when Experiment 2 was conducted under the protocols of TP 20-01 Revision 0 (compare the data points in orange ovals in Figure III.2-6; A and B). In Figure III.2-6, the data points in green ovals in A and B are identical at 95% confidence like the pHr (Figure III.2-3), but the three data points in orange ovals in A and B are different. In the same context of $CO_2(g)$ loss in the Experiment 2 conducted under TP 08-02 Revision 0, Reaction (7) can explain the observation described in Figure III.2-6, i.e., higher partial pressure of $CO_2(g)$ maintained in the Experiment 2 (or less/slower loss of $CO_2(g)$) conducted under TP 20-01 Revision 0 suppressed the Reaction (7) from proceeding to the right.

---

[23] SNL WIPP Geochemistry is considering implementation of a real-time (or close to real-time) data monitoring system to screen such outliers.

[24] SNL WIPP Geochemistry is considering to set low/high detection limits for analytical instruments, including mandating the use of a calibration standard of lowest concentration of analyte in the sample injection queue as a check standards.

Table III.2-5. Time-dependent measurements of ΣPb (M, mol/L) under TP 08-02 Revision 0.

ΣPb (M)	Aging time (Days)							
Reactor ID	741	1020	1069	1118	1167	1293	1379	1461
PbCO3 0.01/0.15-1	1.12E-06	5.83E-07	1.59E-06	5.96E-07	3.49E-06	1.11E-06	1.97E-07	8.95E-07
PbCO3 0.01/0.15-2	7.10E-07	3.92E-06	2.23E-06	1.31E-06	1.42E-06	2.16E-06	1.87E-06	*1.04E-05*
PbCO3 0.05/0.15-1	2.94E-06	4.96E-06	5.14E-06	3.69E-06	4.02E-06	6.25E-06	3.73E-06	3.65E-06
PbCO3 0.05/0.15-2	2.94E-06	4.73E-06	5.03E-06	4.35E-06	4.44E-06	6.73E-06	4.27E-06	*1.44E-05*
PbCO3 0.5/0.15-1	2.58E-05	*9.64E-05*	7.14E-05	6.57E-05	6.24E-05	7.49E-05	6.55E-05	8.17E-05
PbCO3 0.5/0.15-2	2.69E-05	4.48E-05	4.65E-05	5.04E-05	5.04E-05	5.27E-05	6.69E-05	6.25E-05
PbCO3 1.0/0.15-1	5.83E-05	8.90E-05	9.94E-05	1.05E-04	1.09E-04	1.13E-04	1.22E-04	*1.53E-04*
PbCO3 1.0/0.15-2	6.04E-05	8.11E-05	9.28E-05	9.72E-05	9.89E-05	9.78E-05	1.19E-04	1.02E-04
PbCO3 1.0/0.3-1	6.67E-05	1.25E-04	1.27E-04	1.38E-04	1.13E-04	1.37E-04	1.61E-04	1.32E-04
PbCO3 1.0/0.3-2	7.12E-05	9.14E-05	1.06E-04	1.07E-04	1.43E-04	1.11E-04	1.19E-04	1.43E-04

Italics in red fonts: considered outliers based on the red dashed error bars in Figure III.2-4 (marked with green ovals in Figure III.2-4).

Figure III.2-4. Plot of the time-dependent measurements of ΣPb (M, mol/L) under TP 08-02 Revision in Table III.2-5. For high loading of NaCl at 0.3 m, no outliers were noticed when all measurements were considered. Low precision for PbCO3 0.01/0.15-(1,2), i.e., error bar extending to the negative concentration region after statistically reducing the data once, indicates the ΣPb are below the lower detection limit of ICP-AES for the reactors. Green ovals indicate outliers that were deemed valid data under the SNL QA program and no screening of such data had been performed at the time.

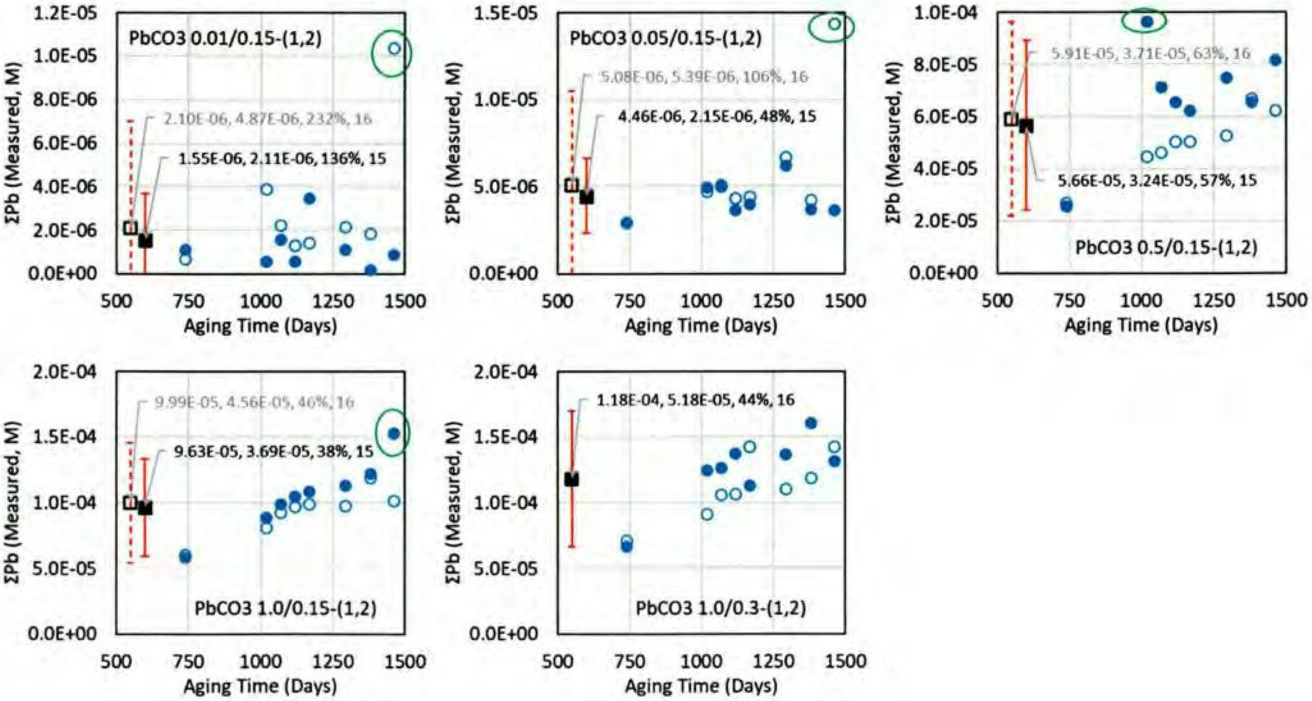

Table III.2-6. Statistics of measurements of ΣPb (M, mol/L) under TP 08-02 Revision 0 in Table III.2-5.

All Data				
Reactor ID	Average	2SD	%2SD	Counts
PbCO3 0.01/0.15-(1,2)	2.10E-06	4.87E-06	232%	16
PbCO3 0.05/0.15-(1,2)	5.08E-06	5.39E-06	106%	16
PbCO3 0.5/0.15-(1,2)	5.91E-05	3.71E-05	63%	16
PbCO3 1.0/0.15-(1,2)	9.99E-05	4.56E-05	46%	16
PbCO3 1.0/0.3-(1,2)	1.18E-04	5.18E-05	44%	16
Once-Reduced Data				
Reactor ID	Average	2SD	%2SD	Counts
PbCO3 0.01/0.15-(1,2)*	1.55E-06	2.11E-06	136%	15
PbCO3 0.05/0.15-(1,2)	4.46E-06	2.15E-06	48%	15
PbCO3 0.5/0.15-(1,2)	5.66E-05	3.24E-05	57%	15
PbCO3 1.0/0.15-(1,2)	9.63E-05	3.69E-05	38%	15
PbCO3 1.0/0.3-(1,2)#	1.18E-04	5.18E-05	44%	16

* Measurements seem to have been conducted close to or below the detection limit of the analytical instrument.
#No outliers were noticed when all measurements were considered. No statistical reduction performed, so the statistics are the same as in the upper part of this table.

Table III.2-7. Time-dependent measurements of ΣPb (M, mol/L) in Experiment 2 conducted under TP 20-01 Revision 0.

Aging time (Days)	47	91
Reactor ID (n =)	1	2
PbCO3-0.01-NaHCO3-1-n	3.50E-06	2.25E-06
PbCO3-0.01-NaHCO3-2-n	2.86E-06	2.09E-06
PbCO3-0.05-NaHCO3-1-n	3.90E-06	3.90E-06
PbCO3-0.05-NaHCO3-2-n	4.64E-06	3.92E-06
PbCO3-0.5-NaHCO3-1-n	1.68E-05	1.94E-05
	1.26E-05	*1.53E-05*
PbCO3-0.5-NaHCO3-2-n	1.78E-05	1.39E-05
PbCO3-1.0-NaHCO3-1-n	3.67E-05	2.75E-05
PbCO3-1.0-NaHCO3-2-n	2.91E-05	3.30E-05
PbCO3-1.0/0.3-NaHCO3-1-n	3.20E-05	4.21E-05
PbCO3-1.0/0.3-NaHCO3-2-n	3.03E-05	2.72E-05

Italics in red fonts: Flagged by lab. Not used in the statistics. They are comparable to the valid measurements. Sensitivity linearity and/or low detection limits of the instrument need to be discussed in the future.

Figure III.2-5. Plot of the time-dependent measurements of ΣPb (M, mol/L) under TP 20-01 Revision in Table III.2-7. Orange circles are the data flagged by lab and not included in calculating the statistics. Black squares and red error bars located on 20 days are averages and twice the standard deviations of all the measurements displayed to the right at their aging time (blue dots and circles, which represent data from duplicate reactors).

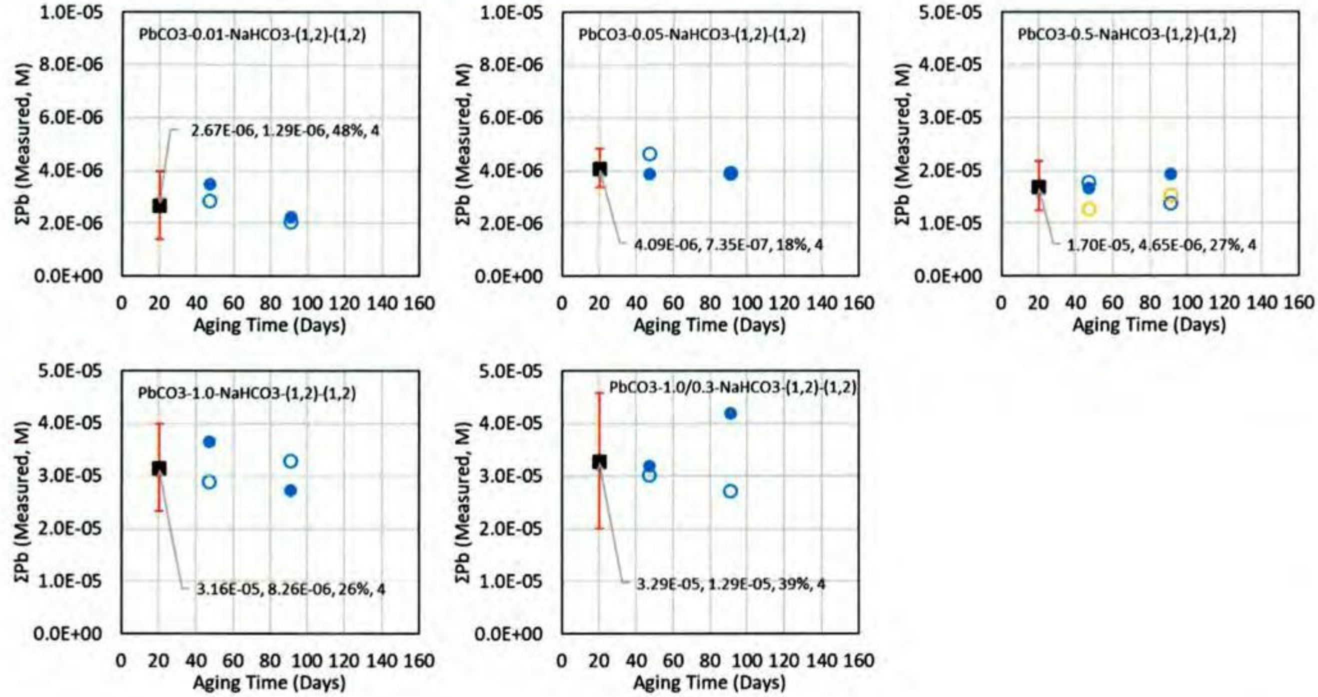

Table III.2-8. Statistics of measurements of ΣPb (M, mol/L) under TP 20-01 Revision 0 in Table III.2-7.

Reactor ID	Average	2SD	%2SD	Counts
PbCO3-0.01-NaHCO3-(1,2)-(1,2)	2.67E-06	1.29E-06	48%	4
PbCO3-0.05-NaHCO3-(1,2)-(1,2)	4.09E-06	7.35E-07	18%	4
PbCO3-0.5-NaHCO3-(1,2)-(1,2)	1.70E-05	4.65E-06	27%	4
PbCO3-1.0-NaHCO3-(1,2)-(1,2)	3.16E-05	8.26E-06	26%	4
PbCO3-1.0/0.3-NaHCO3-(1,2)-(1,2)	3.29E-05	1.29E-05	39%	4

Figure III.2-6. Plots of the statistics of ΣPb (M, mol/L) in A. Table III.2-6 (TP 08-02 Revision 0); B. Table III.2-8 (TP 20-01 Revision 0). Data labels are listed in the order of average, 2SD, %2SD, and counts of measurements. For the last two data points, i.e., the fourth and fifth from the left, the $NaHCO_3$ loading is the same, but the loading of NaCl was double for the last data point, i.e., the fifth from the left. Green ovals indicate a group of reactors showing statistically similar ΣPb values between A and B, and yellow ovals indicate another group of reactors showing different ΣPb values between A and B.

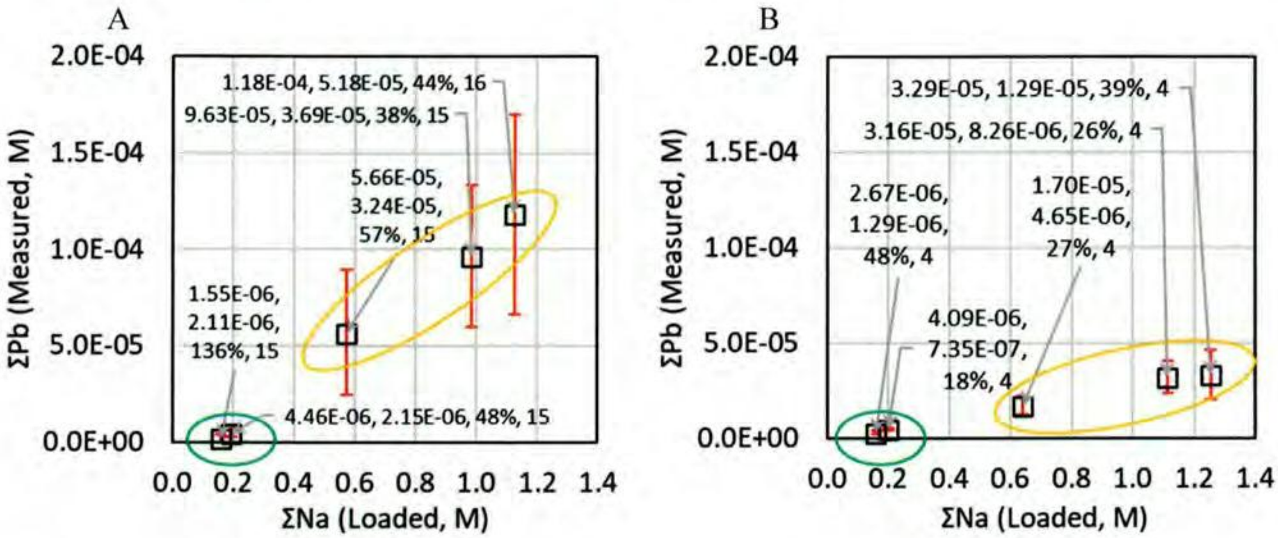

III.2.3. ΣCO3

The behavior of ΣCO3 is crucial to confirm the interpretation made for pHr and ΣPb in Sections III.2.1 and III.2.2. Measurements of ΣCO3 are available for Experiment 2 conducted under TP 08-02 Revision 0, but not available for Experiment 2 conducted under TP 20-01 Revision 0 as of 6/21/2021.

Presented in Table III.2-9 are the time-dependent measurements of ΣCO3. The plots are presented in Figure III.2-7. Statistics are summarized in Table III.2-10 and displayed in Figure III.2-9A.

Carbonate is a reactive species; the dissolution of $PbCO_3$(s) increases the ΣCO3 over the loaded ΣCO3 by addition of $NaHCO_3$:

$$\Sigma CO_3^{2-} = [NaHCO_3]_{Loaded} + [PbCO_3(s)]_{Dissolved}$$

$$= [NaHCO_3]_{Loaded} + \Sigma Pb \qquad (8)$$

, where $[PbCO_3(s)]_{Dissolved}$ = ΣPb by mass balance. $PbCO_3$(s) is the sole source of dissolved lead. Carbonate is loaded by adding the $NaHCO_3$ to the solutions and the lowest loading is 8.58E-03 M (Table II.2-1). ΣPb is less than 10^{-5} M at the lowest loading of $NaHCO_3$ (Table III.2-5, Figure III.2-4, and Table III.2-6). The ratio of $[NaHCO_3]_{Loaded}$/ΣPb is over 100. Thus, it is difficult to observe positive %Deviation of measured ΣCO3 from the loaded $NaHCO_3$ concentration via the dissolution of $PbCO_3$(s); that is, in Equation (8), $[NaHCO_3]_{Loaded} >> [PbCO_3(s)]_{Dissolved}$ = ΣPb, and ΣCO3 ≡[25]

[25] "≡" means "Can be equated to".

$[NaHCO_3]_{Loaded}$ within 1%. Although carbonate is a reactive component due to the dissolution of $PbCO_3(s)$, it can be considered a conservative component under the condition of the Experiment 2 unless it is lost by Reaction (6).

From Experiment 1 conducted under TP 08-02 Revision 0, the ΣCO3 showed scatter at the lowest loading of $NaHCO_3$. The scattering of data is negligible at higher loadings of $NaHCO_3$ (Table III.2-9, Figure III.2-7, and Table III.2-10). The precision, i.e., %2SD, decreased from 29% to 9% as the loading of $NaHCO_3$ increased. With 29% of %2SD, the lowest loading[26] of $NaHCO_3$ seems below the lower detection limit of the instrument (coulometer).

Consistent underestimation of ΣCO3 was noticed by the negative %Deviations, reaching down to -26% (Figure III.2-7, Table III.2-10, and Figure III.2-9A). From the statistical analysis presented in Figure III.2-9, it can be stated with 95% confidence that $CO_2(g)$ was lost during the aging of Experiment 2 samples, except at the lowest loading of $NaHCO_3$ where the measurements seem to have been conducted below the lower detection limit of the coulometer, resulting in lower precision (i.e., 2SD = 29%, highest values in Table III.2-10). Lower recovery of ΣCO3 can be explained by the inaccurate loading of $NaHCO_3$, but this explanation can be excluded by the higher accuracy (i.e., smaller %Deviation) of ΣNa measurements (See Section III.2.4; Figure III.2-12A), i.e., $NaHCO_3$ is the common source of ΣNa and ΣCO3 (Recipes in Table II.2-1 and Table II.2-2).

Consistent negative %Deviation indicates $CO_2(g)$ loss, not $CO_2(g)$ intrusion, and is consistent with the observed increase of pHr due to Reaction (6) in page 40, and the suppression of Pb due to Reaction (7) in page 45.

Measurements of ΣCO3 from Experiment 2 performed under TP 20-01 Revision 0 will be reported as the measurements become available.

Table III.2-9. Time-dependent measurements of ΣCO3 (M, mol/L) under TP 08-02 Revision 0.

ΣCO3 (M)	Aging time (Days)							
Reactor ID	741	1020	1069	1118	1167	1293	1379	1461
PbCO3 0.01/0.15-1	8.95E-03	8.18E-03	7.94E-03	6.30E-03	5.20E-03	7.61E-03	7.29E-03	6.81E-03
PbCO3 0.01/0.15-2	8.56E-03	6.51E-03	6.35E-03	5.57E-03	6.52E-03	6.90E-03	7.82E-03	6.83E-03
PbCO3 0.05/0.15-1	3.66E-02	3.30E-02	3.28E-02	3.41E-02	4.12E-02	3.30E-02	4.02E-02	3.42E-02
PbCO3 0.05/0.15-2	3.73E-02	3.10E-02	3.10E-02	3.30E-02	3.72E-02	3.42E-02	3.38E-02	3.46E-02

[26] 8.58 mmol/L $NaHCO_3$ × 1 mmol C/mmol $NaHCO_3$ × 12 mg C/mmol C = 103 mg C/L = 103 ppm C.

PbCO3 0.5/0.15-1	3.58E-01	2.98E-01	2.79E-01	2.99E-01	2.73E-01	2.84E-01	2.93E-01	2.82E-01
PbCO3 0.5/0.15-2	3.64E-01	3.06E-01	3.22E-01	3.41E-01	3.29E-01	3.25E-01	3.37E-01	3.17E-01
PbCO3 1.0/0.15-1	6.82E-01	6.39E-01	6.91E-01	6.03E-01	6.87E-01	6.77E-01	6.60E-01	6.38E-01
PbCO3 1.0/0.15-2	7.01E-01	6.27E-01	6.80E-01	6.83E-01	6.84E-01	6.78E-01	6.57E-01	6.49E-01
PbCO3 1.0/0.3-1	6.92E-01	6.59E-01	6.68E-01	6.63E-01	6.03E-01	6.59E-01	7.31E-01	6.22E-01
PbCO3 1.0/0.3-2	6.65E-01	6.91E-01	6.99E-01	6.88E-01	6.89E-01	6.83E-01	6.77E-01	6.75E-01

Figure III.2-7. Plot of the time-dependent measurements of ΣCO3 (M, mol/L) under TP 08-02 Revision 0 in Table III.2-9. Orange dots are initial loading of $NaHCO_3$. Black squares and red error bars located on 600 days are averages and twice the standard deviations of all the measurements displayed to the right at their aging time (blue dots and circles, which represent data from duplicate reactors).

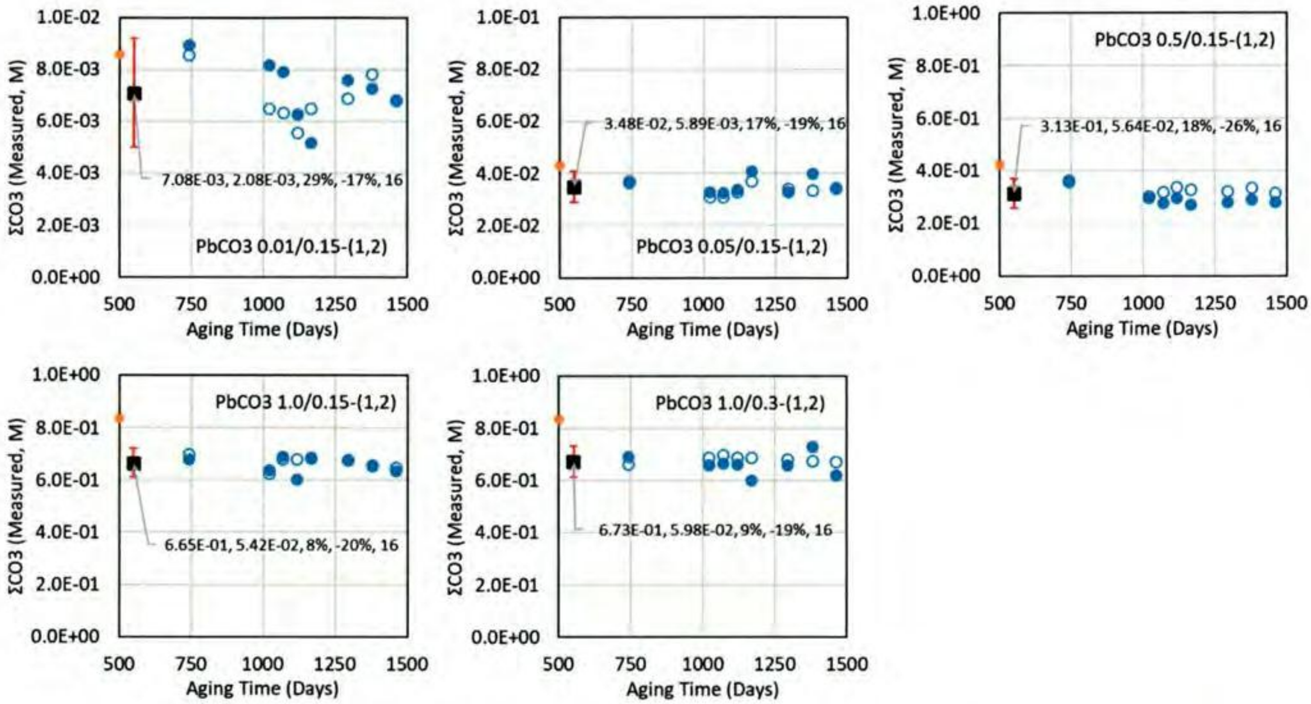

Table III.2-10. Statistics of measurements of ΣCO3 (M, mol/L) under TP 08-02 Revision 0 in Table III.2-9.

Reactor ID	Average	2SD	%2SD	%Deviation	Counts
PbCO3 0.01/0.15-(1,2)	7.08E-03	2.08E-03	29%	-17%	16
PbCO3 0.05/0.15-(1,2)	3.48E-02	5.89E-03	17%	-19%	16
PbCO3 0.5/0.15-(1,2)	3.13E-01	5.64E-02	18%	-26%	16
PbCO3 1.0/0.15-(1,2)	6.65E-01	5.42E-02	8%	-20%	16
PbCO3 1.0/0.3-(1,2)	6.73E-01	5.98E-02	9%	-19%	16

Table III.2-11. Time-dependent measurements of ΣCO3 under TP 20-01 Revision 0.

No measurements as of 6/20/2021

Figure III.2-8. Plot of the time-dependent measurements of ΣCO3 under TP 20-01 Revision in Table III.2-11.

No measurements as of 6/20/2021

Table III.2-12. Statistics of measurements of ΣCO3 under TP 20-01 Revision 0 in Table III.2-11.

No measurements as of 6/20/2021

Figure III.2-9. Plot of the statistics of ΣCO3 in Table III.2-10 (TP 08-02 Revision 0).

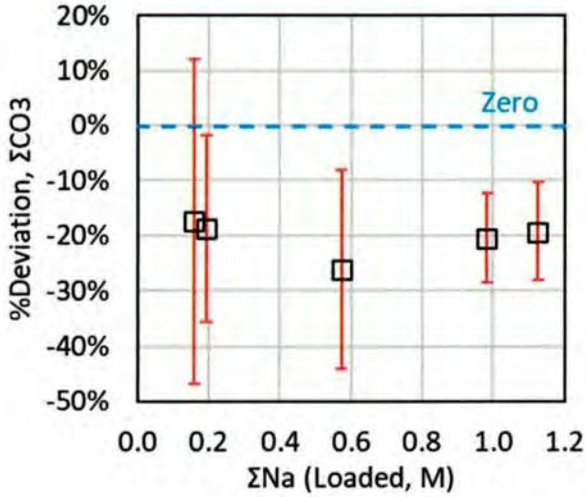

III.2.4. ΣNa

Sodium can be considered a non-reactive/conservative component unless removed by the precipitation of abellaite. Total dissolved sodium concentration, ΣNa, is defined:

$$\Sigma Na = [NaHCO_3]_{Loaded} + [NaCl]_{Loaded} \quad (9)$$

From Experiment 1 conducted under TP 08-02 Revision 0, the ΣNa were stable through the aging time. The time-dependent measurements of ΣNa are presented in Table III.2-13 and plotted in Figure III.2-10. Statistics are summarized and illustrated in Table III.2-14 and Figure III.2-12A. The measurements of ΣNa were accurate and precise. The precision, i.e., %2SD, ranged from 3 - 11%, and the accuracy, i.e., %Deviation, ranged from -8 to 5%.

Measurements of ΣNa from Experiment 2 performed under the protocols of TP 20-01 Revision 0 are tabulated in Table III.2-15. They are stable and independent of the dilution techniques (Figure III.2-11).

In the Experiment 2 under the protocols of TP 20-01 Revision 0, ΣNa was measured in the background solutions prior to adding the solid, $PbCO_3(s)$, in addition to the measurements after commencing the dissolution. The samples injected to the instrument for measurements of ΣNa in the background solution prior to the addition of $PbCO_3(s)$ were prepared by volume-to-volume dilution. The samples for the measurements of ΣNa in the filtered supernatants after commencing the dissolution were prepared by mass-to-volume dilution. All the measurements of ΣNa are summarized in Table III.2-15 and plotted in Figure III.2-11.

While the mass-to-volume dilution technique frequently underestimated ΣNa in the Experiment 1 conducted under TP 20-01 Revision 0 (Section III.1.4; Figure III.1-11), the technique showed better accuracy in reproducing the loaded ΣNa in the Experiment 2 conducted under TP 20-01 Revision 0 (This section; Figure III.2-11). While the volume-to-volume dilution technique accurately reproduced ΣNa in the Experiment 1 conducted under TP 20-01 Revision 0 (Section III.1.4; Figure III.1-11), the technique showed lower accuracy in reproducing the loaded ΣNa in the Experiment 2 conducted under TP 20-01 Revision 0 (This section; Figure III.2-11). While in theory the mass-to-volume dilution technique is more accurate for denser solutions than volume-to-volume dilution, it is not clear why the opposite is observed from the measurements of ΣNa performed for Experiments 1 and 2. The two dilution techniques do not result in observable differences for the range of solution densities considered in the recipe (Table II.1-2 and Table II.2-2) under the overall laboratory operation of SNL WIPP Geochemistry Program.

Statistical analysis of the data is summarized in Table III.2-16 and Figure III.2-12B. Experiments conducted under both TPs show identical results.

Table III.2-13. Time-dependent measurements of ΣNa (M, mol/L) under TP 08-02 Revision 0.

ΣNa (M)	Aging time (Days)							
Reactor ID	741	1020	1069	1118	1167	1293	1379	1461
PbCO3 0.01/0.15-1	1.60E-01	1.82E-01	1.81E-01	1.60E-01	1.75E-01	1.65E-01	1.55E-01	1.69E-01
PbCO3 0.01/0.15-2	1.57E-01	1.76E-01	1.73E-01	1.56E-01	1.70E-01	1.66E-01	1.54E-01	1.63E-01
PbCO3 0.05/0.15-1	1.95E-01	2.04E-01	1.94E-01	1.90E-01	1.98E-01	1.88E-01	1.80E-01	1.92E-01
PbCO3 0.05/0.15-2	1.91E-01	2.08E-01	1.95E-01	1.89E-01	2.00E-01	1.96E-01	1.83E-01	1.91E-01

PbCO3 0.5/0.15-1	5.50E-01	5.55E-01	5.09E-01	4.98E-01	5.28E-01	5.20E-01	5.21E-01	5.18E-01
PbCO3 0.5/0.15-2	5.15E-01	5.36E-01	5.27E-01	5.13E-01	5.44E-01	5.47E-01	5.34E-01	5.34E-01
PbCO3 1.0/0.15-1	9.12E-01	9.05E-01	9.19E-01	9.04E-01	9.32E-01	9.29E-01	9.31E-01	9.21E-01
PbCO3 1.0/0.15-2	9.32E-01	8.94E-01	9.12E-01	9.11E-01	9.28E-01	9.24E-01	9.48E-01	9.15E-01
PbCO3 1.0/0.3-1	9.00E-01	1.05E+00	1.03E+00	1.05E+00	1.09E+00	1.07E+00	1.11E+00	1.05E+00
PbCO3 1.0/0.3-2	1.07E+00	1.05E+00	1.05E+00	1.07E+00	1.07E+00	1.07E+00	1.09E+00	1.04E+00

Figure III.2-10. Plot of the time-dependent measurements of ΣNa (M, mol/L) under TP 08-02 Revision in Table III.2-13. Orange dots on vertical axes are the initial loadings of ΣNa. Black squares and red error bars located on 600 days are averages and twice the standard deviations of all the measurements displayed to the right at their aging time (blue dots and circles, which represent data from duplicate reactors).

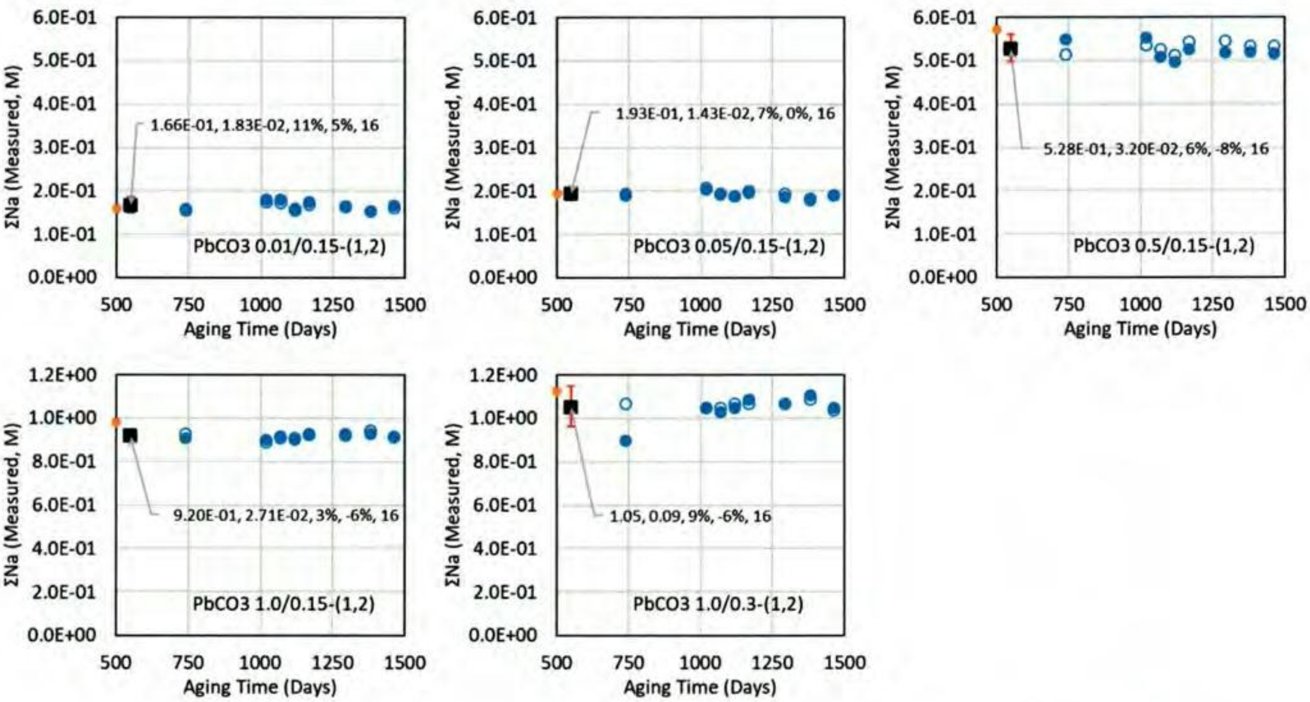

Table III.2-14. Statistics of measurements of ΣNa (M, mol/L) under TP 08-02 Revision 0 in Table III.2-13.

Reactor ID	Average	2SD	%2SD	%Deviation	Counts
PbCO3 0.01/0.15-(1,2)	1.66E-01	1.83E-02	11%	5%	16
PbCO3 0.05/0.15-(1,2)	1.93E-01	1.43E-02	7%	0%	16
PbCO3 0.5/0.15-(1,2)	5.28E-01	3.20E-02	6%	-8%	16
PbCO3 1.0/0.15-(1,2)	9.20E-01	2.71E-02	3%	-6%	16
PbCO3 1.0/0.3-(1,2)	1.05	0.09	9%	-6%	16

Table III.2-15. Time-dependent measurements of ΣNa (M, mol/L) under TP 20-01 Revision 0.

Aging time (Days)	0	47	91
Reactor ID (n =)	Before adding $PbCO_3$[#]	1	2
PbCO3-0.01-NaHCO3-1-n	1.32E-01	1.61E-01	1.59E-01
PbCO3-0.01-NaHCO3-2-n	1.34E-01	1.58E-01	1.59E-01
PbCO3-0.05-NaHCO3-1-n	1.70E-01	1.92E-01	1.94E-01
PbCO3-0.05-NaHCO3-2-n	1.71E-01	1.94E-01	1.89E-01
PbCO3-0.5-NaHCO3-1-n	5.65E-01	5.81E-01	5.78E-01
PbCO3-0.5-NaHCO3-2-n	5.62E-01	5.71E-01	5.73E-01
PbCO3-1.0-NaHCO3-1-n	1.13E+00	1.04E+00	1.03E+00
PbCO3-1.0-NaHCO3-2-n	1.13E+00	9.07E-01	1.01E+00
PbCO3-1.0/0.3-NaHCO3-1-n	9.82E-01	1.35E+00	1.36E+00
PbCO3-1.0/0.3-NaHCO3-2-n	9.80E-01	1.33E+00	1.02E+00

#Duplicate measurements of the six solutions described in Table II.2-2 prior to adding to the solid-containing vials. volume-to-volume dilution.

Figure III.2-11. Plot of the time-dependent measurements of ΣNa (M, mol/L) under TP 20-01 Revision in Table III.2-15. Orange ×s on the vertical axes are the initial loading of ΣNa by the recipe. Black squares and red error bars located on 20 days are averages and twice the standard deviations of all the measurements displayed to the right at their aging time (blue dots and circles, which represent data from duplicate reactors).

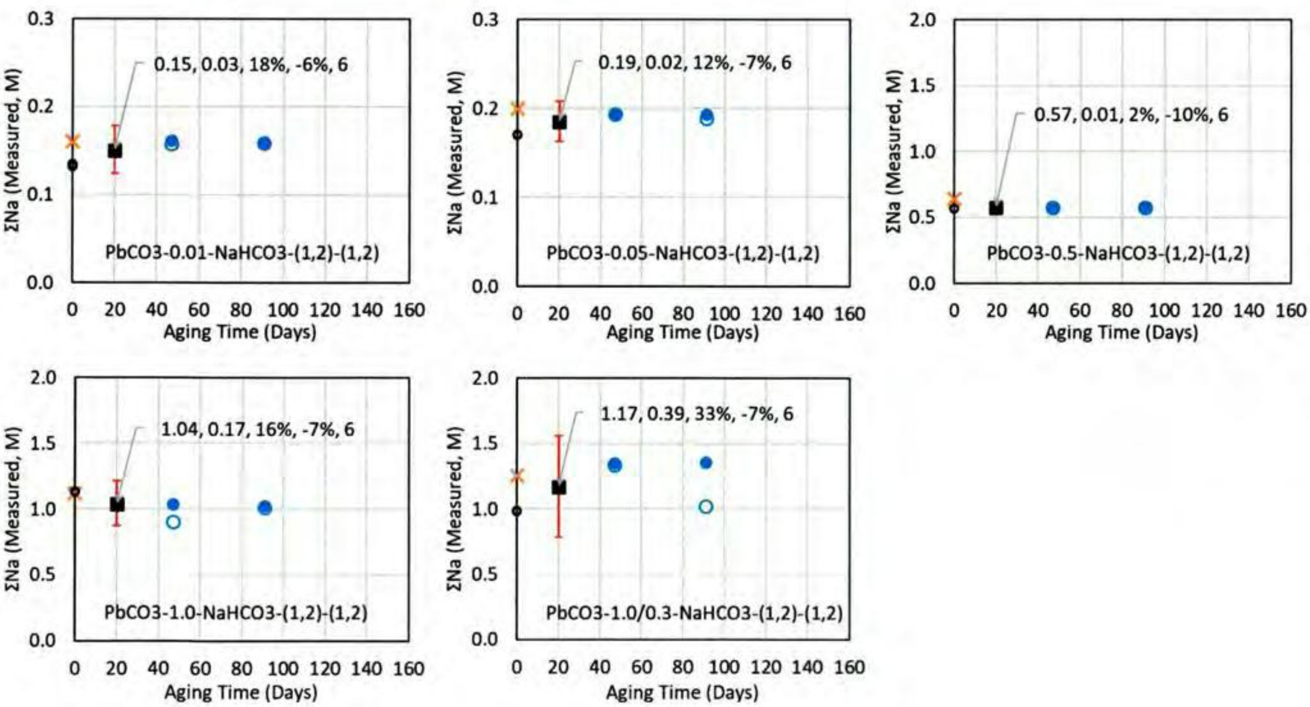

Table III.2-16. Statistics of measurements of ΣNa (M, mol/L) under TP 20-01 Revision 0 in Table III.2-15.

Reactor ID	Average	2SD	%2SD	%Deviation	Counts
PbCO3-0.01-NaHCO3-(1,2)-(1,2)	1.51E-01	2.73E-02	18%	-6%	6
PbCO3-0.05-NaHCO3-(1,2)-(1,2)	1.85E-01	2.29E-02	12%	-7%	6
PbCO3-0.5-NaHCO3-(1,2)-(1,2)	5.72E-01	1.42E-02	2%	-10%	6
PbCO3-1.0-NaHCO3-(1,2)-(1,2)	1.04E+00	1.68E-01	16%	-7%	6
PbCO3-1.0/0.3-NaHCO3-(1,2)-(1,2)	1.17E+00	3.87E-01	33%	-7%	6

Figure III.2-12. Plot of the statistics of ΣNa in A: Table III.2-14 (TP 08-02 Revision 0) and B: Table III.2-16 (TP 20-01 Revision 0).

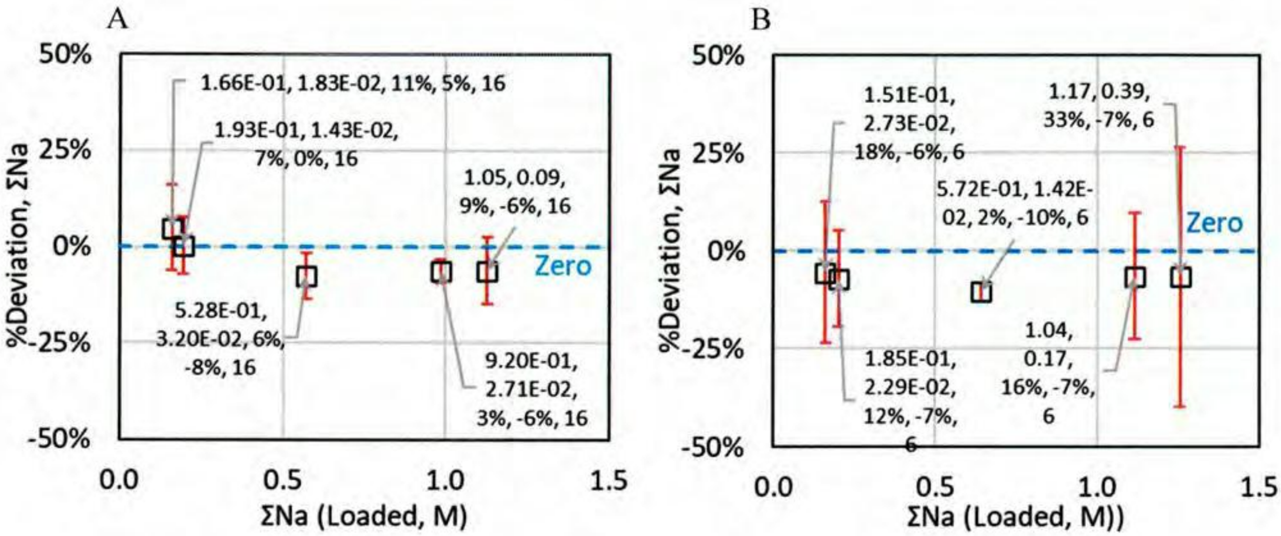

III.2.5. ΣCl

Not available.

Table III.2-17. Time-dependent measurements of ΣCl under TP 08-02 Revision 0.

ΣCl not reported in Kirkes et al. (2014)

Figure III.2-13. Plot of the time-dependent measurements of ΣCl under TP 08-02 Revision in Table III.2-17.

ΣCl not reported in Kirkes et al. (2014)

Table III.2-18. Statistics of measurements of ΣCl under TP 08-02 Revision 0 in Table III.2-17.

ΣCl not reported in Kirkes et al. (2014)

Table III.2-19. Time-dependent measurements of ΣCl under TP 20-01 Revision 0.

No measurements as of 6/20/2021

Figure III.2-14. Plot of the time-dependent measurements of ΣCl under TP 20-01 Revision in Table III.2-19.

No measurements as of 6/20/2021

Table III.2-20. Statistics of measurements of ΣCl under TP 20-01 Revision 0 in Table III.2-19.

No measurements as of 6/20/2021

Figure III.2-15. Plot of the statistics of ΣCl in Table III.2-18 and Table III.2-20.

No measurements as of 6/20/2021

III.2.6. Solid Characterization

One of the duplicates for the loadings of $NaHCO_3$ and NaCl at 0.5 and 0.15 with reactor ID of PbCO3-0.5-0.15-1 showed abellaite ($NaPb_2(CO_3)_2(OH)(s)$) formation (Figure III.2-16). Solids collected from PbCO3-1.0-0.15-1 and PbCO3-1.0-0.3-1 also displayed sign for abellaite formation.

No sign of abellaite formation was observed from the XRD scans of the solid samples generated under TP 20-01 Revision 0 (Figure III.2-17).

Figure III.2-16. XRD scans of solids collected from Experiment 2 conducted under TP 08-02 Revision 0. Two blue elongated rectangles locate the positions of major reference peaks of cerussite, and three red elongated rectangles locate those of abellaite.

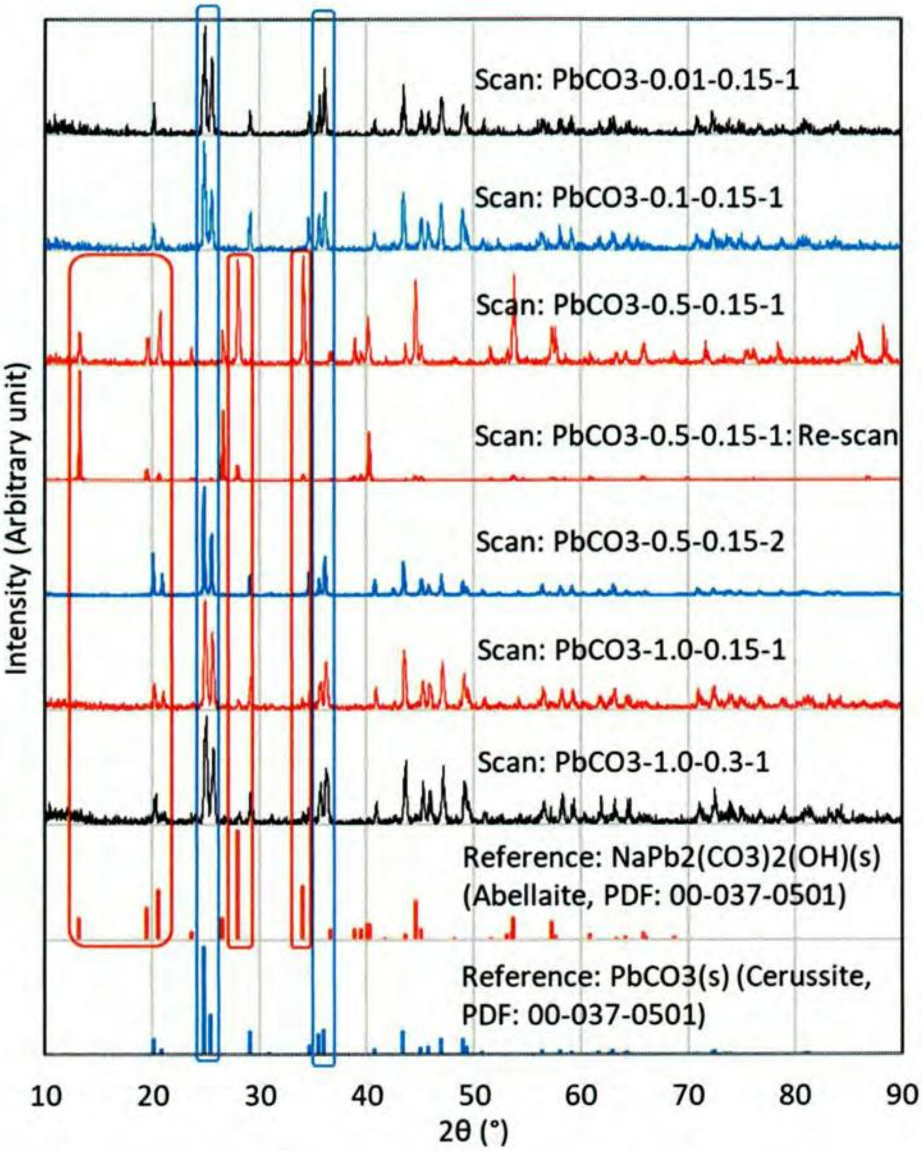

Figure III.2-17. XRD scans of solids collected from Experiment 2 conducted under TP 20-01 Revision 0. The last digit of sample ID, i.e., -1 and -2 stands for solid sample collected after 47 and 91 days of equilibration, respectively. Solid obtained from PbCO3-1.0_0.3 NaHCO3-2-1 is in the queue.

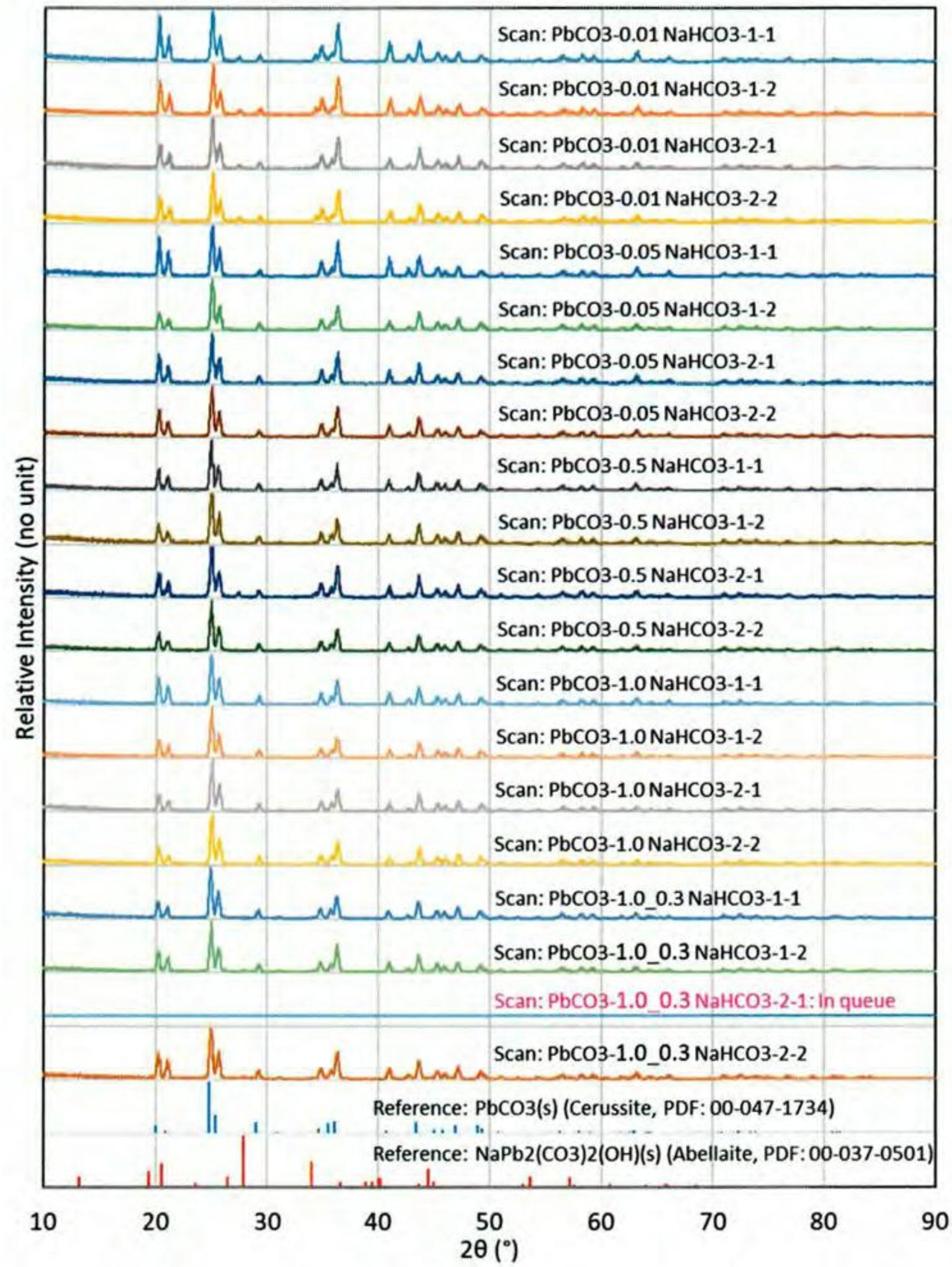

III.2.7. Summary

Experiment 2, where excess $PbCO_3(s)$ (cerussite) was added to background solutions of incremental concentrations of $NaHCO_3$ spiked with a constant NaCl concentration, was performed using protocols in TP 08-02 Revision 0. This experiment was assumed to be subject to $CO_2(g)$ loss (not gain) and inadvertent contamination of the reactors by unknown sources due to repeated entries during sampling and aging times in the order of multiple years. The same experiment was performed under the protocols of TP 20-01 Revision 0 using gloveboxes for minimal CO_2 intrusion. These protocols involved the preparation of multiple replicates at the termination at each timed investigation to exclude the possibilities of $CO_2(g)$ intrusion and inadvertent contamination of the reactors. The last sampling under TP 20-01 Revision 0 was conducted on 91 days of aging, which is much earlier than the first sampling on 741 days of aging under TP 08-02 Revision 0.

The recorded pHr values from Experiment 2 showed two groups (green and orange ovals in Figure III.2-3). The pHr in the green ovals were obtained from reactors of low $NaHCO_3$ loadings (see recipes in Table II.2-1 and Table II.2-2), and the values from the old and new experiments are statistically identical. That is, two different protocols of the TPs did not influence the pHr because the partial pressures of $CO_2(g)$ are close enough to the atmospheric partial pressure of $CO_2(g)$, and as a result, the $CO_2(g)$ loss was minimal.[27] The pHr in the orange ovals were obtained from reactors having higher $NaHCO_3$ loadings (see recipes in Table II.2-1 and Table II.2-2), and the application of different protocols (i.e., use of a glovebox for minimal $CO_2(g)$ intrusion) resulted in statistically different values of pHr. Less $CO_2(g)$ loss under the protocols of TP 20-01 Revision 0 effectively kept the pHr lower than the experiments conducted under the protocols of TP 08-02 Revision 0 via Reaction (6).

The difference of the ΣPb behavior described in Figure III.2-6 can be explained by the extent of loss of $CO_2(g)$ via Reaction (7). More loss of $CO_2(g)$ under the protocols of TP 08-02 Revision 0 resulted in driving Reaction (7) to the right, increasing the ΣPb, while less loss of $CO_2(g)$ under the protocols of TP 20-01 Revision 0 resulted in the suppression of ΣPb.

Statistical comparison of ΣCO3 between the two protocols is not currently available (Figure III.2-9). Statistically, it can be stated with 95% confidence that Experiment 2 under TP 08-02 Revision 0 lost ΣCO3 in four conditions out of five via Reaction (6), which could provide the excess OH^- needed to form abellaite at the expense of cerussite via Reaction (1). Inaccurate loading of $NaHCO_3$ can be one explanation for the lower recovery of ΣCO3, but this can be eliminated given the higher accuracy measurements of ΣNa (Figure III.2-12A) and mass balance calculations.

The difference of H^+ concentration for the last three experimental conditions (marked with orange ovals in Figure III.2-3) can be approximated by a factor of 10, while the difference of ΣPb for the

[27] The calculated initial $P_{CO_2(g)}$ are $10^{-3.1}$ and $10^{-1.7}$ atm under TP 08-02 Revision 0, and $10^{-2.4}$ and $10^{-1.7}$ atm under TP 20-01 Revision 0. Note the slight difference in the $NaHCO_3$ loadings in the reactors of lowest $NaHCO_3$ loading (Table II.2-1 and Table II.2-2).

same set of reactors can be approximated by a factor of 2 (marked with orange ovals in Figure III.2-6), which means that the stoichiometry of Reaction (7) cannot explain the change of pHr.

Considering ΣCO3 > ΣPb by at least one order of magnitude (Figure III.2-7 and Figure III.2-4), the main driver to determine the pHr would be Reaction (6).

The ΣNa are statistically identical (Figure III.2-12), so the possibility of inadvertent addition of Na-containing salts, e.g., NaOH, that can drive Reaction (1) to the right can be eliminated.

One of the replicates where abellaite was observed (Reactor ID: PbCO3 0.5/0.15-1; Figure III.2-16) showed a wider spread of pHr (blue dots in the third panel of upper row of Figure III.2-1). The sudden drop of pHr at around 1400 days could be an indication of abellaite formation by OH^- removal from solution via Reaction (1). This observation implies that the pHr boundary between cerussite and abellaite may be located at pHr of 9.0 ~ 9.5, where cerussite and abellaite could coexist. The reactors PbCO3 0.01/0.15-(1,2) showed similar spread of pHr between the replicates (first panel in Figure III.2-1), but lower loading of ΣNa than PbCO3 0.5/0.15-(1,2) would explain no observation of abellaite. No mineralogical transformation was observed under TP 20-01 Revision 0 (Figure III.2-17), which is supported by less CO_2(g) loss and thus lower pHr (orange oval in A and B of Figure III.2-3).

IV. DISCUSSION

IV.1. Experiment 1

Results of pHr, ΣPb, ΣSO4, and ΣNa under protocols of both TPs are statistically identical (Figure III.1-3 for pHr; Figure III.1-6 for ΣPb; Figure III.1-9 for ΣSO4; Figure III.1-12 for ΣNa). Considering higher accuracy observed in the ΣNa measurements, the measurements of ΣCl under TP 20-01 Revision 0 seem impacted by lower accuracy of the instrument (compare Figure III.1-12B and Figure III.1-15B).

The possibility of CO_2(g) intrusion under TP 08-02 Revision 0 cannot be excluded, but even if it is the case, the repetition of Experiment 1 under the protocols of TP 20-01 Revision 0 with CO_2(g) intrusion excluded proved that the results are statistically identical, and the CO_2(g) intrusion would not influence the thermodynamic interpretation of Experiment 1 conducted under TP 08-02 Revision 0.

Inadvertent contamination of the reactors because of repeated entries for sampling might have happened while Experiment 1 was performed under TP 08-02 Revision 0, but even if it is the case, the repetition of Experiment 1 under TP 20-01 Revision 0 where two replicates were used up in a time-dependent investigation proved that any such contamination is within our experimental and analytical uncertainty.

IV.2. Experiment 2

In Experiment 2, CO_2(g) loss seemed to occur rather than CO_2(g) gain by intrusion, which is supported by the loading of $NaHCO_3$. The behavior observed from the measurements of pHr (Figure III.2-3), ΣPb (Figure III.2-6), and ΣCO3 (Figure III.2-9) is consistent with the mass action law described by Reactions (6) and (7). The source of excess OH^- to drive Reaction (1) to the right also can be attributed to Reaction (6) (c.f., Krauskopf and Bird, 1995).

Inadvertent contamination of the reactors because of repeated entries for sampling might have happened while Experiment 1 was performed under TP 08-02 Revision 0, but even if it is the case, the repetition of Experiment 1 under TP 20-01 Revision 0 where two replicates were used up in the timed investigation proved that such contamination can be considered a negligible source of uncertainty.

IV.3. Aging Time and Status of System Equilibrium

For Experiment 1, the first sampling was conducted after 360 days of aging, and the last sampling after 1368 days of aging under TP 08-02 Revision 0. Under TP 20-01 Revision 0, the first sampling was conducted after 43 days of aging, and the second sampling after 111 days of aging.

For Experiment 2, the first sampling was conducted after 741 days of aging, and the last sampling after 1461 days of aging under TP 08-02 Revision 0. Under TP 20-01 Revision 0, the first sampling was conducted after 47 days of aging, and the second sampling after 91 days of aging.

Interpretation of the experimental data in this report was performed using the averages and twice the standard deviations of the time-dependent measurements. Averages of the concentrations of conservative/non-reactive components showed reliable accuracy (%Deviation from the loadings) and precision (narrow %2SD). Statistically, no sign of consistent time-dependent behavior of measurements was observed. Therefore, both Experiments 1 and 2 reached equilibria under the protocols of both TPs.

IV.4. Bottle Material

Plastic bottles (HDPE) were used when Experiments 1 and 2 were performed under TP 08-02 Revision 0. Borosilicate glass bottles were used when Experiments 1 and 2 were performed under TP 20-01

Revision 0. The uncertainty that can come from the differences in the bottle materials did not show up in the measurements.

V. CONCLUSIONS

From our analyses we can conclude that the results of Experiment 1 performed under the protocols of TP 08-02 Revision 0 were not affected by sample contamination or $CO_2(g)$ intrusion. Both sample contamination and $CO_2(g)$ intrusion can be considered negligible sources of uncertainty as part of our laboratory operations. Thus, the results would be useful to construct or validate a lead-sulfate thermodynamic model after implementing a reliable lead-chloride model (e.g., Jang, 2021b).

The results of Experiment 2 performed under the protocols of TP 08-02 Revision 0 were not affected by sample contamination. No increase of ΣNa was observed that could have driven the Reaction (1) in page 4 to the right. Sample contamination, if it occurred, can be considered a negligible source of uncertainty. Results of Experiment 2 performed under the protocols of TP 08-02 Revision 0 indicated $CO_2(g)$ losses, not gains of $CO_2(g)$ by intrusion. Evidence for $CO_2(g)$ loss is consistent with Reactions (1), (6), and (7). They would be useful to construct or validate a lead-carbonate model after implementing a reliable lead-chloride model.

VI. ACKNOWLEDGMENT

Technical Review was performed by Carlos Jove-Colon. QA review by Shelly Nielsen. Management Review by Paul Shoemaker. Reviews were conducted under SNL WIPP QA Program. Comments and resolutions are documented. Authors are grateful for the constructive comments from the Reviewers.

VII. REFERENCES

Ismail, A. E., M. B. Nemer, G. T. Roselle, and Y. Xiong, 2008. Iron, Lead, Sulfide, and EDTA Solubilities. Test Plan TP 08-02, Revision 0. Sandia National Laboratories, Carlsbad, New Mexico, U.S.A. ERMS 548466.

Jang, J., 2020. Factors for Conversion of Molarity to molality and molality to Molarity. Memo to SNL WIPP Records Center and SNL WIPP Geochemistry. October 16, 2020. Sandia National Laboratories, Carlsbad, New Mexico, U.S.A. ERMS 574276.

Jang, J., 2021a. Memo of Correction for the Third Milestone Report on Test Plan TP 08-02, "Iron, Lead, Sulfide, and EDTA Solubilities", Revision 0 (ERMS 561911), Revision 1 (ERMS 562645), and Revision 2 (ERMS 562947). November 1, 2021, Sandia National Laboratories, Carlsbad, New Mexico, U.S.A. ERMS 576204.

Jang, J., 2021b. Revisit to the Pitzer Geochemical Thermodynamic Model for the $PbCl_2$(s) - HCl - H_2O System. Memo to SNL WIPP Records Center and SNL WIPP Geochemistry, May 25, 2021. Sandia National Laboratories, Carlsbad, New Mexico, U.S.A. ERMS 575309.

Jang, J., P. Hora, L. Kirkes, C. Miller, and L. Zhang, 2021. Analysis Plan for the Analysis Report documenting the Assessment of the Solubility of Lead, EDTA, and other Organic Ligands in Non-Sulfide Systems performed under TP 08-02 Revision 0 and under TP 20-01 Revision 0. Analysis Plan AP-192 Revision 0. Sandia National Laboratories, Carlsbad, New Mexico, U.S.A. ERMS 575694.

Kirkes, L., T. Olivas, J. Jang, S. Kim, and Y. Xiong, 2014. Third Milestone Reports on Test Plan TP 08-02, "Iron, Lead, Sulfide, and EDTA Solubilities", Revision 2, Sandia National Laboratories, Carlsbad, New Mexico, U.S.A., ERMS 562947.

Kirkes, L., and Y. Xiong, 2019. Solid Characterization Milestone Report on Test Plan TP 08-02, "Iron, Lead, Sulfide, and EDTA Solubilities", Revision 1. Sandia National Laboratories, Carlsbad, New Mexico, U.S.A., ERMS 572290.

Kirkes, L., and L. Zhang, 2020. Solubility and Complexation of Lead in Non-Sulfidic Brines of WIPP-Relevance. Test Plan TP 20-01, Revision 0. Sandia National Laboratories, Carlsbad, New Mexico, U.S.A. ERMS 573598.

Krauskopf, K. B., and D. K. Bird, 1995. Chapter 3. Solution - Mineral Equilibria Part 1: Carbonates, IN: K. B. Krauskopf and D. K. Bird, 1995. Introduction to Geochemistry. New York, McGraw-Hill.

Nielsen, S. R., 2020. Analyses. Nuclear Waste Management Procedure NP 9-1 Revision 11. September 15, 2020. Sandia National Laboratories, Carlsbad, New Mexico, U.S.A. ERMS 574015.

Stumm, W., and J. J. Morgan, 1996. *Aquatic Chemistry*. John Wiley & Sons, New York.

Wolery, T., and R. L. Jarek, 2003. Software User's Manual, EQ3/6, Version 8.0, 01/01/2003. Sandia National Laboratories, Carlsbad, New Mexico, U.S.A. ERMS 548926.

(No broken link found by Jay Jang on 11/17/2021. Total line number = 1116 including this line)

Sandia National Laboratories is a multi-mission laboratory managed and operated by National Technology and Engineering Solutions of Sandia, LLC., a wholly owned subsidiary of Honeywell International, Inc., for the U.S. Department of Energy's National Nuclear Security Administration under contract DE-NA-0003525. This research is funded by WIPP programs administered by the Office of Environmental Management (EM) of the U.S. Department of Energy.